

**Phosphorylation dependent stability control of the
deneddylase DenA and its impact on *Aspergillus nidulans*
development**

Dissertation
for the award of the degree
“Doctor rerum naturalium”
of the Georg-August Universität Göttingen

within the doctoral program GAUSS
of the Georg-August University School of Science

submitted by
Josua Sebastian Schinke
from Aalen

Göttingen 2015

Thesis Committee

Prof. Dr. Gerhard H. Braus

Department of Molecular Microbiology and Genetics
Institute of Microbiology and Genetics
Georg-August Universität Göttingen

Prof. Dr. Stefanie Pöggeler

Department of Genetics of Eukaryotic Microorganisms
Institute of Microbiology and Genetics
Georg-August Universität Göttingen

Members of the Examination Board

Reviewer I

Prof. Dr. Gerhard H. Braus

Department of Molecular Microbiology and Genetics
Institute of Microbiology and Genetics
Georg-August Universität Göttingen

Reviewer II

Prof. Dr. Stefanie Pöggeler

Department of Genetics of Eukaryotic Microorganisms
Institute of Microbiology and Genetics
Georg-August Universität Göttingen

Further members of the Examination Board

Prof. Dr. Rolf Daniel

Department of Genomic and Applied Microbiology
Institute of Microbiology and Genetics

PD Dr. Michael Hoppert

Department General Microbiology
Institute of Microbiology and Genetics

Prof. Dr. Kai Tittmann

Department of Molecular Enzymology
Albrecht von Haller Institute

Prof. Dr. Kai Heimel

Department of Molecular Microbiology and Genetics
Institute of Microbiology and Genetics

Date of oral examination: 28.01.2016

Affirmation

I hereby declare that this thesis was written independently and with no other sources and aids than quoted.

Göttingen, 11.12.2015

Josua Sebastian Schinke

This work was accomplished in the group of Prof. Dr. Gerhard H. Braus, at the Department of Molecular Microbiology and Genetics at the Institute of Microbiology and Genetics, Georg-August Universität Göttingen.

Parts of my work are published:

- von Zeska Kress MR, Harting R, Bayram Ö, Christmann M, Irmer H, Valerius O, **Schinke J**, Goldman GH & Braus GH (2012) The COP9 signalosome counteracts the accumulation of cullin SCF ubiquitin E3 RING ligases during fungal development. *Mol Microbiol.* 83: 1162–1177
- Christmann M, Schmalzer T, Gordon C, Huang X, Bayram Ö, **Schinke J**, Stumpf S, Dubiel W & Braus GH (2013) Control of multicellular development by the physically interacting deneddylases DEN1/DenA and COP9 signalosome. *PLoS Genet.* 9: e1003275
- **Schinke J**, Kolog Gulko M, Christmann M, Valerius O, Stumpf SK, Stirz M & Braus GH (2016) The DenA/DEN1 Interacting Phosphatase DipA Controls Septa Positioning and Phosphorylation-dependent Stability of Cytoplasmatic DenA/DEN1 during Fungal Development. *PLoS Genet.* 12: e1005949

TABLE OF CONTENTS

SUMMARY	1
ZUSAMMENFASSUNG	2
1 INTRODUCTION.....	3
1.1 Posttranslational protein modifications (PTMs).....	3
1.1.1 Phosphorylation and dephosphorylation	4
1.2 The family of ubiquitin and ubiquitin-like proteins	6
1.2.1 Ubiquitin.....	6
1.2.2 The ubiquitin-like protein Nedd8	8
1.3 Destruction of proteins	10
1.3.1 Protein degradation by the ubiquitin-proteasome system (UPS)	10
1.4 E3 ubiquitin ligases	11
1.5 Regulation of cullin-RING ligases (CRLs)	12
1.5.1 Neddylolation as a prerequisite for cullin-RING ligase activity	12
1.5.2 The deneddylase COP9 signalosome (CSN).....	14
1.5.3 Deneddylolation of CRLs by the COP9 signalosome	15
1.5.4 The deneddylase 1 (DEN1)	16
1.6 Fungi in science	19
1.6.1 The model organism <i>Aspergillus nidulans</i>	19
1.6.1.1 Vegetative growth and septation	20
1.6.1.2 Sexual development	21
1.6.1.3 Asexual development	23
1.6.2 Regulation of fungal development	23
1.6.3 The deneddylases COP9 signalosome and DEN1 in <i>Aspergillus</i> <i>nidulans</i>	27
1.7 Aims of this study.....	29
2 MATERIALS & METHODS	30
2.1 Chemicals.....	30
2.2 Strains and growth conditions	30
2.3 Plasmid and strain construction	34
2.3.1 Construction of <i>denA</i> overexpression strains	34
2.3.2 Strain construction of DenA-GFP in <i>csn</i> deletion strains	34

2.3.3	Construction of strains carrying an amino acid substituted phosphorylation site of DenA at position S253	34
2.3.4	Construction of strains with triple amino acid substituted phosphorylation sites of DenA at positions S243, S245 and S253	35
2.3.5	BiFC plasmid and strain construction for DenA-DipA interaction studies	36
2.3.6	Plasmid and strain construction for <i>dipA</i> * strain	37
2.3.7	Plasmid and strain construction for the <i>dipA</i> deletion strain	38
2.3.8	Plasmid and strain construction for the DipA-GFP strain	38
2.3.9	Strain construction of DenA-GFP in <i>dipA</i> deletion strain	39
2.3.10	Strain construction of <i>dipA/csnG</i> double deletion strain with DenA-GFP	39
2.4	Nucleic acid methods.....	39
2.4.1	Transformations	39
2.4.2	Constructs for genetic manipulation	40
2.4.3	Recombinant DNA methods	46
2.4.4	DNA isolation and hybridization	46
2.4.5	Sequence analyses.....	46
2.4.6	Quantitative real-time PCR.....	46
2.5	Protein methods.....	47
2.5.1	Protein isolation and western hybridization analyses	47
2.5.2	Antibodies	48
2.5.3	Co-purification methods	48
2.5.3.1	Tandem affinity purification (TAP)-tag purification.....	48
2.5.3.2	GFP-Trap purification	49
2.5.4	Protein staining	50
2.5.5	Tryptic in-gel digestion of proteins (Shevchenko <i>et al</i> , 2006)	50
2.5.6	Identification of proteins and phosphorylation sites by tandem mass spectrometry.....	51
2.5.7	Phos-tag Acrylamide.....	52
2.5.8	Computational methods	52
2.6	Fungal physiology and cell biology	52
2.6.1	Stress-Test.....	52
2.6.2	Microscopy	53
2.6.3	Quantification methods	53

3	RESULTS	54
3.1	Deneddylase deficient <i>A. nidulans</i> strains accumulate neddylated cullins	54
3.2	Accumulation of neddylated proteins caused by an impaired CSN complex can be reduced by elevated <i>denA</i> expression.....	56
3.3	High copy of <i>denA</i> affects the ratio of neddylated to deneddylated cullins in <i>csnG</i> but not in <i>csnE</i> deletion strain	57
3.4	Increased <i>denA</i> expression can partially rescue asexual development in CSN deficient strain.....	59
3.5	Three PCI domain containing CSN subunits as well as the two MPN subunits destabilize DenA in the nucleus.....	61
3.6	DenA stability regulated by distinct phosphorylation events is required for asexual development	63
3.6.1	DenA is phosphorylated	63
3.6.2	DenA possesses an additional phosphorylation at position S253 during asexual development	65
3.6.3	Phosphorylation of DenA S253 destabilizes the protein during fungal development	68
3.6.4	DenA stability control is required for asexual development	70
3.7	Characterization of the phosphatase DipA.....	71
3.7.1	AN10946 encodes a DenA interacting phosphatase (DipA) including a conserved metallophosphatase domain	71
3.7.2	DipA is required for asexual development.....	73
3.7.3	DipA controls intervals of septa positioning	76
3.7.4	DipA is present in the cytoplasm, at septa and is undetectable during late asexual development.....	77
3.8	DenA and DipA physically interact in the cytoplasm and at septa	79
3.8.1	The DenA-DipA interaction complex is dynamically transported.....	80
3.9	Stability of DenA is increased in <i>dipA</i> deletion strain	82
3.10	DipA and CsnG affect stability of DenA in a similar manner	83

4	DISCUSSION	86
4.1	The two deneddylases COP9 signalosome and DenA share cullins as common substrates	86
4.2	DenA provides an auxiliary function to support deneddylation and development in the absence of a functioning CSN complex	89
4.3	The presence of five neighboring CSN subunits targets nuclear DenA for degradation	92
4.4	A specific choreography of changing phosphorylation events at DenA C-terminus regulates its stability and fungal development	95
4.5	The phosphatase DipA targets cytoplasmatic DenA for degradation ...	100
4.6	The phosphatase DipA controls cytokinesis.....	102
4.7	The phosphatase DipA controls development.....	104
4.8	Future outlook	107
	LITERATURE	109
	ABBREVIATIONS	133
	LIST OF FIGURES	137
	LIST OF TABLES.....	139
	ACKNOWLEDGEMENTS.....	140
	CURRICULUM VITAE.....	141

Summary

Malfunctioning protein degradation in higher eukaryotes is associated with numerous diseases, including neurodegenerative disorders and cancer. Understanding regulation mechanisms of protein degradation is thus of particular importance. The ubiquitin-proteasome system selectively degrades intracellular proteins. Cullin-RING ligases, activated by the ubiquitin-like protein Nedd8, recognize target proteins and mediate the transfer of ubiquitin onto the protein. Ubiquitinated proteins are recognized and degraded by the 26S proteasome. The two deneddylases DenA and COP9 signalosome (CSN) remove Nedd8 from different kinds of substrates.

For the model organism *Aspergillus nidulans*, this study reveals that cellular DenA consists of a nuclear and a dynamic cytoplasmatic subpopulation. This study further provides (A) detailed information on the interplay between nuclear DenA and CSN, and (B) uncovers a hitherto uncharacterized phosphatase, DipA, which plays an important role in regulating cytoplasmatic DenA, as well as cell development.

(A) An increased amount of DenA partially compensates the lack of a functional CSN. DenA counteracts the accumulation of neddylated proteins and CSN associated developmental defects. This suggests that both fungal deneddylases have different but also overlapping functions. Further, nuclear DenA physically interacts with CSN and is destabilized during fungal development by five of the eight CSN subunits. These subunits form a functional surface on the CSN, and interaction of DenA with this surface seems an important step in regulating the stability of nuclear DenA.

(B) Cytoplasmatic DenA is co-transported with DipA and enriched at septa. Deletion of *dipA* results in increased DenA stability. This suggests that DipA destabilizes DenA and thus plays a role in cytoplasmatic DenA stability control. In addition, deletion of *dipA* impacts cell development, which manifests itself in an increased amount of septa and defects in light regulated fungal development. This indicates that - beyond DenA stability control - DipA is important for cell differentiation.

The stability of DenA is further regulated via phosphorylation. During vegetative growth, DenA is stabilized by phosphorylation at positions S243 and S245, which is required for initiating subsequent asexual development. After this initiation a change in the phosphorylation pattern of DenA is observed, which destabilizes the protein and results in DenA degradation in later asexual development.

In summary, this study provides insights into complex mechanisms of DenA protein degradation, which might also be relevant for higher eukaryotes.

Zusammenfassung

Ein fehlerhafter Proteinabbau führt in höheren Eukaryoten zu diversen Krankheiten wie z.B. neurodegenerativen Störungen und Krebs. Es ist daher bedeutend die Regulationsmechanismen des Proteinabbaus zu verstehen. Intrazelluläre Proteine werden spezifisch durch das Ubiquitin-Proteasome System abgebaut. Cullin-RING Ligasen, welche durch das ubiquitin-ähnliche Protein Nedd8 aktiviert werden, binden und markieren das Zielprotein mit Ubiquitin. Diese ubiquitinierten Proteine werden durch das 26S Proteasome abgebaut. Die zwei Deneddylasen DenA und COP9 Signalosome (CSN) entfernen Nedd8 von unterschiedlichen Substraten.

Diese Arbeit zeigt im Modellorganismus *Aspergillus nidulans*, dass DenA aus einer Kernfraktion sowie einer dynamischen zytoplasmatischen Subpopulation besteht. Zudem wird (A) das Zusammenspiel zwischen DenA und CSN im Kern untersucht und (B) die bisher unbekannte Phosphatase DipA, welche an der Regulation des zytoplasmatischen DenA und an der Zelldifferenzierung beteiligt ist, charakterisiert.

(A) Eine erhöhte DenA Konzentration kann teilweise das Fehlen eines aktiven CSN kompensieren, indem es der Akkumulation an neddylierten Proteinen und damit CSN assoziierten Entwicklungsstörungen entgegenwirkt. Beide pilzlichen Deneddylasen haben somit unterschiedliche aber auch überlappende Funktionen. Zusätzlich zeigt sich, dass die DenA Kernfraktion, welche mit dem CSN interagiert, in der pilzlichen Entwicklung durch fünf benachbarte CSN Untereinheiten destabilisiert wird. Da diese Untereinheiten eine funktionelle Oberfläche bilden ist anzunehmen, dass die Interaktion von DenA mit dieser Oberfläche wichtig für die Stabilitätskontrolle der DenA Kernsubpopulation ist.

(B) Zytoplasmatisches DenA wird zusammen mit DipA transportiert und akkumuliert an den Septen. Fehlt DipA erhöht sich die DenA Stabilität. Somit spielt DipA eine wichtige Rolle in der zytoplasmatischen DenA Stabilitätskontrolle. Zusätzlich führt das Fehlen von DipA zu einer erhöhten Septenbildung und Defekten in der lichtabhängigen Zellentwicklung des Pilzes. DipA wird somit, neben der DenA Stabilitätskontrolle, für die Zelldifferenzierung benötigt.

Die Stabilität der zwei DenA Subpopulationen wird zusätzlich durch Phosphorylierung reguliert. Während vegetativen Bedingungen wird DenA durch die Phosphorylierung von S243 und S245 stabilisiert, was für die Initiierung der nachfolgenden asexuellen Entwicklung wichtig ist. Anschließend wird DenA durch eine Änderung des Phosphorylierungsmusters destabilisiert und abgebaut. Zusammenfassend zeigt diese Studie Einblicke in komplexe Mechanismen des DenA Proteinabbaus, welche womöglich auch in höheren Eukaryoten relevant sind.

1 Introduction

1.1 Posttranslational protein modifications (PTMs)

All living organisms must constantly monitor their internal and external environment to sense signals for growth, development and reproduction. Transcription of new mRNAs, alternative RNA splicing and translation of new proteins create a continuously fine-tuned regulatory network to adapt to environmental alterations. A major mechanism to directly respond to changing circumstances without expanding the size of the genome or varying the cellular gene expression is represented by posttranslational protein modifications (PTMs). PTMs increase the functional diversity of protein variants by adding chemical groups or other proteins to one or more of its amino acid residues. Often, multiple residues are modified on the same protein. This may happen through the same type of modification on various sites as well as through different types of modifications on multiple, or overlapping sites (Prabakaran *et al*, 2012). Multiple PTMs lead to an exponential increase of potential molecular states. These modifications alter protein surfaces, lead to differences in the interaction with other proteins and can affect stability, activity or localization of targeted substrates (Mann & Jensen, 2003; Duan & Walther, 2015). PTMs control a wide range of cellular pathways including development, cell-cycle control, DNA repair, cell growth and signaling (Seo & Lee, 2004; Deribe *et al*, 2010; Chung & Dellaire, 2015). They can vary in a temporal and spatial manner depending on the respective environmental condition. Defects in posttranslational protein modifications have been linked to a variety of diseases and developmental disorders demonstrating the importance of PTMs in maintaining normal cell viability (Karve & Cheema, 2011).

More than 200 kinds of PTMs are known to modify eukaryotic proteins (Walsh & Jefferis, 2006). Several were discovered years ago and their broader significance has emerged only slowly. Some PTMs such as glycosylation, lipidation and disulfide bridge formation are stable and have essential roles in maturation and proper folding of newly synthesized proteins. Others, including phosphorylation, sumoylation, ubiquitination and neddylation are reversible and are important for intracellular signaling (Figure 1) (Deribe *et al*, 2010; Wang *et al*, 2014). These flexible PTMs are controlled by forward and reverse enzymes, which create a

dynamically regulated network. Analyses of these modifications and participating enzymes are challenging due to their transient occurrence, but they provide indispensable insights into biological functions of proteins and increase the possibilities to develop therapeutic proteins (Walsh & Jefferis, 2006; Pratt *et al.*, 2015).

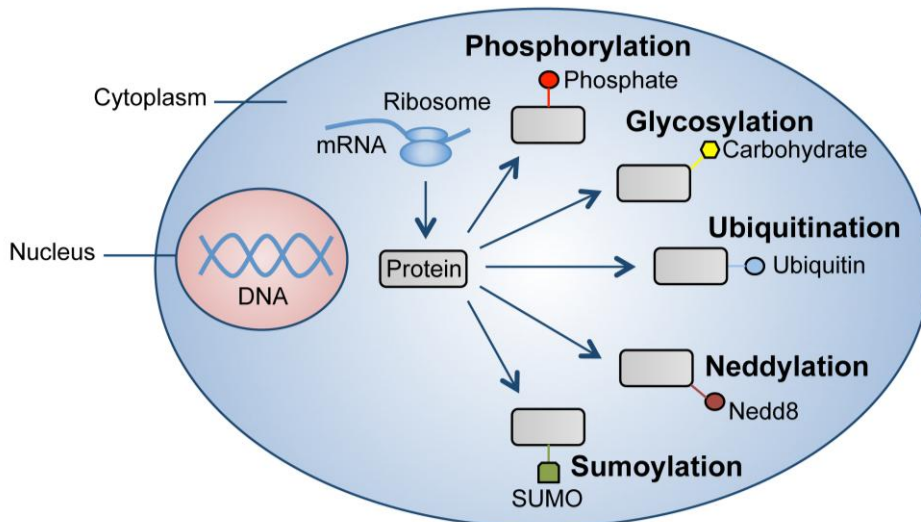


Figure 1: Posttranslational modifications of proteins.

After protein synthesis, posttranslational modifications (PTMs) increase the diversity of the cellular proteome without altering the transcriptome. The attachment of functional groups or proteins can change the function of targeted substrates. PTMs include phosphorylation, glycosylation, ubiquitination, neddylation, as well as sumoylation and can affect the stability, activity, interaction or localization of the modified target protein.

1.1.1 Phosphorylation and dephosphorylation

Phosphorylation was one of the first posttranslational modifications described (Fischer & Krebs, 1955). Phosphorylation of cellular proteins is a dynamic process that depends on the activity of protein kinases and protein phosphatases (Hunter, 1995). A kinase catalyzes the transfer of γ -phosphate from ATP to its protein substrate, whereas a phosphatase removes the phosphate by hydrolysis (Figure 2). Although kinase encoding genes constitute 2% of eukaryotic genomes, they phosphorylate more than 30% of all cellular proteins (Ubersax & Ferrell, 2007). Since kinases and phosphatases have severe impacts on their substrates, the recognition and interaction with the target protein has to be precisely regulated and the protein modification must be strictly controlled in a specific temporal order

(Rogers *et al*, 2015). Kinases and phosphatases can either identify their substrates by a specific consensus sequence of the phosphorylation site in the substrate or by interaction motifs spatially separated from the modified residue. Additional levels of substrate specificity are provided by the amino acid composition of the respective catalytic core and the co-localization of kinases/phosphatases with their particular substrates in the same cellular compartment (Ubersax & Ferrell, 2007; Cheng *et al*, 2011). The addition of a phosphate group occurs in eukaryotes primarily on the amino acid residues of serine, threonine and tyrosine, which adds two negative charges to the substrate. This can lead to conformational changes affecting the biological function of the protein (Nishi *et al*, 2011; Duan & Walther, 2015).

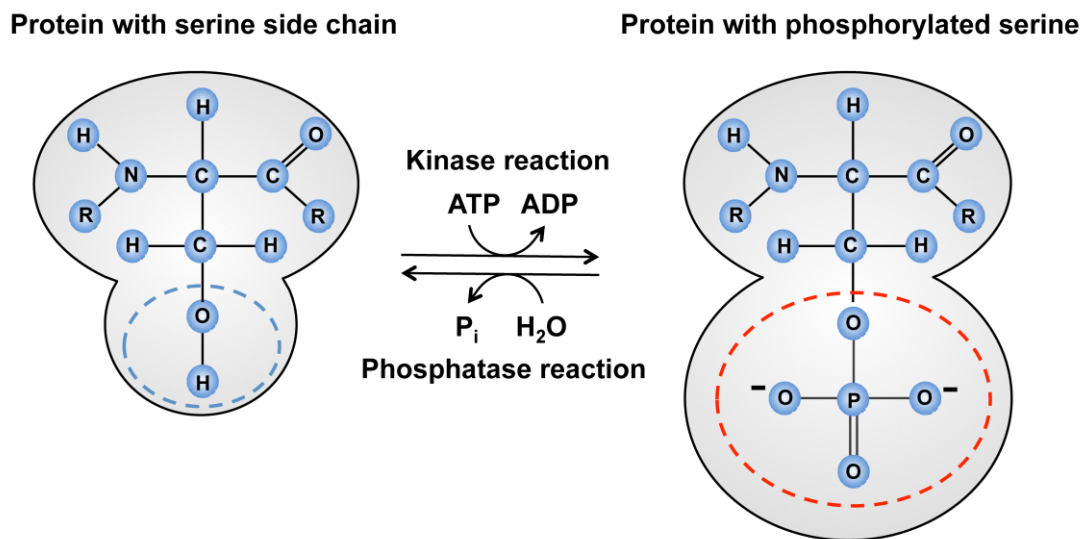


Figure 2: Mechanism of phosphorylation and dephosphorylation of proteins.

Proteins can be phosphorylated on serine/threonine side chains (dashed blue circle) by serine/threonine specific kinases and dephosphorylated by serine/threonine phosphatases. The reaction involves ATP as the phosphate donor in the phosphorylation reaction and water to hydrolyze the phosphate group (dashed red circle) in the dephosphorylation reaction. This results in a changed structure, activity or stability of the substrate (illustrated in a simplified form as a change of the grey periphery).

Due to different amino acids that can be modified by a phosphate group, two major families of kinases and phosphatases exist. One group is specific for tyrosine side chains and another one targets serine/threonine residues. Phosphorylation and dephosphorylation of tyrosines play an important role in signal transduction whereas serine/threonine alterations have a central role in mitosis and cytokinesis (Stoker,

2005; Barr *et al*, 2011). Around 98% of reversibly protein-bound phosphate in eukaryotic cells affects serine/threonine residues (Olsen *et al*, 2006). Serine/threonine phosphatases can be divided into the family of phosphatases metallo-dependent (PPM) and the phospho-protein phosphatases (PPPs). Both types of enzymes contain a conserved domain with an active site consisting of two metal ions, such as manganese (Mn^{2+}) and iron (Fe^{2+}), which are surrounded by a set of conserved amino acid residues (Shi, 2009). These bound metal ions are crucial to coordinate the phosphorus of the substrate and to stabilize its negative charge, thus facilitating nucleophilic attack on the phosphate group by a water molecule and hydrolysis of the phosphate ester bond (Goldberg *et al*, 1995; Barr *et al*, 2011).

1.2 The family of ubiquitin and ubiquitin-like proteins

1.2.1 Ubiquitin

In contrast to phosphorylation, the process of ubiquitination is a posttranslational modification by which a small protein is attached to a substrate. Ubiquitin was initially discovered in the mid 1970s as a ubiquitous protein with lymphocyte differentiating properties (Goldstein *et al*, 1975). Research on ATP-dependent proteolysis revealed that the heat-stable polypeptide APF1 (ATP-dependent proteolysis factor 1) covalently binds to other proteins, which is required for protein breakdown (Ciechanover *et al*, 1980; Hershko *et al*, 1980; Ciechanover, 2015). Subsequent studies revealed that APF1 is identical to the previously described ubiquitin (Wilkinson *et al*, 1980). In 2004 Aaron Ciechanover, Avram Hershko and Irwin Rose were honored with the Nobel Price in chemistry for their discovery of ubiquitin-dependent protein degradation.

Ubiquitin is conserved in all eukaryotic cells and consists of 76 amino acids. The binding of ubiquitin to a substrate affects a plethora of cellular processes. Ubiquitination can target a modified substrate for degradation, regulate cellular localization, activate and inactivate proteins, change protein-protein interactions and it is involved in DNA double strand break repair (Hershko & Ciechanover, 1992; Schnell & Hicke, 2003; Mukhopadhyay & Riezman, 2007; Brown & Jackson, 2015). Ubiquitin proteins are encoded and expressed as multimeric head-to-tail repeats (Ozkaynak *et al*, 1987). An isopeptidase recognizes and hydrolyzes these isoforms

resulting in monomeric ubiquitin exposing a C-terminally di-glycine motif (GG) located at position glycine75 and glycine76 (Reyes-Turcu *et al*, 2006; 2008; Grou *et al*, 2015). Single ubiquitin molecules are attached to substrates by an ATP-dependent enzyme cascade consisting of an E1 activating enzyme, E2 conjugating enzyme and E3 ligating enzyme (Hershko & Ciechanover, 1992; Kerscher *et al*, 2006). A single ubiquitin molecule is linked to its substrate through an isopeptide bond between G76 and a lysine (K) residue of the target protein.

The impact of ubiquitin on its substrate depends on the type of ubiquitination. The attachment of an ubiquitin monomer, monoubiquitination, or modification of several lysine residues with numerous ubiquitin molecules within a substrate protein, multiubiquitination, are involved in endocytosis, DNA repair and transcription (Hicke, 2001; Miranda & Sorkin, 2007; Brown & Jackson, 2015). The seven lysine residues in ubiquitin (K6, K11, K27, K29, K33, K48, and K63) can form polyubiquitin chains (Spasser & Brik, 2012; Lee & Diehl, 2014). Polyubiquitin chains are created by the formation of an isopeptide bond between a specific lysine residue from the preceding ubiquitin molecule to the C-terminal glycine residue of the next ubiquitin molecule. These chains can have different conformations depending on the involved lysine residues, resulting in a variety of cellular effects. The most abundant types of ubiquitin chains are linked via the internal K48 or K63. A chain emerging on K48 has a closed conformation, whereas ubiquitin molecules connected via K63 display an extended conformation (Varadan *et al*, 2004; 2005). Site-directed mutagenesis experiments revealed that ubiquitin chain formation on K48 targets the substrate for degradation (Butt *et al*, 1988; Finley *et al*, 1994; Ciechanover, 1994). Using competitor ubiquitin chains of different lengths demonstrated that at least four molecules are required for recognition by the 26S proteasome, which represents the cellular protein degradation machinery (Thrower *et al*, 2000). In contrast, ubiquitin chains linked via K63 are involved in membrane trafficking, stress response, DNA repair and translation (Arnason & Ellison, 1994; Pickart & Fushman, 2004; Li & Ye, 2008; Brown & Jackson, 2015). In addition to conjugation, the ubiquitination status of a protein is also regulated by ubiquitin cleavage. The isopeptidases responsible for removal of ubiquitin from the substrate are called deubiquitinases (DUBs). These enzymes play important roles as potential drug targets in various diseases including cancer and neurodegeneration (Millard & Wood, 2006; Komander *et al*, 2009; Pfoh *et al*, 2015).

1.2.2 The ubiquitin-like protein Nedd8

Proteins with similarities to ubiquitin regarding sequence homology and especial structural properties are summarized as ubiquitin-like proteins (UBLs) (Hochstrasser, 2009; van der Veen & Ploegh, 2012). More than ten UBLs have been identified and the focus of current research is most dominantly on Nedd8 (neural precursor cell expressed, developmentally downregulated 8), SUMO (small ubi^ubi^uti^un-related modifier), FAT10 (human leukocyte antigen F-associated 10), ISG15 (interferon-stimulated gene 15), ATG8 (autophagy-related protein 8) and ATG12 (Streich & Lima, 2014). The attachment of UBLs to substrates affects enzymatic activity, subcellular localization or regulates protein interactions (Herrmann *et al*, 2007; van der Veen & Ploegh, 2012). As a consequence, UBLs generate extensive interest as therapeutic targets (Marsh, 2015).

Among all ubiquitin-like proteins, Nedd8 is most identical to ubiquitin with 60% amino acid and high structural identity (Figure 3). It consists of 81 amino acids, including a lysine residue at position K48 (Kumar *et al*, 1993; Jones *et al*, 2008). Nedd8 was detected in several organisms and is essential in most model systems such as *Arabidopsis thaliana*, *Schizosaccharomyces pombe*, *Drosophila melanogaster*, *Caenorhabditis elegans*, mice and the filamentous fungus *Aspergillus nidulans* (Rabut & Peter, 2008; von Zeska Kress *et al*, 2012). In contrast, deletion of the Nedd8 encoding gene in *Saccharomyces cerevisiae* results in viable cells (Liakopoulos *et al*, 1998; Lammer *et al*, 1998).

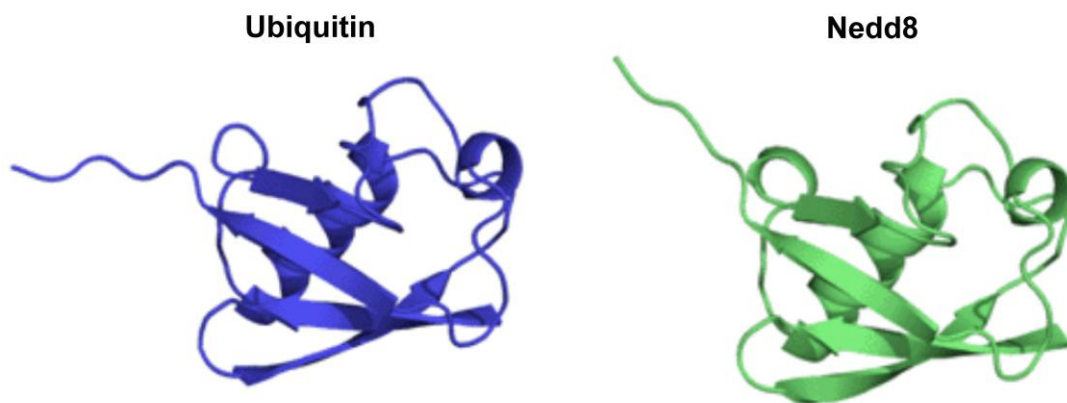


Figure 3: Structures of ubiquitin and the ubiquitin-like protein Nedd8.

Ribbon diagrams of ubiquitin and Nedd8. Both posttranslational modifiers share high structural similarities. Modified from (Ha & Kim, 2008).

Similar to ubiquitin, Nedd8 translation results in a non-conjugatable precursor with an extended C-terminus. C-terminal hydrolases process the precursor in order to generate the mature Nedd8 isoform with an exposed di-glycine motif at position G75 and G76 (Figure 4). It has been shown that several enzymes catalyze the maturation of Nedd8. Among them is the mammalian UCH-L3 (ubiquitin C-terminal hydrolase L3) which also possesses activity towards ubiquitin precursors (Wada *et al*, 1998; Frickel *et al*, 2007). In addition, the corresponding ortholog YUH1 (yeast ubiquitin hydrolase 1) of budding yeast as well as the Nedd8 specific ubiquitin like protease 1 (ULP1) family protein DEN1 are capable of processing Nedd8 to expose G76 required for conjugation (Linghu *et al*, 2002; Gan-Erdene *et al*, 2003; Wu *et al*, 2003; Mendoza *et al*, 2003). The mature Nedd8 variant is subsequently activated and ligated in a similar ATP-dependent enzymatic cascade as ubiquitin.

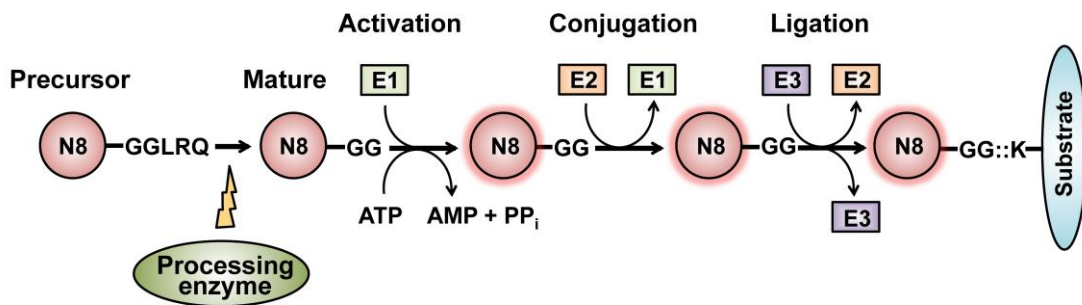


Figure 4: Nedd8 maturation and its ligation cascade.

Neddylation is a posttranslational protein modification by which the ubiquitin-like protein Nedd8 (N8) is covalently bound to a substrate. The precursor of N8 is enzymatically processed to expose the C-terminal di-glycine motif (GG). Mature N8 is activated by E1 in an energy consuming process, conjugated to E2 and the final ligation to a lysine residue (K) of the target protein is facilitated by E3. According to (Enchev *et al*, 2015).

The mammalian E1 heterodimer consisting of APPBP1 and UBA3 activates mature Nedd8 in an ATP-consuming reaction (Huang *et al*, 2004; Schulman & Harper, 2009). Amino acid substitution revealed that a single conserved arginine in APPBP1-UBA3 acts as a selectivity gate, preventing misactivation of the structural similar ubiquitin (Walden *et al*, 2003). Activated Nedd8 is transferred to the conjugating E2 enzyme UBC12 (Huang *et al*, 2005a; 2007). The final conjugation step of Nedd8 from the E2 to the substrate is often facilitated by an E3 ligase (Streich & Lima, 2014). E3s have at least two domains of which one recruits the E2 and the

other binds the substrate (Morimoto *et al*, 2003; Kurz *et al*, 2008). Similar to ubiquitin, Nedd8 is conjugated to its target protein (neddylation) by a covalent linkage between its C-terminally located G76 and a lysine (K) of the substrate. Whereas ubiquitination regulates a vast amount of proteins, only a limited number of neddylated substrates have been described to date (Welchman *et al*, 2005; Mergner *et al*, 2015; Enchev *et al*, 2015). The best studied substrates modified with Nedd8 are E3 ubiquitin cullin-RING ligases (CRLs) representing an essential component of ubiquitin mediated protein degradation (Petroski & Deshaies, 2005; Deshaies & Joazeiro, 2009; Vittal *et al*, 2015).

1.3 Destruction of proteins

1.3.1 Protein degradation by the ubiquitin-proteasome system (UPS)

Proteins are continuously synthesized and degraded by the cell to respond to changing environmental conditions and to assure maintenance of cellular processes. The appropriate protein degradation pathway depends on the substrates origin. Foreign dietary proteins are digested in the lumen of the gastrointestinal tract. They are degraded to non-antigenic amino acids that can be absorbed and reused for synthesis of endogenous proteins (Erickson & Kim, 1990). The ubiquitin-proteasome system (UPS) represents a protein degradation pathway, which is essential for the destruction of the majority of intracellular proteins (Ciechanover, 1994; Rock *et al*, 1994; Glickman & Ciechanover, 2002). Among them are misfolded and damaged proteins as well as transcription factors and time-limited cell cycle proteins (Piva *et al*, 1999; Vlachostergios *et al*, 2012). Therefore, the UPS plays an important role in a plethora of cellular processes, including cell cycle control, signal transduction, development immune response and coordination of DNA repair response (Ciechanover *et al*, 2000; Chung & Dellaire, 2015). Considering the importance of these numerous processes, it is crucial that protein degradation by the UPS is highly specific and precisely regulated. Misregulation is associated to a variety of diseases, including cancer and neurodegenerative defects such as Alzheimer's and Parkinson's disease (Glickman & Ciechanover, 2002; Reinstein & Ciechanover, 2006; Carlucci & D'Angiolella, 2015).

Ubiquitin and Nedd8 represent two posttranslational modifiers that do not only share similar structural properties but are also involved in protein degradation regulated by the UPS. The activated Nedd8 is attached to a lysine residue of an ubiquitin ligase. This neddylation process stabilizes and activates the ligase which mediates the transfer of ubiquitin to a bound substrate (Saha & Deshaies, 2008). Repeating cycles of ubiquitination generates a polyubiquitin chain attached to the target protein (Figure 5). The ubiquitinated substrate is recognized by the 26S proteasome (Thrower *et al*, 2000). This multisubunit protein complex degrades ubiquitinated proteins to small peptides and amino acids that can be reused for protein synthesis whereas the attached ubiquitin molecules are recycled and re-enter the ubiquitination cycle (Verma *et al*, 2002; Glickman & Ciechanover, 2002; Lu *et al*, 2015).

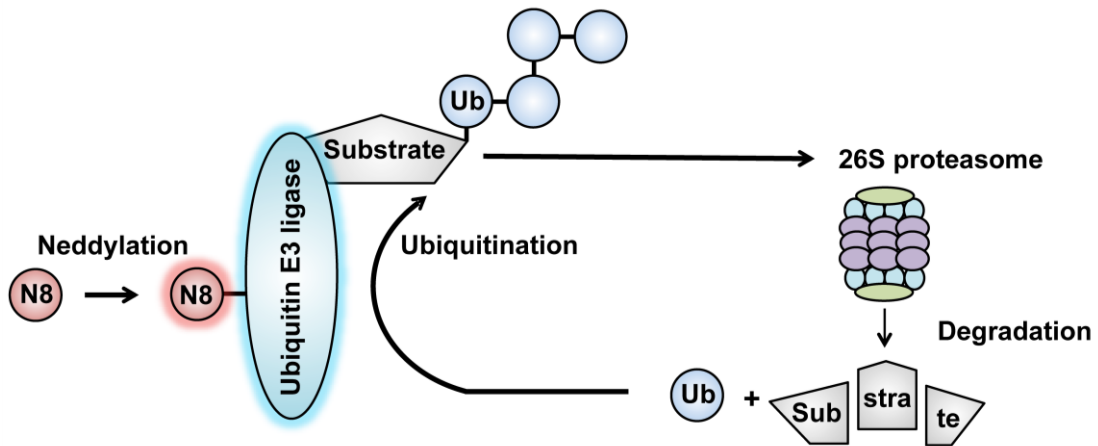


Figure 5: Protein degradation by the ubiquitin-proteasome system.

The covalent attachment of Nedd8 (N8) activates ubiquitin E3 ligases, which mediate the transfer of ubiquitin (Ub) to substrate proteins. Repeated rounds of ubiquitination create a polyubiquitin chain that labels the substrate for degradation. Ubiquitinated proteins are recognized by the 26S proteasome, which degrades the substrate and recycles ubiquitin. According to (Deshaies & Joazeiro, 2009; Lu *et al*, 2015).

1.4 E3 ubiquitin ligases

E3 ubiquitin ligases determine specificity of substrate ubiquitination and degradation by the 26S proteasome. Two types of E3s, either defined by a HECT domain (homologous to the E6-AP carboxyl terminus) or a RING motif (really interesting new gene), are present in eukaryotes (Pickart, 2001; Metzger *et al*, 2012; Vittal *et al*, 2015). The main difference between both classes is the transfer of ubiquitin to the substrate. In contrast to HECT E3s, E3 ligases with a RING motif do

not form a catalytic intermediate with ubiquitin (Schwarz *et al*, 1998; Lorick *et al*, 1999; Kerscher *et al*, 2006). RING E3s bind the ubiquitin-linked E2 and the substrate protein simultaneously. They promote the transfer of ubiquitin to the bound substrate by bringing them in proximity so that ubiquitin is transferred from E2 to the substrate (Duda *et al*, 2008; Deshaies & Joazeiro, 2009). The most intensively studied ubiquitin E3 ligase family is represented by cullin-RING ligases (Hua & Vierstra, 2011; Genschik *et al*, 2013). CRLs are multi-protein complexes with a central cullin which serves as a scaffold to mediate substrate binding and ubiquitin transfer. In mammals seven cullins (CUL1-CUL7) and the closely related p53-associated parkin-like cytoplasmatic protein (PARC) are known to be modified with Nedd8 (Sarikas *et al*, 2011). In addition to the cullin backbone, CRLs consist of an adapter that links a substrate binding protein to the cullin and a RING module that recruits E2-ubiquitin.

The prototypical CRL is referred to as the SCF (Skp1/CUL1/F-Box) ligase (Figure 6). SCFs consist of a cullin backbone and a C-terminally located Rbx1 (RING box protein 1), which harbors the characteristic RING motif. At the N-terminus a substrate recognition unit is attached that consists of the adaptor protein Skp1 (S-phase kinase associated protein 1) and an F-Box protein (Schulman *et al*, 2000; Lee & Diehl, 2014). F-Box proteins deliver the appropriate substrates to the SCFs and play a crucial role in determining specific degradation of proteins. They contain an F-Box motif and a variable protein-interaction domain that binds selectively the substrate which will be labeled for degradation (Skowyra *et al*, 1997; Kipreos & Pagano, 2000; Randle & Laman, 2015). To assure specific substrate degradation of a wide range of intracellular proteins around 70 F-Box encoding genes are present in humans whereas in *A. thaliana* around 700 F-Box domain containing proteins are described (Gagne *et al*, 2002; Jin *et al*, 2004).

1.5 Regulation of cullin-RING ligases (CRLs)

1.5.1 Neddylation as a prerequisite for cullin-RING ligase activity

CRLs target a variety of oncoproteins, transcription factors, cell cycle specific cyclins, cyclin-dependent kinase inhibitors and other regulatory proteins for degradation by mediating ubiquitination. Repeating cycles of activation and

inhibition control the function of CRLs. The covalent attachment of Nedd8 to a conserved lysine residue of the cullin is essential for the function of CRLs. Neddylation enhances ubiquitination activity and stabilizes the E3 complex (Saha & Deshaies, 2008; Bornstein & Grossman, 2015). Nedd8 stimulates the transfer of ubiquitin to the substrate by an increase of E2-Ub recruitment and conformational change of the E3 ligase complex (Figure 6). The attachment of Nedd8 to the cullin orients ubiquitin in close proximity to the bound substrate and thus facilitates ubiquitination (Kawakami *et al*, 2001; Duda *et al*, 2008; Merlet *et al*, 2009).

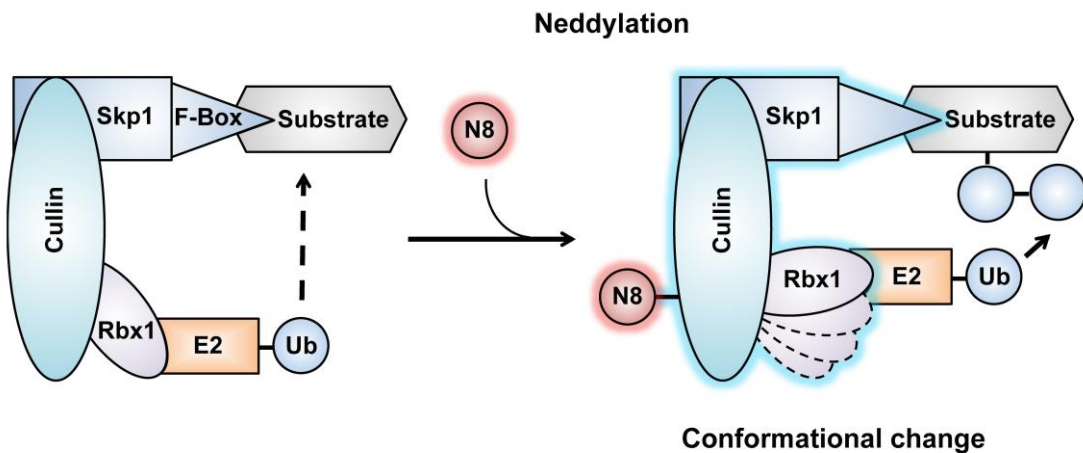


Figure 6: Attachment of Nedd8 promotes CRL activity.

The SCF ligase is composed of a cullin scaffold with a C-terminally attached Rbx1. The adaptor Skp1 and the substrate recognizing F-Box protein are N-terminally bound. Activated Nedd8 (N8) binds covalently to cullin and induces a conformational change of Rbx1. This flexibility brings E2-ubiquitin in proximity to the bound substrate resulting in the transfer of ubiquitin (Ub). According to (Duda *et al*, 2008; Merlet *et al*, 2009).

Deactivation of CRLs is achieved by removal of Nedd8. Deneddylation of cullins results in disassembly of the CRL complex. The substrate recognition unit consisting of Skp1 and F-Box protein dissociates and allows rearrangement of CRL composition. Since F-Box proteins determine substrate specificity, repeating cycles of neddylation and deneddylation assure binding of new F-Box proteins and as a consequence degradation of new subsets of target proteins (Deshaies & Joazeiro, 2009; Hua & Vierstra, 2011; Mergner & Schwechheimer, 2014). Two proteins are described in eukaryotes that hydrolyze cullin-Nedd8 conjugates, namely the deneddylases COP9 (constitutive photomorphogenesis 9) signalosome and DEN1 (deneddylase 1).

1.5.2 The deneddylase COP9 signalosome (CSN)

The deneddylase COP9 signalosome (CSN) was initially discovered in *A. thaliana* where it is a component of a large light-signaling complex. In plants it is required for the repression of photomorphogenic seedling development in the dark (Wei *et al*, 1994). The main function of the CSN complex is to regulate the activity of SCF complexes by deneddylation (Chapter 1.5.3). Through the regulatory function of CSN in ubiquitin-dependent protein degradation it is involved in complex cellular processes such as transcription, DNA repair and cell development (Chamovitz, 2009; Beckmann *et al*, 2015; Meir *et al*, 2015). The CSN is conserved from fungi to human and consists of up to eight subunits termed CSN1 through CSN8, according to their descending number of molecular weights (Figure 7).

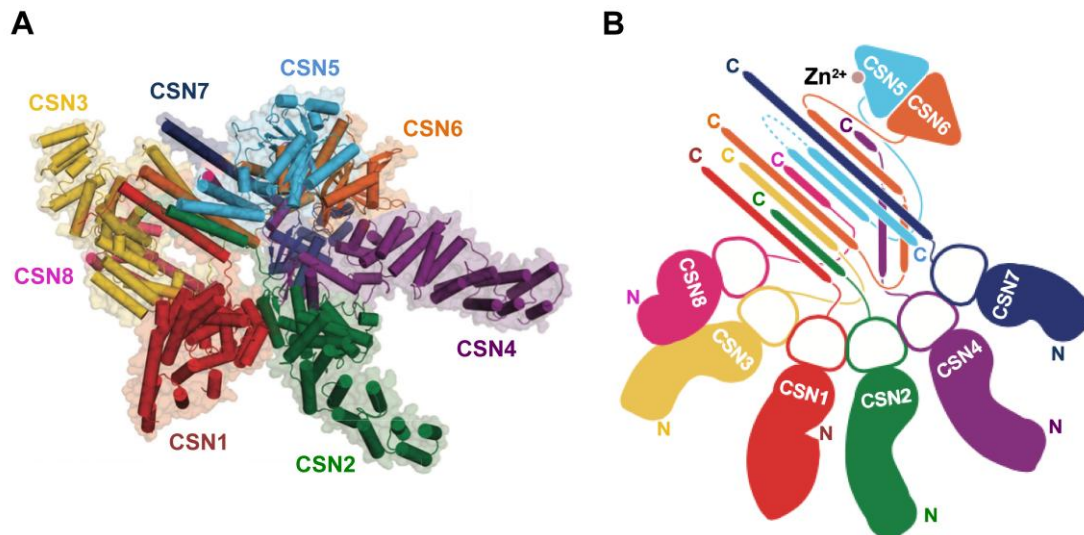


Figure 7: Subunit composition of the COP9 signalosome deneddylase.

(A) Cartoon representation of all eight CSN subunits assembled in a CSN holocomplex. Domain boundaries are indicated. (B) A flattened schematic representation of the three-dimensional structure of CSN. Six PCI domain containing subunits form an open ring and all eight subunits are connected by a bundle of α -helices. A heterodimer formed by the MPN domains of CSN5 and CSN6 is located on the helical bundle. Modified from (Lingaraju *et al*, 2014).

The CSN complex shares similarities regarding structure and subunit composition with the LID of the 26S proteasome and with the eukaryotic translation initiation factor 3 (eIF3), suggesting they derived from a common ancestor (Kapelari *et al*, 2000; Enchev *et al*, 2010; Meister *et al*, 2015). Each of them possesses six subunits with a PCI domain (proteasome-LID, CSN, eIF3) and two subunits with an MPN domain (Mpr1p and Pad1p N-terminal) (Glickman *et al*, 1998; Hinnebusch,

2006; Pick & Pintard, 2009). The six PCI domain proteins of human CSN form a horseshoe-like ring, the MPN containing proteins create a stable dimer and all eight subunits are connected by a bundle of C-terminal α -helices (Lingaraju *et al*, 2014). The PCI domains are thought to be important for protein-protein interactions and thereby for assembly of the eight subunit CSN complex, but also for the interaction with CSN associated proteins (Scheel & Hofmann, 2005; Hu *et al*, 2015).

Beside its primary function of deneddylation, CSN acts as an assembly platform recruiting a variety of proteins involved in protein modification such as ubiquitination and phosphorylation. Several CSN associated proteins are phosphorylated in a CSN mediated kinase reaction, resulting in a changed stability of the modified substrate (Uhle *et al*, 2003; Wu *et al*, 2006; Huang *et al*, 2009; Yoshida *et al*, 2013).

1.5.3 Deneddylation of CRLs by the COP9 signalosome

The only known intrinsic enzymatic function of the COP9 signalosome is represented by its MPN isopeptidase activity towards cullins modified with Nedd8 (Lyapina *et al*, 2001). The catalytic active subunit is CSN5 with a zinc ion in its active center. CSN5 is the last subunit, which assembles to the seven subunit pre-CSN complex (Cope *et al*, 2002; Beckmann *et al*, 2015). Only when CSN5 is incorporated, the CSN is active (Beckmann *et al*, 2015). Binding of CSN to neddylated CRLs is sensed by CSN4, and communicated to CSN5 with the assistance of CSN6, which results in activation of the deneddylase (Lingaraju *et al*, 2014). All eight CSN subunits are necessary for the holocomplex to acquire enzymatic activity. Loss of one subunit leads to impairment of the entire active complex causing accumulation of neddylated substrates, primarily represented by cullins (Serino & Deng, 2003; Sharon *et al*, 2009; Pick *et al*, 2012; Beckmann *et al*, 2015).

Cullin-RING ligases modified with Nedd8 are more active than their deneddylated variants (Saha & Deshaies, 2008) and CSN inhibits the ubiquitination activity of CRLs *in vitro* (Zhou *et al*, 2003). Based on these results, it was expected that CRLs are constitutively active in CSN mutants. Paradoxically, reduced CSN activity attenuated rather than enhanced CRL function *in vivo* suggesting that CSN is required for the activation of CRLs (Liu *et al*, 2003; Doronkin *et al*, 2003; Pintard *et*

et al., 2003). This so-called CSN paradox was solved by the observation that CSN's inhibitory enzymatic activities demonstrated *in vitro* prevent the autocatalytic degradation of CRL substrate adaptors *in vivo*, thus promoting CRL activity (Schmidt *et al.*, 2009; Dubiel, 2009). This is in agreement with the discovery that in humans and in *S. pombe* the deubiquitinating enzyme USP15/Ubp12 interacts with CSN to prevent ubiquitination of CRL components (Zhou *et al.*, 2003; Hetfeld *et al.*, 2005). It is hypothesized that CSN mediated CRL inhibition is a prerequisite for the proper assembly and maintenance of active ubiquitin ligase complexes. Structural and biochemical analyses revealed that CSN binds both SCF functional sites, the catalytic Rbx1-CUL1 C-terminal domain as well as the N-terminal substrate receptor. This demonstrates that CSN binding prevents SCF interactions with Ub-E2 and an ubiquitination substrate (Enchev *et al.*, 2012). Cycles of neddylation and deneddylation as well as the abundance of adaptor modules are critical for CRLs to exert their enzymatic activity (Figure 8) (Wolf *et al.*, 2003; Wee *et al.*, 2005; Cope & Deshaies, 2006; Bennett *et al.*, 2010).

Another factor that affects CRL activity is the cullin-associated Nedd8-dissociated protein 1 (CAND1). CAND1 wraps around deneddylated cullins and interacts with both, the N-terminus, where it competes with the substrate adaptor for binding, and the C-terminus, where it blocks the neddylation site of cullin (Figure 8) (Liu *et al.*, 2002; Goldenberg *et al.*, 2004). Binding of CAND1 triggers the exchange of the substrate-specific receptor. CAND1 does not inactivate CRLs, but instead ensures the formation of a new subset of CRL complexes by mediating substrate adaptor exchange (Cope & Deshaies, 2003; Goldenberg *et al.*, 2004; Pierce *et al.*, 2013; Wang & Martin, 2015). CAND1 promotes the assembly of new F-Box containing cullin-RING ligases and controls the recruitment of less abundant substrates (Dubiel, 2009; Schmidt *et al.*, 2009; Lydeard *et al.*, 2013; Wu *et al.*, 2013).

1.5.4 The deneddylase 1 (DEN1)

The second known enzyme with deneddylating activity is the deneddylase 1 (DEN1). In contrast to CSN, DEN1 is a single protein and belongs to the ubiquitin-like-specific protease 1 (ULP1) family of cysteine proteases with a conserved catalytic triad consisting of the amino acids histidine, aspartate and cysteine. DEN1 is thought to have a different substrate specificity when compared to CSN. Whereas the

main substrate of the CSN is represented by mononeddylated cullins, it was suggested that DEN1 acts primarily on non-cullin proteins (Chan *et al*, 2008; Christmann *et al*, 2013; Enchev *et al*, 2015; Mergner *et al*, 2015). However, *in vitro* studies revealed that DEN1 can act towards neddylated cullins in a concentration-dependent manner (Wu *et al*, 2003; Zhou & Watts, 2005). Low concentrated human DEN1 deconjugates cullins modified with several Nedd8 molecules to yield a mononeddylated form. Elevated concentrations of DEN1 are capable to catalyze the complete removal of Nedd8 from cullins. In contrast, CSN did not efficiently cleave multineddylated cullins, suggesting that they are not the main substrates for this deneddylase (Wu *et al*, 2003). Among the postulated non-cullin proteins that represent DEN1 specific substrates are ribosomal proteins and transcription factors. DEN1 seems to regulate Nedd8-based signaling in response to cellular stresses (Enchev *et al*, 2015). In addition to the deconjugation process of Nedd8, it was shown that mammalian DEN1 is capable of processing the precursor of Nedd8 to achieve the conjugatable mature Nedd8 variant with the exposed di-glycine motif (Figure 8), (Wu *et al*, 2003). Therefore, DEN1 might represent a dual functional protease acting on Nedd8 maturation and deconjugation. DEN1 activity is highly specific towards neddylated substrates as neither ubiquitin nor SUMO conjugates are cleaved (Gan-Erdene *et al*, 2003; Mendoza *et al*, 2003). A single-residue difference in the C-terminus of Nedd8 (Ala72) and ubiquitin (Arg72) contributes to the ability of DEN1 to discriminate between them (Shen *et al*, 2005; Shin *et al*, 2011).

DEN1 was initially discovered in mammalian cells (Wu *et al*, 2003; Gan-Erdene *et al*, 2003; Mendoza *et al*, 2003), but subsequent studies found homologs in fungi, plants and insects, demonstrating that DEN1 is highly conserved throughout evolution (Christmann *et al*, 2013; Mergner *et al*, 2015; Kim *et al*, 2015). Two DEN1 related sequences were identified in *S. pombe*. The respective proteins Nep1 and Nep2 showed deneddylation activity against cullins *in vitro* and Nep1 was co-purified with CSN5 (Zhou & Watts, 2005). In mammalian cells it was shown that chemotherapy increases DEN1 levels with activity towards the neddylated E3 ligase MDM2 (murine double minute 2). This results in MDM2 destabilization and activation of tumor suppressor p53, suggesting a role of DEN1 in regulating apoptosis (Watson *et al*, 2010).

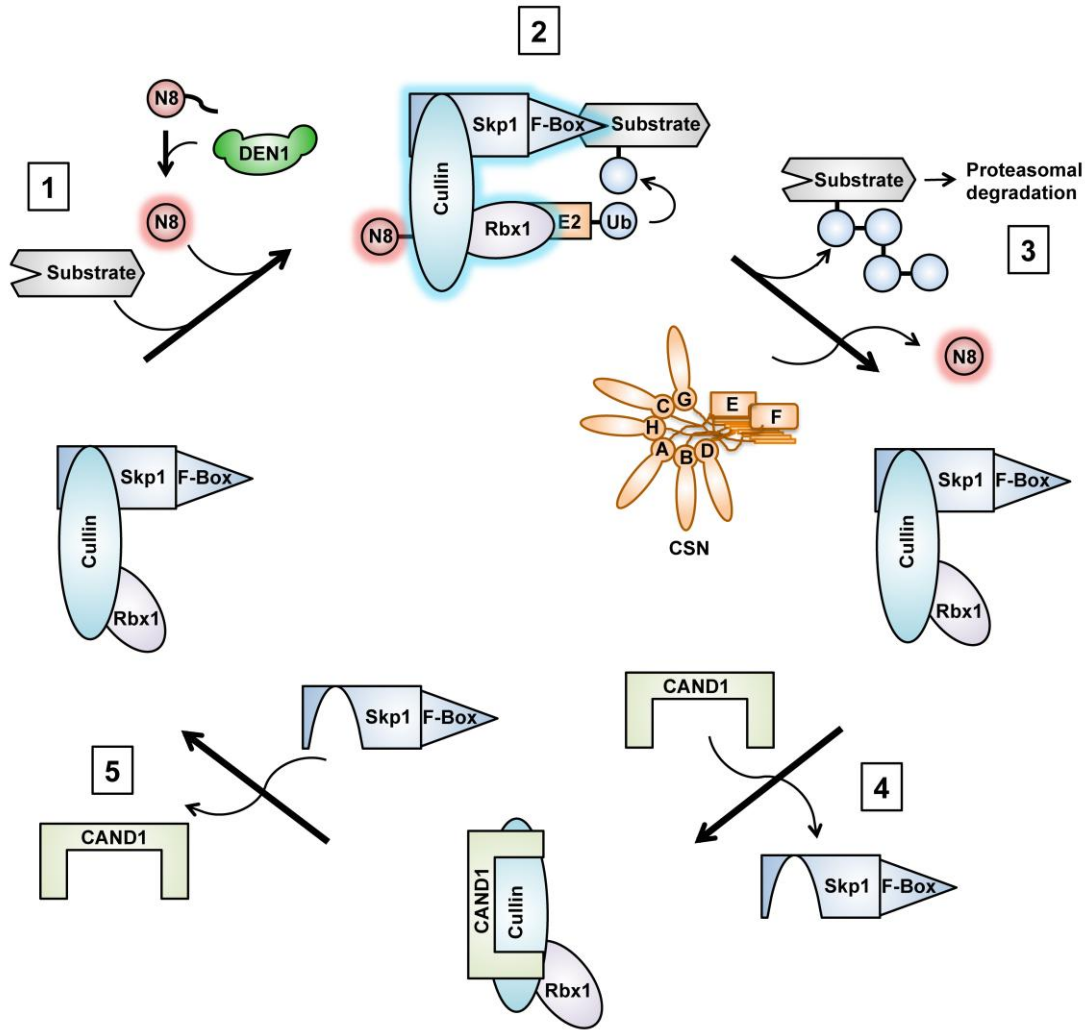


Figure 8: Regulation of CRL activity by dynamic alterations of its architecture.

(1) The cullin-RING ligase binds the protein to be degraded via its substrate recognition unit consisting of Skp1 and a respective F-Box protein. The deneddylase DEN1 processes the Nedd8 precursor, which then covalently binds the ligase resulting in its activation. (2) The activated CRL mediates ubiquitination of the bound substrate by facilitating the transfer of ubiquitin. (3) The ubiquitinated substrate is recognized and degraded by the 26S proteasome. The CSN removes Nedd8 from CRL, which then is unfavorable for E2-Ub binding but displays high affinity for CAND1. (4) Binding of CAND1 blocks the neddylation site and results in the disassembly of the substrate recognition unit. (5) Recruitment of a new substrate recognition unit results in CAND1 release. The newly assembled CRL binds a different subset of substrates, which are targeted for degradation. According to (Pierce *et al*, 2013; Lydeard *et al*, 2013).

1.6 Fungi in science

Fungi are important organisms that resemble animals more than plants and were classified in the late 1960's into the separate "Kingdom of Fungi" (Whittaker, 1969). It is estimated that 1.5 to 2 million species of fungi exist on planet earth of which only about 100.000 have been properly described. Through their adaptability to utilize nutrients, fungi perform essential roles in global ecosystems such as carbon recycling and biomass degradation. Since Alexander Fleming discovered in 1929 that *Penicillium chrysogenum* produces penicillin, several species are used to synthesize medically important antibiotics (Kawaguchi *et al*, 2013). Industrial relevant fungal species play central roles in alcohol production (*S. cerevisiae*), rice fermentation (*Aspergillus oryzae*), extraction of citric acid (*Aspergillus niger*) and enzyme production including lipases (*Aspergillus oryzae*) and cellulases (*Humicola insolens*) (Bennett, 1998). Despite the broad range of benefits, some fungal species are pathogenic to humans and plants (Dean *et al*, 2012; Scharf *et al*, 2014). Around 1.5 to 2 million people die of a fungal infection each year (Denning & Bromley, 2015). The estimated number of unknown cases might be even higher as fungal cells were found in brain sections from Alzheimer's disease patients (Pisa *et al*, 2015). The most common human pathogen is *Aspergillus fumigatus*. *A. fumigatus* causes invasive fungal infections in immunocompromised patients displaying a mortality rate of up to 90% (Latgé, 1999). Fungal plant pathogens contaminate crops, which results in a worldwide loss of agricultural yields of more than 10%, representing an enormous economic problem (Normile, 2010). Since fungal proteins are similar to mammalian proteins, several fungal species are used in laboratories to study fundamental cellular processes of eukaryotic cells. The most prominent fungal model organisms are *S. cerevisiae*, *Neurospora crassa* and species that belong to the genus *Aspergillus*.

1.6.1 The model organism *Aspergillus nidulans*

Aspergillus nidulans is a filamentous fungus that belongs to the phylum Ascomycota. Within the genus *Aspergillus*, it belongs to the few species, which are able to form sexual spores through meiosis. *A. nidulans* is homothallic, meaning beside its sexual reproduction by mating a respective partner, it is self-fertile and can fuse its own nuclei (Pöggeler *et al*, 2006; Bayram & Braus, 2012). *A. nidulans* was introduced to science in 1953 (Pontecorvo *et al*, 1953) and represents a key model

organism for genetics and cell biology. The impact of gene deletions or mutations can be observed as phenotypes due to the haploid genome. Research studies with *A. nidulans* for more than 60 years led to important progress in our understanding of metabolic regulation, cytoskeletal function, mitosis, cell cycle, development and pathogenicity (Arst & Cove, 1973; Xiang & Plamann, 2003; Osmani & Mirabito, 2004; Bayram & Braus, 2012; Sarikaya-Bayram *et al*, 2015). Its 31 Mb genome is distributed among eight chromosomes and was fully sequenced (Galagan *et al*, 2005). It encodes around 9500 genes of which around 90% are still uncharacterized (Cerqueira *et al*, 2014). *A. nidulans* has a short life cycle and an amenable and well-characterized genetic system. Findings on the molecular level can be transferred to its industrial and pathogenic relatives as well as to higher eukaryotic organisms.

1.6.1.1 Vegetative growth and septation

Life of *A. nidulans* starts with a spore that undergoes an initial period of isotropic expansion and depending on the nutritional status it already completes a nuclear division (Harris, 1999). The elongating germ tube, hypha, grows in a polarized manner by apical extension and branching to form a network of interconnected cells, known as mycelium. This vegetative phase represents the simplest form of fungal growth and requires the expansion of the plasma membrane, biosynthesis of cell wall components and the apical body of the Spitzenkörper as the vesicle supply center (Steinberg, 2007; Harris, 2009; Fajardo-Somera *et al*, 2015). Multiple rounds of nuclear division occur until hypha reaches a certain cell size (Wolkow *et al*, 1996). The size threshold triggers formation of the first septum at the base of the germinating spore. Septa are internal hyphal cross walls which are formed via invagination of the plasma membrane and aggregation of cell wall material, to increase the rigidity and to withstand turgor pressure (Harris, 2001; Mouriño-Pérez, 2013). A small pore allows the cytoplasm, organelles and nuclei to pass through the septum (Mouriño-Pérez, 2013). The septal pore can be plugged upon injury by structures known as Woronin bodies to prevent cytoplasmic leakage and cell death (Collinge & Markham, 1985; Jedd & Chua, 2000; Momany *et al*, 2002). Furthermore, it can ensure hyphal heterogeneity by impeding cytoplasmic continuity to maintain diversity of RNA and protein composition between hyphae (Bleichrodt *et al*, 2012; 2015).

The cytoskeleton plays a key role in vegetative growth and during septum formation in different filamentous fungi (Liu & Morris, 2000; Mouriño-Pérez, 2013; Manck *et al*, 2015). The polarized tip growth of hyphae requires the continuous transport of cell wall precursors to the tip and organelles like nuclei need to be positioned within the elongating cell. Cytoskeletal polymers such as microtubules and actin filaments do not only provide mechanical support to sustain the cell shape but also function as tracks for intracellular transport processes and participate in organelle positioning. Motor proteins attach to the cytoskeleton and perform ATP-dependent transport processes of vesicles, organelles and other cargos (Soldati & Schliwa, 2006; Egan *et al*, 2012; Takeshita *et al*, 2015). A coordinated shuttling of cell components is critical for fungal growth and misregulation alters septation (Liu & Morris, 2000; Taheri-Talesh *et al*, 2012).

After a defined period of vegetative growth, which ranges from 16 h to 20 h, hyphal cells reach a stage of developmental competence (Figure 9). They become responsive to external stimuli resulting in the induction of either sexual or asexual development, (Axelrod *et al*, 1973; Adams *et al*, 1998; Pöggeler *et al*, 2006; Bayram & Braus, 2012).

1.6.1.2 Sexual development

Developmental competent cells of *A. nidulans* develop primarily sexually in the absence of light and under elevated carbon dioxide concentrations. The sexual cycle starts with fusion of two ascogonial hyphae that form a dikaryon (Figure 9). This is followed by the formation of nest-like structures composed of thick-walled Hülle cells. These specialized cells have a protecting and nursing function for the developing fruiting body as mutant strains that are strongly reduced in Hülle cell production, reveal a decreased number of sexual structures, which are reduced in size (Sarıkaya-Bayram *et al*, 2010). The proposed nursing function is in accordance with the observation that tissue specific gene products, as laccase II, are synthesized in Hülle cells. Such proteins can then be transferred to the immature sexual fruiting body called primordium that is formed inside the nest (Hermann *et al*, 1983; Scherer & Fischer, 1998). The primordium matures to a closed fruiting body, termed cleistothecium, in which nuclear fusion and meiosis take place (Sohn & Yoon, 2002). After mitosis, asci are formed of which each contains eight nuclei. This is followed

by an additional mitotic division that generates binucleate ascospores. The mature cleistothecium accumulates the characteristic red pigmented secondary metabolite asperthecin and after seven days it can contain up to 80.000 ascospores (Howard & Raistrick, 1955; Szewczyk *et al*, 2008). Secondary metabolites are produced during development and function e.g. as defense mechanism against predators or support the host invasion of human and plant pathogens (Bayram & Braus, 2012; Scharf *et al*, 2014; Presti *et al*, 2015).

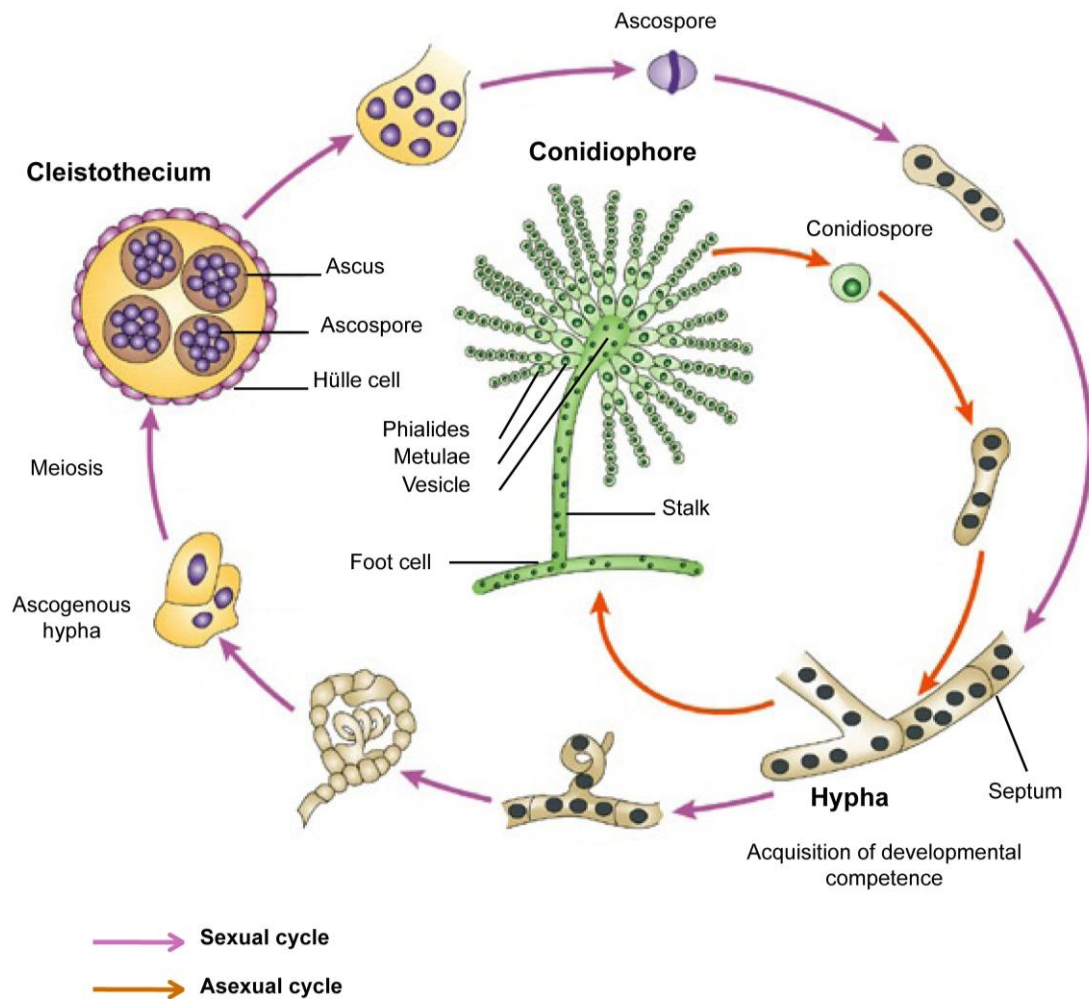


Figure 9: Life cycle of *Aspergillus nidulans*.

Vegetative hypha derived from a germinating spore contains several nuclei. Septum formation separates the hypha in single, but connected compartments. After reaching developmental competence the mycelium can enter two distinct life cycles depending on environmental factors. In darkness, the sexual pathway is favored (purple arrows). Ascogenous hyphae develop the sexual fruiting body, which is surrounded by Hülle cells. After meiosis and two post-meiotic mitoses the cleistothecium encloses asci, of which each harbors eight sexual ascospores. In light, the competent cells enter the asexual life cycle (orange arrows). Hyphae form a stalk and a multinucleate vesicle. The vesicle produces primary and secondary sterigmata (metulae and phialides) that give rise to asexual conidiospores. Modified from (Casselton & Zolan, 2002).

1.6.1.3 Asexual development

Developmental competent cells of *A. nidulans* develop predominantly asexually when exposed to an air interface in the presence of light and normal carbon dioxide concentrations (Adams *et al*, 1998). The first visible effect of asexual development is the occurrence of aerial hypha that elongates from a thick-walled foot-cell to form an aseptate conidiophore stalk (Figure 9), (Mims *et al*, 1988). After reaching a height of about 70 μm - 100 μm the tip of the stalk begins to swell and the phase of initial asexual development continues with the development of a conidiophore vesicle, which contains several nuclei. Budding of the vesicle produces around 60 primary sterigmata termed metulae. Each metula encloses one nucleus (Clutterbuck, 1969b; Oliver, 1972). Metulae bud twice to form uninucleate secondary sterigmata termed phialides. Phialides are mitotically highly active and produce long rows of up to 100 uninucleate conidiospores by repeated rounds of budding. After three days the mature conidiophore gives rise to around 10,000 asexual conidiospores. Advanced asexual development is followed by the distribution of asexual conidia by wind. These conidiospores display a characteristic dark green pigmentation resulting from spore-specific gene products, which protect the content from ultraviolet radiation (Aramayo *et al*, 1989; Mayorga & Timberlake, 1990; Adams *et al*, 1998).

1.6.2 Regulation of fungal development

A. nidulans is a soil borne fungus and its life is, like in most other organisms, regulated by light. Light sensing is crucial to adapt to changing environmental conditions. For spreading hyphae it is a major difference whether they grow on or under the surface in terms of abiotic and biotic factors such as illumination, oxygen concentration, osmotic stress and reactive oxygen species (Rodríguez-Romero *et al*, 2010; Bayram & Braus, 2012; Jaimes-Arroyo *et al*, 2015). The choice of entering the asexual or sexual developmental program is not a black/white decision. Light predominantly induces asexual (conidiophore) development and represses sexual (cleistothecia) development. After competence is acquired, induction of spore formation occurs through intracellular programmed events, which include the processes of signaling and signal transduction (Yu, 2010; Dasgupta *et al*, 2015).

A. nidulans senses light with a variety of different light receptors. The fungal phytochrome FphA is a sensor kinase that represses sexual development and induces asexual spore formation under red-light conditions (Blumenstein *et al*, 2005; Brandt *et al*, 2008). Phytochromes exist in two different conformations that can change upon light perception of a certain wavelength. The ratio between the two forms determines the signaling state of the phytochrome (Bayram *et al*, 2010). Cryptochromes are blue/UV light receptors that presumably originated from the DNA photolyase protein family, which are light-activated DNA-repair enzymes (Lin & Todo, 2005). Blue-light receptors of *A. nidulans* are encoded by *lreA* (light receptor A) and *lreB*. These transcription factors are homolog to the white-collar proteins of *N. crassa* WC1/WC2 that regulate the circadian rhythm. LreA and LreB stimulate sexual development and are associated to FphA (Purschwitz *et al*, 2008; Chen *et al*, 2010; Bayram & Braus, 2012; Dasgupta *et al*, 2015). The nuclear photolyase-like protein CryA (Cryptochrome A) senses UV-light and represses sexual development. Deletion of *cryA* results in abnormal formation of Hülle cells in submerged culture and increased cleistothecia formation during UV or blue-light illumination (Bayram *et al*, 2008a; Dasgupta *et al*, 2015).

A key protein involved in the regulation of light dependent developmental is encoded by *veA*. The velvet protein VeA is a conserved transcription factor that is supposed to affect the expression of hundreds of genes and physically interacts with FphA (Purschwitz *et al*, 2008; Dhingra *et al*, 2012; Sarikaya-Bayram *et al*, 2015). Deletion of *veA* results in a block of sexual development and reduces the production of secondary metabolites such as the aflatoxin precursor sterigmatocystin and the antibiotic penicillin (Kato *et al*, 2003; Bayram & Braus, 2012; Gerke & Braus, 2014). Light controls cellular localization of VeA. During illumination, VeA is associated to the velvet-like protein VelB and predominantly localized in the cytoplasm (Figure 10). In darkness the two velvet family proteins VeA-VelB interact with importin KapA (karyopherin A) to enter the nucleus (Stinnett *et al*, 2007; Bayram *et al*, 2008b). The nuclear VeA-VelB heterodimer forms the trimeric velvet complex by binding the histone methyltransferase LaeA (lack of *afIR* expression A), which is a master regulator of secondary metabolism (Sarikaya-Bayram *et al*, 2010). The trimeric velvet complex VelB-VeA-LaeA is essential to coordinate secondary metabolism and development by inducing the expression of sexual as well as secondary metabolite genes (Bayram *et al*, 2008b; Sarikaya-Bayram *et al*, 2015).

Beside LaeA, two other methyltransferases namely VipC (VeA interacting protein C) and VapB (VipC associated protein B) interact with VeA. The VipC-VapB dimer forms a complex with the membrane protein VapA (VipC associated protein A) to allow the nuclear *velvet* complex VelB-VeA-LaeA to induce transcription of genes important for sexual development in the dark. The release of membrane bound VipC-VapB by external signals results in VeA interaction, leading to a reduced import of the VeA-VelB dimer into the nucleus (Sarıkaya-Bayram *et al*, 2014; 2015). VelB might be part of a second complex as it interacts with the transcription factor VosA in the nucleus. The VelB-VosA heterodimer regulates the expression of genes important for cell wall biosynthesis and is required for spore viability and repression of asexual development in the dark (Sarıkaya-Bayram *et al*, 2010; Park *et al*, 2015).

Asexual development of *A. nidulans* is a precisely timed and genetically coordinated process, in which light regulates expression of several hundred genes in developmentally competent mycelium (Ruger-Herreros *et al*, 2011). The central regulatory pathway is composed of the genes *brlA*, *abaA* and *wetA* (Figure 10). Respective proteins control asexual development-specific genes and determine the order of gene expression during conidiation (Mirabito *et al*, 1989; Timberlake, 1990; Adams *et al*, 1998). The master regulator BrlA, whose transcription is induced by upstream regulators such as FlbB, is a transcription factor that is expressed in early asexual development when the conidiophore vesicles start to form (Momany, 2015). BrlA is localized in vesicles, metulae and phialides. Deletion of *brlA* leads to fungal colonies with elongated stalks, unable to develop vesicles or any other subsequent structures, thus the respective phenotype was named “*bristle*” (Clutterbuck, 1969a). BrlA is required for the expression of developmentally regulated genes (Boylan *et al*, 1987). Expression of *abaA* depends on BrlA activity and is initiated during phialide formation (Yu, 2010). Mutants deleted for *abaA* produce aconidial conidiophores that develop sterigmata but are incapable to form sporogenous phialides. Therefore, deletion of *abaA* results in the repetition of phialide-like structures rather than chains of conidia (Sewall *et al*, 1990b). *brlA* is overexpressed in *abaA* mutants, but *abaA* overexpression results in expression of *wetA* and *brlA*, demonstrating that AbaA has suppressive as well as promoting activities towards *brlA* (Aguirre, 1993; Sewall *et al*, 1990b). The third protein participating in the central regulatory pathway of asexual development is WetA. Expression of *wetA* is induced by AbaA in late conidiophore differentiation (Mirabito *et al*, 1989). The *wetA* gene product is required for

activating the *wetA* gene, indicating an autoregulatory expression mechanism (Boylan *et al*, 1987). WetA activates genes required for spore formation and maturation (Sewall *et al*, 1990a). Other light induced genes contribute to spore resistance in a dry environment (Suzuki *et al*, 2013).

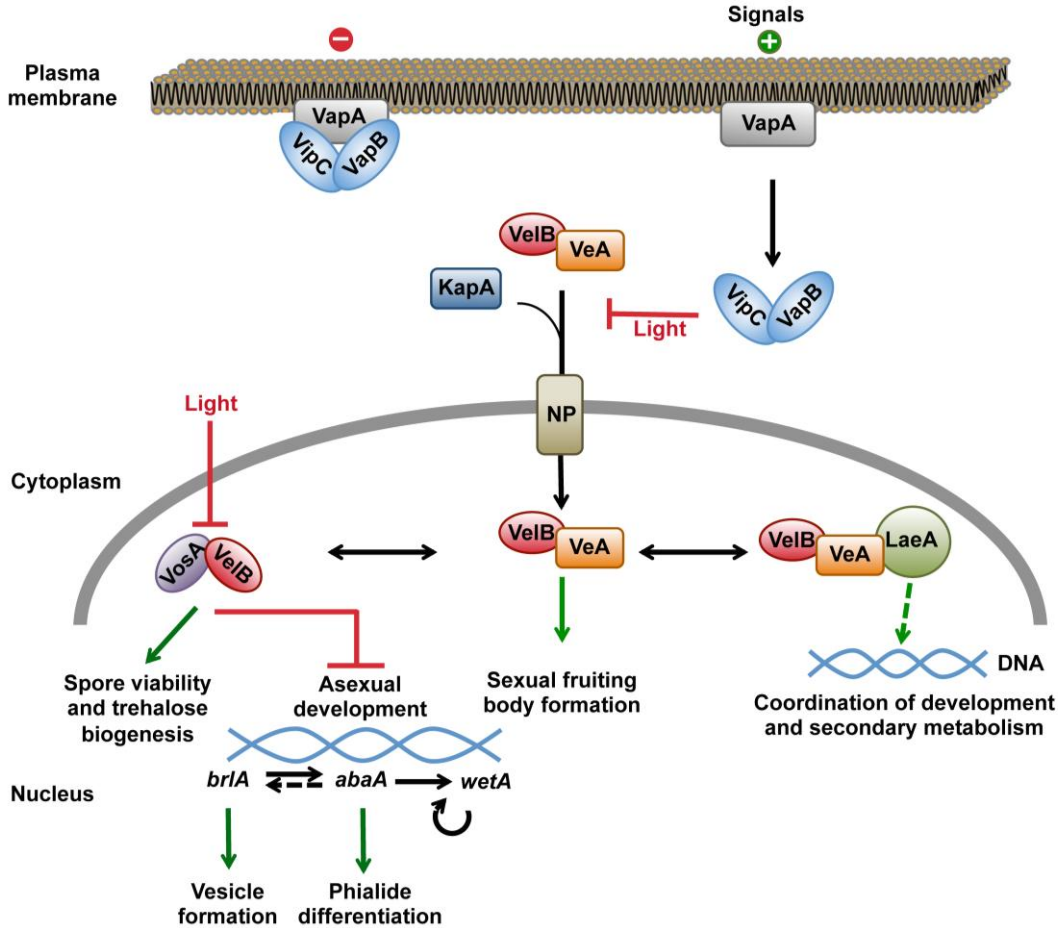


Figure 10: Light-dependent regulation of *A. nidulans* development.

In darkness, the VeA-VelB dimer interacts with importin KapA to enter the nucleus through the nuclear pore (NP). VapA binds the methyltransferases VipC and VapB to the membrane. Light as well as the membrane unbound VipC-VapB dimer repress nuclear import of the VeA-VelB complex. In the nucleus, VeA-VelB can interact with the methyltransferase LaeA to form the trimeric *velvet* complex, which coordinates sexual development and secondary metabolism. In addition, VelB forms a dimer with VosA that inhibits asexual development in the dark and is crucial for spore viability by activating trehalose biogenesis. Light decreases cellular levels of VosA and VelB and promotes asexual development, which is controlled by a central regulatory pathway. BrlA and the downstream transcription factors AbaA and WetA constitute the central regulatory pathway of conidiation. Increased *brlA* expression is crucial for conidiophore vesicle formation and conidiophore maturation. BrlA activates expression of *abaA* and *wetA*. AbaA is required for phialide differentiation and has activating as well as repressing functions towards *brlA*. *abaA* induces expression of *wetA*, which has an autoregulatory expression mechanism and is crucial for spore maturation. Modified from (Bayram & Braus, 2012; Sarikaya-Bayram *et al*, 2014).

An additional key player to complete asexual development in *A. nidulans* is VosA that also interacts with VelB in response to light. The VosA encoding gene is expressed during the formation of both sexual and asexual spores. VosA is conserved in most fungi and controls the late phase of conidiation. VosA is required for activating genes involved in spore maturation, but represses certain development-specific genes (Ni & Yu, 2007; Park *et al*, 2015). Strains deleted for *vosA* reveal a loss of trehalose accumulation in spores that is crucial to protect cells against environmental stresses (Ni & Yu, 2007).

1.6.3 The deneddylases COP9 signalosome and DEN1 in *Aspergillus nidulans*

Neddylation and deneddylation regulate the activity of SCF E3 ubiquitin ligases. All genes of the neddylation machinery, including the three cullins CulA/CUL1, CulC/CUL3 and CulD/CUL4, are highly conserved in *A. nidulans* (Galagan *et al*, 2005). The fungal genome encodes genes for around 74 different F-Box proteins, which is a similar amount of substrate binding proteins as found in humans (Jin *et al*, 2004; Galagan *et al*, 2005). Despite their central role in protein turnover, only few of them have been described. The F-Box protein GrrA is required during late fruiting body maturation as a *grrA* deletion strain produces cleistothecia with empty asci (Krappmann *et al*, 2006). F-Box15 and F-Box23 accumulate in a CSN deficient strain and are linked to development. Deletion of *fbx15* results in reduced asexual and sexual development, whereas an *fbx23* mutant forms sexual fruiting bodies during asexual conditions. These data suggest that the fungal CSN complex prevents the accumulation of development specific E3 ubiquitin cullin-RING ligases and is required for sexual development (Busch *et al*, 2003; von Zeska Kress *et al*, 2012; Beckmann *et al*, 2015). It was shown that several protein encoding genes involved in the neddylation machinery such as Nedd8 as well as UbcL, which represents the corresponding E2-Nedd8 conjugating enzyme UBC12 in *A. nidulans*, are indispensable to sustain fungal life (von Zeska Kress *et al*, 2012). In contrast, deletion of *csn* genes results in viable strains of *A. nidulans*, whereas they are essential in higher eukaryotes (Busch *et al*, 2003; 2007; Lee *et al*, 2011; Beckmann *et al*, 2015). While other fungi such as *N. crassa* or the fission yeast *S. pombe* possess only smaller versions of the CSN complex with seven, respective six subunits, *A. nidulans* encodes the full set of eight CSN subunits (CsnA-CsnH), including the

catalytic active subunit CsnE (Mundt *et al*, 2002; Galagan *et al*, 2005; Wang *et al*, 2010). This subunit composition corresponds to the situation found in plants and humans (Wei & Deng, 1999). Deletion of any of the eight *A. nidulans* CSN subunits results in a pleiotropic phenotype with an incomplete sexual development. Respective deletion strains are blocked in early sexual fruiting body formation at the stage of primordia (Busch *et al*, 2003; Beckmann *et al*, 2015). Since multicellular development and secondary metabolism are linked in *A. nidulans*, *csn* deletion strains display an altered secondary metabolism. Deletion of *csnE* causes accumulation of more than 100 metabolites that are produced by secondary metabolite gene clusters, which are silent under standard laboratory conditions (Nahlik *et al*, 2010). This results in an accumulation of red pigments caused by orcinol and orcellinic acid-derived compounds within hyphae and the surrounding medium (Busch *et al*, 2003; Nahlik *et al*, 2010; Beckmann *et al*, 2015).

The second deneddylase and homolog of DEN1, is called DenA in *A. nidulans*. DenA has a molecular weight of 29.5 kDa and shares 32% identical amino acids with human DEN1. Deletion of the DenA encoding gene did not lead to obvious phenotypes in several tested eukaryotic organisms, but in *A. nidulans* DenA contributes to asexual spore formation during limited pyrimidine supply (Christmann *et al*, 2013). Similar to mammalian DEN1, fungal DenA is capable to deneddylate cullins as well as non-cullin proteins. But in contrast to the human protein, fungal DenA does not display processing activity against the Nedd8 precursor (Christmann *et al*, 2013). The cellular DenA population is divided into subpopulations, which are located in the nucleus and the cytoplasm, and there especially enriched at septa. The nuclear DenA proportion interacts with CSN. The physical interaction between both deneddylases is conserved from fungi to human and results in DenA degradation. However, the major interacting subunits seem to have changed during evolution. Human DEN1 predominantly interacts with CSN1 as shown by far-western experiments. In contrast, yeast-two-hybrid tests revealed that the related Nep1 and Nep2 of *S. pombe* have a high binding affinity towards CSN2, whereas DenA of *A. nidulans* binds most dominantly to the seventh CSN subunit CsnG, and additionally but to lower extent to CsnA/CSN1, CsnE/CSN5 and CsnF/CSN6 (Christmann *et al*, 2013).

1.7 Aims of this study

Eukaryotic cells possess two known enzymes with deneddylation isopeptidase activity, the COP9 signalosome and the Deneddylase 1. Enzymatic CSN function is mostly responsible for deneddylating cullins, whereas DenA/DEN1 deneddylation activity is primarily associated to non-cullin proteins and hardly affects the neddylation status of cullins. Previously it was shown that DenA and CSN represent two developmental deneddylases, which play an important role in two different developmental processes. The CSN complex is essential for the sexual life cycle and coordination of secondary metabolism, while DenA is involved in asexual development (Busch *et al*, 2003; Christmann *et al*, 2013; Beckmann *et al*, 2015). DenA is localized in the nucleus as well as in the cytoplasm. It was demonstrated that the seventh CSN subunit, CsnG, interacts with nuclear DenA. As DenA is stabilized in a *csnG* deletion strain, it was suggested that the interaction targets nuclear DenA for degradation (Christmann *et al*, 2013).

The focus of this study was to unveil the stability control and the functions of the nuclear and cytoplasmatic subpopulations of the deneddylase DenA/DEN1 using the multicellular mold *A. nidulans* as model. Special emphasis was put on the interplay of DenA and the CSN complex. *A. nidulans* represents an attractive model to study the function and interrelation of the two deneddylases in multicellular development due to the different impact of CSN and DenA on individual fungal developmental programs. The first aim was to analyze whether DenA can compensate the lack of a functional CSN complex regarding deneddylation of cullins and developmental defects. The observation of a CsnG mediated stability control of DenA raised additionally the question whether among all CSN subunits CsnG exclusively controls DenA stability. To provide a comprehensive understanding, all eight CSN subunits and their contribution to degradation of nuclear DenA were analyzed. Another approach aimed to identify additional DenA binding proteins that contribute to localization and stability of the cytoplasmatic DenA subpopulation. Of particular interest was to find indications explaining the role of DenA in asexual development.

2 Materials & Methods

2.1 Chemicals

Growth media, buffers and solutions were prepared by using products from CARL ROTH GMBH & CO. KG (Karlsruhe, D), MERCK (Darmstadt, D), INVITROGEN GMBH (Karlsruhe, D), SIGMA-ALDRICH CHEMIE GMBH (Steinheim, D), VWR INTERNATIONAL GMBH (Darmstadt, D), APPLIChem GMBH (Darmstadt, D), SERVA ELECTROPHORESIS GMBH (Heidelberg, D), FLUKA (Neu-Ulm, D) and BD BIOSCIENCES (Heidelberg, D).

2.2 Strains and growth conditions

Escherichia coli strain DH5 α (INVITROGEN) was used for plasmid DNA preparations. *E. coli* was cultivated in lysogeny broth (LB) medium (1% tryptophan, 0.5% yeast extract, 1% NaCl) (Bertani, 1951) at 37°C in the presence of 100 mg/ml ampicillin. Solid media contained 2% agar.

Aspergillus nidulans strains TNO2a3 (Nayak *et al*, 2006), AGB551 (Bayram *et al*, 2012) and AGB152 (Busch *et al*, 2003) were used as wild type hosts to transform deletion constructs, overexpression plasmids or plasmids expressing genes that encode for proteins linked to a tag. All *A. nidulans* strains used in this study are listed in table 1. Respective strains were grown in minimal medium (1% glucose, 2 mM MgSO₄, 70 mM NaNO₃, 7 mM KCl, 11.2 mM KH₂PO₄, 0.1% trace element solution (Käfer, 1977) pH5.5). For solid media 2% agar was added. Supplements such as 0.1% pyridoxine-HCl, 5 mM uridine, 5 mM uracil, 100 ng/ml pyrithiamine, 120 ng/ml nourseothricin and 10 μ g/ml phleomycin were added in appropriate amounts. Vegetative cultures were grown in liquid medium for 16-40 h in baffled flasks on a rotary shaker. Asexual development was induced either by distributing spores on solid medium or in case of developmental synchronization by transferring pre-grown vegetative mycelia onto solid medium. Plates were incubated at 30°C or 37°C during constant white light exposure. Mycelia were harvested at time points as indicated in respective figure legends.

Table 1: *Aspergillus nidulans* strains constructed and used in this study.

Strain	Genotype	Reference
TNO2a3	<i>pyrG89;pyroA4;argB2;ΔnkuA::argB</i>	(Nayak <i>et al</i> , 2006)
AGB152	<i>pyrG89;pyroA4</i>	(Busch <i>et al</i> , 2003)
AGB160	<i>pyrG89;pyroA4; pyr4⁺</i>	(Busch <i>et al</i> , 2003)
AGB195	<i>pyrG89;pyroA4;ΔcsnD::pyr4⁺</i>	(Busch <i>et al</i> , 2003)
AGB209	<i>pyrG89;pyroA4;ΔcsnE::pyr4⁺</i>	(Busch <i>et al</i> , 2003)
AGB223	<i>pyrG89;pyroA4;ΔcsnA::pyr4⁺</i>	(Busch <i>et al</i> , 2007)
AGB238	<i>pyrG89;pyroA4;ΔcsnB::pyrG⁺_{af}</i>	(Busch <i>et al</i> , 2007)
AGB316	<i>pyrG89;pyroA4;ΔdenA::pyr4⁺</i>	(Christmann <i>et al</i> , 2013)
AGB318	<i>pyrG89;pyroA4;ΔdenA::pyr4⁺;denA⁺;phleo^R</i>	(Christmann <i>et al</i> , 2013)
AGB466	<i>pyrG89;pyroA4;ΔnkuA::argB;ΔcsnE::ptrA^R</i>	(Christmann <i>et al</i> , 2013)
AGB551	<i>pyrG89;pyroA4</i>	(Bayram <i>et al</i> , 2012)
AGB596	<i>P_{gpdA}::gfp::phleo^R;pabaA1;yA2;veA⁺</i>	(Bayram <i>et al</i> , 2012)
AGB630	<i>pyrG89;pyroA4;ΔdenA::pyr4⁺; P_{niaD}::cyfp::niaD^T /P_{niiA}::denA^{cDNA}::nyfp::niiA^T;ptrA^R</i>	(Christmann <i>et al</i> , 2013)
AGB631	<i>pyrG89;pyroA4;ΔcsnG::ptrA^R</i>	(Beckmann <i>et al</i> , 2015)
AGB632	<i>pyrG89;pyroA4;ΔcsnE::ptrA^R;ΔdenA::pyr4⁺</i>	(Christmann <i>et al</i> , 2013)
AGB634	<i>pyrG89;pyroA4;P_{denA}::denA::gfp::nat^R:: denA^T</i>	(Christmann <i>et al</i> , 2013)
AGB635	<i>pyrG89;pyroA4;ΔcsnA::pyr4⁺; P_{denA}::denA::gfp::nat^R::denA^T</i>	(Christmann, 2012)
AGB636	<i>pyrG89;pyroA4;P_{denA}::denA::ctap::nat^R::denA^T</i>	(Christmann, 2012)

Strain	Genotype	Reference
AGB640	<i>pyrG89;pyroA4;</i> ^P <i>denA::denA::gfp::nat^R::denA^T;</i> <i>gpdA::mrfp::h2A::hisB^T;pyrG⁺_{af}</i>	(Christmann <i>et al</i> , 2013)
AGB641	<i>pyrG89;pyroA4;mrfp::h2A;phleo^R</i>	(Christmann <i>et al</i> , 2013)
AGB649	<i>pyrG89;pyroA4;ΔcsnE::pyr4⁺;</i> <i>denA::denA::gfp::nat^R::denA^T</i>	Christmann pers. comm.
AGB667	<i>pyrG89;pyroA4;sasA::ctap::</i> ^P <i>gpdA::nat^R</i>	(Gerke <i>et al</i> , 2012)
AGB708	<i>pyrG89;pyroA4;</i> ^P <i>denA::denA::gfp::nat^R::denA^T;</i> <i>ΔcsnG::ptrA^R;</i> ^P <i>gpdA::mrfp::h2A::hisB^T;pyrG⁺_{af}</i>	(Christmann <i>et al</i> , 2013)
AGB718	<i>pyrG89;pyroA4;ΔcsnC::pyrG⁺_{af}</i>	(Beckmann <i>et al</i> , 2015)
AGB720	<i>pyrG89;pyroA4;ΔcsnF::pyrG⁺_{af}</i>	(Beckmann <i>et al</i> , 2015)
AGB722	<i>pyrG89;pyroA4;ΔcsnH::pyrG⁺_{af}</i>	(Beckmann <i>et al</i> , 2015)
AGB959	<i>pyrG89;pyroA4;ΔdenA::pyr4⁺;</i> <i>niaD::dipA^{cDNA}::cyfp::niaD^T</i> <i>/</i> ^P <i>niiA::denA^{cDNA}::nyfp::niiA^T;ptrA^R</i>	This study
AGB960	<i>pyrG89;pyroA4;ΔdipA::ptrA^R</i>	This study
AGB961	<i>pyrG89;pyroA4;ΔdenA::pyr4⁺;</i> <i>niaD::dipA^{cDNA}::cyfp::niaD^T</i> <i>/</i> ^P <i>niiA::denA^{cDNA}::nyfp::niiA^T;ptrA^R;</i> ^P <i>gpdA::mrfp::h2A::hisB^T;phleo^R</i>	This study
AGB962	<i>pyrG89;pyroA4;</i> ^P <i>niiA::denA::niiA^T;pyrG⁺_{af}</i>	This study
AGB963	<i>pyrG89;pyroA4;</i> <i>niaD::dipA^{cDNA}::cyfp::niaD^T</i> <i>/</i> ^P <i>niiA::denA::niiA^T;pyrG⁺_{af};ΔcsnE::ptrA^R</i>	This study
AGB964	<i>pyrG89;pyroA4;</i> <i>niaD::dipA^{cDNA}::cyfp::niaD^T</i> <i>/</i> ^P <i>niiA::denA::niiA^T;pyrG⁺_{af};ΔcsnG::ptrA^R</i>	This study
AGB965	<i>pyrG89;pyroA4;ΔdipA::ptrA^R;</i> <i>denA::denA::gfp::nat^R::denA^T</i>	This study
AGB966	<i>pyrG89;pyroA4;</i> <i>denA::denA^{S243A-S245A-S253A}::gfp::nat^R::denA^T</i>	This study

Strain	Genotype	Reference
AGB967	<i>pyrG89;pyroA4;</i> <i>P_{denA}::denA^{S243D-S245D-S253D}::gfp::nat^R::denA^T</i>	This study
AGB968	<i>pyrG89;pyroA4;</i> <i>P_{dipA}::dipA::gfp::nat^R::dipA^T</i>	This study
AGB969	<i>pyrG89;pyroA4;ΔcsnB::pyrG⁺_{af};</i> <i>P_{denA}::denA::gfp::nat^R::denA^T</i>	This study
AGB970	<i>pyrG89;pyroA4;ΔcsnC::pyrG⁺_{af};</i> <i>P_{denA}::denA::gfp::nat^R::denA^T</i>	This study
AGB971	<i>pyrG89;pyroA4;ΔcsnD::pyr4⁺;</i> <i>P_{denA}::denA::gfp::nat^R::denA^T</i>	This study
AGB972	<i>pyrG89;pyroA4;ΔcsnF::pyrG⁺_{af};</i> <i>P_{denA}::denA::gfp::nat^R::denA^T</i>	This study
AGB973	<i>pyrG89;pyroA4;ΔcsnH::pyrG⁺_{af};</i> <i>P_{denA}::denA::gfp::nat^R::denA^T</i>	This study
AGB974	<i>pyrG89;pyroA4;ΔdipA::ptrA^R;</i> <i>P_{denA}::denA::gfp::nat^R::denA^T;ΔcsnG::pyroA_{af}</i>	This study
AGB975	<i>pyrG89;pyroA4;</i> <i>P_{denA}::denA^{S253A}::gfp::nat^R::denA^T</i>	This study
AGB976	<i>pyrG89;pyroA4;</i> <i>P_{denA}::denA^{S253D}::gfp::nat^R::denA^T</i>	This study
AGB977	<i>pyrG89;pyroA4;</i> <i>P_{denA}::denA::gfp::nat^R::denA^T;</i> <i>P_{dipA}::dipA^{D51A-H73A-D76A}::6xhis::pyrG::dipA^T</i>	This study
AGB978	<i>pyrG89;pyroA4;ΔdenA::pyr4⁺;</i> <i>P_{niaD}::dipA^{cDNA}::cyfp::niaD^T</i> <i>/P_{niiA}::denA^{cDNAS243A-S245A-S253A}::nyfp::niiA^T;ptrA^R;</i>	This study
AGB979	<i>pyrG89;pyroA4;ΔdenA::pyr4⁺;</i> <i>P_{niaD}::dipA^{cDNA}::cyfp::niaD^T</i> <i>/P_{niiA}::denA^{cDNAS243D-S245D-S253D}::nyfp::niiA^T;ptrA^R;</i>	This study
AGB980	<i>pyrG89;pyroA4;</i> <i>P_{dipA}::dipA::gfp::nat^R::dipA^T;</i> <i>P_{gpdA}::mrfp::h2A::hisB^T;phleo^R</i>	This study
AGB981	<i>pyrG89;pyroA4;ΔdipA::ptrA^R;</i> <i>P_{denA}::denA::gfp::nat^R::denA^T;</i> <i>P_{gpdA}::mrfp::h2A::hisB^T;phleo^R</i>	This study

P = promoter; T = terminator; R = resistance; *nat* = nourseothricin; *ptrA* = pyrithiamine; *phleo* = phleomycin; *af* = *Aspergillus fumigatus*. pers. comm. = personal communication

2.3 Plasmid and strain construction

2.3.1 Construction of *denA* overexpression strains

For overexpression of *denA* in different genetic backgrounds plasmid pME4068, carrying *denA* under control of a nitrate promoter, was integrated ectopically into AGB152 (WT), AGB631 ($\Delta csnG$) and AGB466 ($\Delta csnE$) resulting in AGB962, AGB964 and AGB963. Ectopical integration was verified by Southern analysis using *HindIII* for digestion. A probe against the nitrate promoter amplified with primers OLKM67/OLKM68 detected a band for wild type at 2.7 kb and for the *denA* overexpression strains an additional band at 5.2 kb. qRT-PCR was performed by using primers 5'RT MC1/3'RT MC2 and 5'RT H2A/3'RT H2A to validate similar *denA* expression levels.

2.3.2 Strain construction of DenA-GFP in *csn* deletion strains

csn deletion strains carrying a C-terminal fusion of DenA with GFP under control of the native *denA* promoter were obtained by transforming a 5.5 kb *denA-gfp-nat^R* cassette, digested with *ClaI/NotI* from pME3900, into *csn* deletion strains AGB238 ($\Delta csnB$), AGB718 ($\Delta csnC$), AGB195 ($\Delta csnD$), AGB720 ($\Delta csnF$) and AGB722 ($\Delta csnH$). The resulting strains were named AGB969, AGB970, AGB971, AGB972 and AGB973. Homologous recombination was verified by microscopy and Southern hybridization of *AvaI* digested samples. A probe against the 5' flanking region of *denA* was amplified with primers JS65/JS66, which detected a band at 3.5 kb in wild type and at 4.7 kb for the *denA-gfp* fusion construct integrated at the endogenous *denA* locus in the *csn* deletion strains.

2.3.3 Construction of strains carrying an amino acid substituted phosphorylation site of DenA at position S253

For strains containing a DenA-GFP version with substituted amino acids mimicking either a constant phosphorylated or a constant dephosphorylated status at position S253 the respective codon was exchanged either to alanine or aspartate. Single amino acid substituted DenA-GFP versions with an exchanged codon S253

were obtained by using primers MC1/JS201 to amplify a 2.2 kb fragment containing the 5' flanking region as well as the first 1116 bp of *denA* ORF. With primers JS202/MC2 or JS203/MC2 serine S253 either was substituted to alanine or to aspartate, respectively. The amplicons contained a C-terminally located GFP fused to *nat* resistance under control of the constitutive *gpdA* promoter and followed by 3' flanking region. Single fragments were fused by PCR (Szewczyk *et al*, 2006) with primers MC1/MC2 and the resulting 5.5 kb cassette was subcloned into pJET1.2/blunt vector giving plasmids pME4406 and pME4407, respectively. After digestion with *ClaI/NotI* the constructs were integrated at the native *denA* locus of TNO2a3 resulting in strains AGB975 and AGB976. Homologous recombination was verified by Southern hybridization of *AvaI* digested samples. A probe against the 5' flanking region of *denA* was amplified with primers JS65/JS66 and detected a band for wild type at 3.5 kb and at 4.7 kb for the *denA-gfp* fusion construct integrated at the endogenous *denA* locus.

2.3.4 Construction of strains with triple amino acid substituted phosphorylation sites of DenA at positions S243, S245 and S253

Constructions of DenA-GFP strains with three substituted DenA phosphorylation sites at positions S243, S245 and S253 were obtained in a similar way as described in chapter 2.3.3. Primers MC1/JS148 were used to amplify a 2.2 kb fragment containing the 5' flanking region as well as the first 1086 bp of *denA* ORF. A fragment containing S243, S245 and S253 substituted to alanine was obtained by PCR with primers JS150/JS162. Similarly, primers JS158/JS163 were used to substitute S243, S245 and S253 to aspartate. The C-terminal part of *denA* with downstream located GFP fused to *nat* resistance under control of the constitutive *gpdA* promoter and followed by the 3' flanking region was amplified with primers JS167/MC2. All fragments were fused by PCR (Szewczyk *et al*, 2006) using primers MC1/MC2 and ligated into pJET1.2/blunt vector resulting in pME4404 and pME4405, respectively. The 5.5 kb cassette was excised with *ClaI/NotI* and transformed into TNO2a3 giving strains AGB966 and AGB967. Southern hybridization was performed according to the previous described strategy of AGB975 and AGB976.

2.3.5 BiFC plasmid and strain construction for DenA-DipA interaction studies

BiFC studies were performed with each half of a split *yfp* fused to proteins to test for interaction. Fusion proteins were under control of a bidirectional nitrate promoter. cDNA of *denA* was connected C-terminally with a linker to the N-terminal part of *yfp* (*nyfp*), which was amplified from pME3897 with primers MC171/MC30. The 1.2 kb fragment was ligated into the *PmeI* restriction site of pSK409, giving plasmid pME4401. The C-terminal part of *yfp* (*cyfp*) and the appropriate linker was obtained using pME3897 as template and primers JS90/JS91 and JS89/JS92, respectively. Both fragments were fused (Szewczyk *et al*, 2006) with primers JS89/JS91 and the product with a size of 312 bp was ligated into the *SwaI* restriction site of pME4401 resulting in plasmid pME4418. *dipA* cDNA with a size of 2.1 kb was amplified with primers JS96/JS97 from TNO2a3 cDNA pool. This fragment was fused with the *cyfp*-linker fragment, obtained from plasmid pME4418 by PCR with primers JS93/JS91, using primers JS96/JS91. The resulting 2.4 kb product was ligated into the *SwaI* restriction site of pME4401, giving plasmid pME4402. Transformation of pME4402 into AGB316 resulted in strain AGB959. Ectopical integration was examined with Southern analyses using *BglII* digested samples. A probe against the nitrate promoter was amplified with primers OLKM67/OLKM68. The probe detected a band for wild type at 7.1 kb and an additional band at 4.2 kb for the BiFC construct. For visualizing nuclei, the plasmid pME3857 was transformed into AGB959 and ectopic integration of the *mrfp::h2A* construct was verified by microscopy. The resulting strain was named AGB961.

BiFC plasmids with mutations in the codons for the DenA phosphorylation sites were constructed by codon substitutions. cDNA of *dipA* connected with a linker to the C-terminal part of *yfp* (*cyfp*) was amplified from pME4402 with primers JS91/JS96. The 2.4 kb fragment was ligated into the *SwaI* restriction site of pSK409, resulting in plasmid pME4408. PCR with the primers MC30/JS204 were used to amplify cDNA of *denA* to substitute S243, S245 and S253 to alanine. The N-terminal half of *yfp* (*nyfp*) was amplified with primers JS205/MC171. Both fragments were fused (Szewczyk *et al*, 2006) with primers MC30/MC171 and the product with a size of 1.3 kb was ligated into the *PmeI* restriction site of pME4408, giving plasmid pME4409. Primers MC30/JS206 were used to substitute S243, S245 and S253 to aspartate. The obtained 776 bp fragment was fused to the N-terminal part of *yfp* (*nyfp*). The resulting product with a size of 1.3 kb was ligated into the *PmeI*

restriction site of pME4408, giving plasmid pME4410. Transformation of pME4409 and pME4410 in *denA* deletion strain AGB316 resulted in strains AGB978 and AGB979, respectively. Ectopical integration of pME4409 and pME4410 was verified with Southern analyses using *Bgl*II. A probe against the nitrate promoter was amplified with primers OLKM67/OLKM68. Wild type revealed a band at 7.1 kb and respective BiFC strains showed an additional band at the size of 4.2 kb.

2.3.6 Plasmid and strain construction for *dipA strain**

The three amino acids D51, H73 and D76, which belong to the predicted catalytic core of DipA, were substituted to neutral alanine. PCR with primers JS219/JS221 was used to amplify the 5' flanking region of AN10946 and to mutate D51. To assure that the in close proximity lying neighboring gene AN10959 is not disturbed, the amplified 3.1 kb fragment included the gene locus of AN10959. Primers JS222/JS223 were used to obtain a 184 bp fragment with substituted H73 and D76. PCR with primers JS224/JS220 amplified a fragment of 5 kb containing the C-terminal *dipA* fused to GFP and a *nat*-marker under control of the constitutive *gpdA* promoter followed by the 3' flanking region of AN10946. PCR mediated fusion (Szewczyk *et al*, 2006) of all three fragments using primers JS219/JS220 resulted in a 8.2 kb product, that was ligated into pJET1.2/blunt vector giving plasmid pME4419. pME4419 was used as a template for primers JS219/JS228 to amplify a fragment of 5.3 kb containing the mutated *dipA* gene fused to 6xHis-tag. PCR with primers JS225/JS226 resulted in amplified *pyrG*-marker with a size of 2 kb. The 3' flanking region had a size of 900 bp and was generated with primers JS227/JS220. Fusion PCR (Szewczyk *et al*, 2006) with all three fragments using primers JS219/JS220 resulted in a 8.2 kb product which was ligated into pJET1.2/blunt vector giving plasmid pME4420. A 7.4 kb cassette was excised with *Psi*I/*Sna*BI and transformed into AGB634 resulting in AGB977. Homologous recombination was verified by Southern hybridization using *Hind*III digested samples. A probe against the 5' flanking region of *dipA* was amplified with primers JS138/JS233. The probe detected a band for wild type at 5.7 kb and at 6.1 kb for the mutated version of *dipA*.

2.3.7 Plasmid and strain construction for the *dipA* deletion strain

For deleting the *dipA* gene locus (AN10946) the 5' flanking region was amplified with primers JS131/JS132. To assure that the in close proximity lying neighboring gene AN10959 is not disturbed, the amplified 2.6 kb fragment included the gene locus of AN10959. The 3' flanking region had a size of 1 kb and was obtained by PCR with primers JS135/JS136. Both products had an overhang to the *ptrA* marker (Kubodera *et al*, 2000), which was amplified with primers JS133/JS134. The *dipA* deletion cassette was fused by PCR (Szewczyk *et al*, 2006) using primers JS131/JS136 and subcloned into pJET1.2/blunt vector resulting in plasmid pME4399. The 5.6 kb cassette was excised with *EcoRV* and transformed into AGB551 giving strain AGB960. Homologous recombination was confirmed by Southern analysis using *BamHI* digested samples. A probe against the 3' flanking region of *dipA* was amplified with primers JS135/JS136. The probe detected a band for wild type at 6.6 kb and at 4.2 kb for the *dipA* deletion strain.

2.3.8 Plasmid and strain construction for the DipA-GFP strain

For localization studies of DipA, the 5' upstream fragment including the ORF of *dipA* with a size of 5.3 kb was amplified with primers JS171/JS168. It contained a linker and an overhang for GFP cassette. The 2.1 kb *gfp* cassette fused to *nat* resistance under control of the constitutive *gpdA* promoter was obtained by PCR with primers ÖZG207/JS169. The 3' flanking region of *dipA* with an overhang to the *nat* resistance was amplified with primers JS170/JS172. By using primers JS171/JS172 the three fragments were fused and subcloned into pJET1.2/blunt vector giving plasmid pME4400. The 8.2 kb *dipA-gfp* cassette was excised with *NdeI* and transformed into *dipA* deletion strain AGB960 resulting in strain AGB968. As the cassette was transformed into *dipA* deletion strain, AGB968 was used as complementation strain. Homologous recombination was verified by microscopy and Southern analysis using the same strategy as described for AGB960. The wild type revealed a band at 6.6 kb, whereas the complemented strain showed a band at 8.7 kb. AGB968 was further transformed with pME3857 for ectopic integration of an *mrfp::h2A* construct to visualize nuclei. The resulting strain was named AGB980.

2.3.9 Strain construction of DenA-GFP in *dipA* deletion strain

dipA deletion strain AGB960 was used to transform a 5.5 kb *denA-gfp-nat^R* cassette excised with *ClaI/NotI* from pME3857 resulting in strain AGB965. Homologous recombination was verified by microscopy and Southern hybridization of *AvaI* digested samples. A probe against the 5' flanking region of *denA* was amplified with primers JS65/JS66 and detected a band for wild type at 3.5 kb and at 4.7 kb for the *denA-gfp* fusion construct integrated at the endogenous *denA* locus. For visualizing nuclei, the plasmid pME3857 was transformed into AGB965 and ectopic integration of the *mrfp::h2A* construct was verified by microscopy. The resulting strain was named AGB981.

2.3.10 Strain construction of *dipA/csnG* double deletion strain with DenA-GFP

For deleting *csnG* in AGB965, the 2.2 kb 5' flanking region of *csnG* was amplified with primers JS180/JS181. The 1.9 kb 3' flanking region was amplified with primers JS184/JS185. The 2 kb *pyroA* fragment was obtained from template pME3979 by using primers JS182/JS183. All three fragments were fused together with primers JS180/JS185 resulting in a 6 kb *csnG* deletion cassette which was ligated into pJET1.2/blunt vector, giving plasmid pME4403. The construct was excised with *Bgl/II* and transformed into AGB965 resulting in strain AGB974. Homologous recombination was verified by Southern analysis using *BamHI* digested DNA samples. Primers JS188/JS181 amplified a probe against the *csnG* 5' flanking region, which detected a band for wild type at 5.2 kb and at 6.2 kb for *csnG* deletion strain.

2.4 Nucleic acid methods

2.4.1 Transformations

Transformations of *E. coli* were performed as described earlier (Inoue *et al*, 1990). Transformation of *A. nidulans* was performed in a modified form as described by (Punt & van den Hondel, 1992). The respective parental strain was grown under rotation in 200 ml medium of an 1 L flask with indentations at 37°C. The mycelium was filtrated through a sterile Miracloth filter (MERCK), washed with citrate buffer

(150 mM KCl, 580 mM NaCl, 50 mM Na-citrate pH 5.5) and transferred into a sterile 300 mL flask without indentations. An appropriate amount of glucanase/lysozyme mixture (30 mg/ml Vinoflow (NOVOZYMES, Bagsvaerd, DNK) and 15 mg/ml lysozyme (SERVA) dissolved in citrate buffer) was added to the mycelium and incubated at 30°C under gentle agitation for around 1.5 hours. Protoplasts were harvested by pouring the mixture through a sterile Miracloth filter (MERCK) into a new sterile reaction tube. Ice-cold STC1700 buffer (1.2 M sorbitol, 10 mM Tris pH 5.5, 50 mM CaCl₂, 35 mM NaCl) was added prior to centrifugation for 12 min at 2500 rpm at 4°C. The supernatant was discarded, the precipitate was resuspended and washing, centrifugation and resuspension steps were repeated. The protoplasts were incubated with respective DNA (2-15 µg) in ice for 25 min. PEG4000 solution (10 mM Tris pH 7.5, 50 mM CaCl₂, 60% PEG4000) was added successively in three steps (250 µl, 250 µl, 850 µl), carefully mixed with protoplasts and incubated on ice for 20 min. 15 ml ice-cold STC1700 buffer was added followed by 15 min centrifugation at 2500 rpm at 4°C. The supernatant was removed and precipitated protoplasts were resuspended and distributed with Top-Agar (0.7% agar in selective sorbitol medium) on plates containing sorbitol. Plates were incubated at 37°C for three to seven days.

2.4.2 Constructs for genetic manipulation

Plasmids used in this study for transformations are listed in table 2 and details about construction strategies are described in chapter 2.3. Oligonucleotides (EUROFINS GENOMICS GMBH, Ebersberg, D) used to construct respective plasmids are shown in table 3.

Table 2: Plasmids constructed and used in this study.

Plasmid	Description	Reference
pJET1.2/blunt	cloning vector	THERMO SCIENTIFIC GMBH, Schwerte, D
pSK409	$P_{niaD}::niaD^T / P_{niiA}::niiA^T; ptrA^R$	unpublished
pME3160	$P_{niaD}::niaD^T / P_{niiA}::niiA^T; pyrG^+_{af}$	(Bayram <i>et al</i> , 2008b)
pME3857	$P_{gpdA}::mrfp::h2A::hisB^T; phleo^R$ in pBlueII SK+	(Bayram <i>et al</i> , 2012)
pME3887	$5^{',csnG}::ptrA^R::3^{',csnG}$ in pJET1.2/blunt	This study
pME3897	$P_{niaD}::csnG^{cDNA}::cyfp::niaD^T / P_{niiA}::denA^{cDNA}::nyfp::niiA^T; pyrG^+_{af}$	unpublished
pME3900	$5^{',denA}::denA::gfp::nat^R::3^{',denA}$ in pJET1.2/blunt	(Christmann <i>et al</i> , 2013)
pME3901	$5^{',denA}::denA::ctap::nat^R::3^{',denA}$ in pJET1.2/blunt	This study
pME3979	$5^{',ulpA}::pyroA_{af}::3^{',ulpA}$ in pJET1.2/blunt	(Harting <i>et al</i> , 2013)
pME4068	gDNA <i>denA</i> in pME3160	(Harting <i>et al</i> , 2013)
pME4399	AN10959:: $5^{',dipA}::ptrA^R::3^{',dipA}$ in pJET1.2/blunt	This study
pME4400	AN10959:: $5^{',dipA}::dipA::gfp::nat^R::3^{',dipA}$ in pJET1.2/blunt	This study
pME4401	$P_{niaD}::niaD^T / P_{niiA}::denA^{cDNA}::nyfp::niiA^T; ptrA^R$	This study
pME4402	$P_{niaD}::dipA^{cDNA}::cyfp::niaD^T / P_{niiA}::denA^{cDNA}::nyfp::niiA^T; ptrA^R$	This study

Plasmid	Description	Reference
pME4403	5 ['] <i>csnG</i> :: <i>pyroA</i> _{af} ::3 ['] <i>csnG</i> in pJET1.2/blunt	This study
pME4404	5 ['] <i>denA</i> :: <i>denA</i> ^{S243A-S245A-S253A} :: <i>gfp</i> :: <i>nat</i> ^R ::3 ['] <i>denA</i> in pJET1.2/blunt	This study
pME4405	5 ['] <i>denA</i> :: <i>denA</i> ^{S243D-S245D-S253D} :: <i>gfp</i> :: <i>nat</i> ^R ::3 ['] <i>denA</i> in pJET1.2/blunt	This study
pME4406	5 ['] <i>denA</i> :: <i>denA</i> ^{S253A} :: <i>gfp</i> :: <i>nat</i> ^R ::3 ['] <i>denA</i> in pJET1.2/blunt	This study
pME4407	5 ['] <i>denA</i> :: <i>denA</i> ^{S253D} :: <i>gfp</i> :: <i>nat</i> ^R ::3 ['] <i>denA</i> in pJET1.2/blunt	This study
pME4408	P _{<i>niaD</i>} :: <i>dipA</i> ^{cDNA} :: <i>cyfp</i> :: <i>niaD</i> ^T / P _{<i>niiA</i>} :: <i>niiA</i> ^T ; <i>ptrA</i> ^R	This study
pME4409	P _{<i>niaD</i>} :: <i>dipA</i> ^{cDNA} :: <i>cyfp</i> :: <i>niaD</i> ^T / P _{<i>niiA</i>} :: <i>denA</i> ^{cDNAS243A-S245A-S253A} ::: <i>nyfp</i> :: <i>niiA</i> ^T ; <i>ptrA</i> ^R	This study
pME4410	P _{<i>niaD</i>} :: <i>dipA</i> ^{cDNA} :: <i>cyfp</i> :: <i>niaD</i> ^T / P _{<i>niiA</i>} :: <i>denA</i> ^{cDNAS243D-S245D-S253D} ::: <i>nyfp</i> :: <i>niiA</i> ^T ; <i>ptrA</i> ^R	This study
pME4418	P _{<i>niaD</i>} :: <i>cyfp</i> :: <i>niaD</i> ^T / P _{<i>niiA</i>} :: <i>denA</i> ^{cDNA} ::: <i>nyfp</i> :: <i>niiA</i> ^T ; <i>ptrA</i> ^R	This study
pME4419	AN10959::5 ['] <i>dipA</i> :: <i>dipA</i> ^{D51A;H73A;D76A} :: <i>gfp</i> ::: <i>nat</i> ^R ::3 ['] <i>dipA</i> in pJET1.2/blunt	This study
pME4420	AN10959::5 ['] <i>dipA</i> :: <i>dipA</i> ^{D51A-H73A-D76A} ::: <i>6xhis</i> :: <i>pyrG</i> ::3 ['] <i>dipA</i> in pJET1.2/blunt	This study

P = promoter; T = terminator; R = resistance; *nat* = nourseothricin; *ptrA* = pyrithiamine; *phleo* = phleomycin; af = *Aspergillus fumigatus*

Table 3: Oligonucleotides used in this study.

Designation	5' – sequence – 3'	Size
MC1	GTA ATC GAT GTC ATC GCT GAA AAG GG	26mer
MC2	CCT GCG GCC GCT CTA CAT GGG TAT GAC TAG AG	32mer
MC30	CAA TGC GCG ACG GAG GGC TAG G	22mer
MC125	TAC CGA GAC TAT CAA GGG AC	20mer
MC126	CAT CTA GGC CTC GTG GCT GGT GTT GTT GG	29mer
MC127	ACC AGC CAC GAG GCC TAG ATG GCC TCT TGC	30mer
MC128	ACA ATG AGA TGG GCC ACT CAG GCC AAT TGA	30mer
MC129	CTG AGT GGC CCA TCT CAT TGT ACG GTT CAG G	31mer
MC130	TAC TCG AGC GCT GCA AAA CGA AAC ACC A	28mer
MC171	TCA CAT GAT ATA GAC GTT GTG GCT	24mer
MC175	ATC AAG ACC CGA GGC AAT TTG AC	23mer
MC176	CAG GCG CTC TAC ATG AGC ATG CCC TGC CCC TGA TAG TTG GCC CGA CCG CTT CTA C	55mer
MC177	CTT TTT CCA TCT TCT CTT ACC ACC GCT ACC ACC CTC AAT ACG CGG CGG ACT CCT C	55mer
MC178	ATC GCC GAA TCA GAG GCC AAT GT	23mer
5'RT MC1	GAC GAT TCA CCA ACC CAA GAG A	22mer
3'RT MC2	CTA CCT TCC AGC CAC CCA AAC T	22mer
5'RT H2A	TGC GGT CGT GTT AAG CGT TT	20mer
3'RT H2A	CGG ATG GCA AGC TGT AGG TG	20mer
OLKM67	CCA TAA CCC TAT TGC CAC TAG	21mer
OLKM68	GTA TGG GAT AGG AAA ATA ATA TAG	24mer
JS89	ATG CGC CCG GCC TGC AAG	18mer
JS90	AAC AGA AGG TCA TGA ACC ACG CCG ACA AGC AGA AGA ACG	39mer
JS91	TCA CTT GTA CAG CTC GTC CA	20mer
JS92	GCC GTT CTT CTG CTT GTC GGC GTG GTT CAT GAC CTT CTG TTT	42mer
JS93	CGC CCG GCC TGC AAG ATC	18mer
JS96	ATG GCT TCT CCC CGT CCC	18mer

Designation	5' – sequence – 3'	Size
JS97	CAG GAT CTT GCA GGC CGG GCG GGC GTC GCC AGA TGC AGC	39mer
JS131	GAT ATC GAC AAC CTC TCC ACT TAT	24mer
JS132	TAC CAA TGG GAT CCC GTA ATG GGG AGG AAG CAA GCC AAG	39mer
JS133	CCT TGG CTT GCT TCC TCC CCA TTA CGG GAT CCC ATT GGT AA	41mer
JS134	TAA TAG GTC AAA GTC ATG CCG CAT CTT TGT TTG TAT TAT ACT G	43mer
JS135	TAT AAT ACA AAC AAA GAT GCG GCA TGA CTT TGA CCT ATT AG	41mer
JS136	GAT ATC GAA GCT TGA CTT ATT TGG T	25mer
JS148	AGC TCT GGA GGA CCA TGC G	19mer
JS150	CGC ATG GTC CTC CAG AGC TGC CTT AGC CCC TTC AGG AAA GA	41mer
JS158	CGC ATG GTC CTC CAG AGC TGA CTT AGA CCC TTC AGG AAA G	40mer
JS162	TAC GCG GCG GGG CCC TCG ATT TCT TTC CTG AAG	33mer
JS163	TAC GCG GCG GGT CCC TCG ATT TCT TTC CTG AAG	33mer
JS167	CCG CCG CGT ATT GAG GGT	18mer
JS168	GCT CAC CAT ACC ACC GCT ACC ACC GGC GTC GCC AGA TGC AG	41mer
JS169	TAA TAG GTC AAA GTC ATG CCT CAG GGG CAG GGC ATG CT	38mer
JS170	AGC ATG CCC TGC CCC TGA GGC ATG ACT TTG ACC TAT TA	38mer
JS171	CAT ATG CCA TCT CGC ACC CT	20mer
JS172	CAT ATG GTA TAG TCT GGT CTT A	22mer
JS180	AGA TCT CGA CAA TTT TCC GAG A	22mer
JS181	ACC CAA CAA CCA TGA TAC CAC AGT GCT GAG TGC TGG AGC	39mer
JS182	AGC TCC AGC ACT CAG CAC TGT GGT ATC ATG GTT GTT GGG T	40mer
JS183	CTG AAC CGT ACA ATG AGA TGA GCA TCC ACA TGA TCG ACA G	40mer

Designation	5' – sequence – 3'	Size
JS184	TGT CGA TCA TGT GGA TGC TCA TCT CAT TGT ACG GTT CAG G	40mer
JS185	AGA TCT TCG ATT AAA TTC TGC CA	23mer
JS201	CCT CGA TTT CTT TCC TGA AGG	21mer
JS202	CTT CAG GAA AGA AAT CGA GGG CCC CGC CGC GTA TTG AG	38mer
JS203	CTT CAG GAA AGA AAT CGA GGG ACC CGC CGC GTA TTG AG	38mer
JS204	CTC AAT ACG CGG CGG GGC CCT CGA TTT CTT TCC TGA AGG GGC TAA GGC AGC TGA TC	56mer
JS205	CCG CCG CGT ATT GAG CGC	18mer
JS206	CTC AAT ACG CGG CGG GTC CCT CGA TTT CTT TCC TGA AGG GTC TAA GTC AGC TGA TC	56mer
JS219	GTT TTT CAG CAA GAT CAT ATG CCA TCT CGC ACC CT	35mer
JS220	ATC TTC TAG AAA GAT CAT ATG GTA TAG TCT GGT CTT A	37mer
JS221	TCG CAC AGC TGC AAT ACA CAA AAT TCT TAC TGG GC	35mer
JS222	ATT GCA GCT GTG CGA GGT ATG TCC CTG CGC AAT TA	35mer
JS223	CAA AAG CAC CGG TAG CGA TAA TGT GGT CTG CGC GGG CTT G	40mer
JS224	TAT CGC TAC CGG TGC TTT TGG TTT TTA CGA TGA TAC TTC G	40mer
JS225	CAT CAC CAT CAC CAT CAC TGA AAT TCG CCT CAA ACA ATG CT	41mer
JS226	CTA ATA GGT CAA AGT CAT GCC CTG TCT GAG AGG AGG CAC T	40mer
JS227	AGT GCC TCC TCT CAG ACA GGG CAT GAC TTT GAC CTA TTA G	40mer
JS228	TCA GTG ATG GTG ATG GTG ATG ACC ACC GCT ACC ACC GGC GTC GCC AGA TGC AGC	54mer
ÖZG192	TCA GGG GCA GGG CAT GCT CAT GTA GAG	27mer
ÖZG207	GGT GGT AGC GGT GGT ATG GTG AGC	24mer
ÖZG209	GGT GGT AGC GGT GGT AAG AGA AGA TGG AAA AAG AAT TTC ATA G	43mer

A = adenine; C = cytosine; G = guanine; T = thymine

2.4.3 Recombinant DNA methods

PCR reactions were performed with various DNA polymerases, including *Taq*, *Pfu* or Phusion High-Fidelity (THERMO SCIENTIFIC GMBH, Schwerte, D). Restriction enzymes were purchased from THERMO SCIENTIFIC GMBH (Schwerte, D). All reactions were performed as described in manufacturer's instructions.

2.4.4 DNA isolation and hybridization

Extraction of DNA from agarose gels was performed using the QIAquick Gel Extraction Kit (QIAGEN, Hilden, D). Isolation of plasmid DNA from *E. coli* was carried out using the QIAGEN Plasmid MINI-Kit or the QIAGEN Plasmid Plus Midi Kit. Instructions were followed according to user's manual. Genomic DNA from *A. nidulans* was isolated as described previously (Lee, 1990). Southern hybridization was performed using the non-radioactive AlkPhos Direct Labeling and Detection System referring to manufacture's instructions (GE HEALTHCARE, München, D).

2.4.5 Sequence analyses

Plasmids were sequenced at the Göttingen Genomics Laboratory and at SeqLab Sequence Laboratories Göttingen. Respective sequences were analyzed with the software of Lasergene (DNA STAR INC., Madison, WI, USA) and 4Peaks (MEKENTOSJ, Amsterdam, NL). Gene information was provided by CADRE (Mabey Gilsenan *et al*, 2012) or AspGD (Cerqueira *et al*, 2014).

2.4.6 Quantitative real-time PCR

Aspergillus nidulans total RNA was obtained from 0.3 ml of ground mycelia by using RNeasy Plant Kit (QIAGEN, Hilden, D), referring to the manufacture's specifications. cDNA synthesis was performed in duplicates by using 0.8 µg of RNA with the QuantiTect Reverse Transcription Kit (QIAGEN, Hilden, D). Amplification was performed in a LightCycler 2.0 (ROCHE, Basel, CH) by the use of the RealMaster SYBR Rox Kit (5PRIME GMBH, Hamburg, D). Applied real-time (RT) primers are listed in table 3. Amplification conditions were as follows: 95°C for 2:20 min, 95°C

for 0:20 min, 60°C for 0:22 min, 72°C for 0:22 min, 39 cycles, 95°C for 0:10 min, melting curve 65°C to 95°C. Increment 0.5°C. Gene of interest relative to histone *h2A* RNA was quantified using the Δ CT method (Pfaffl *et al*, 2002).

2.5 Protein methods

2.5.1 Protein isolation and western hybridization analyses

A. nidulans mycelium was harvested at indicated time points, dried with paper towels and frozen in liquid nitrogen. Proteins from *A. nidulans* were isolated using ground mycelia and extraction buffer B* (100 mM Tris-HCl pH 7.5, 300 mM NaCl, 10% glycerol, 2 mM EDTA pH 8.0, 0.02% NP-40, freshly supplemented with 2 mM DTT and Complete protease inhibitor cocktail (ROCHE, Basel, CH)). In case of identification of DenA phosphorylation sites phosphatase inhibitor mix (1 mM NaF, 0.5 mM sodium-orthovanadate, 8 mM β -glycerolphosphate disodium pentahydrate) was added to all respective buffers. Protein concentration was determined by a modified Bradford assay (Bradford, 1976) with Roti-Quant assay solution (ROTH) (25% Bradford assay solution, 75% H₂O). Protein solutions were transferred to a 96-wellplate and for measurement of protein concentration the 96-plate reader was used (BIO-RAD LABORATORIES GMBH, München, D) with the Magellan (TECAN, Männedorf, CH) software (M200). The extinction rate was measured at 595 nm and the protein concentration was equalized with a BSA-standard system, which ranged from 0.1 mg/ml to 2.0 mg/ml. For SDS-PAGE, proteins were mixed with 3x sample buffer (250 mM Tris-HCl pH 6.8, 15% β -mercaptoethanol, 30% glycerol, 7% SDS, 0.3% bromphenol blue). After denaturation at 95°C for 8 minutes, equal amounts of proteins were separated by 12% SDS-PAGE gels. Proteins were transferred onto nitrocellulose membrane (WHATMAN GMBH, DASSEL, D). The PageRuler Prestained Protein Ladder (THERMO SCIENTIFIC GMBH, Schwerte, D) was used as molecular weight standard. In case of protein samples derived from asexual development Ponceau S (SIGMA-ALDRICH, 0.2% Ponceau S, 3% TCA) was used as reference for equally loaded protein amounts because the level of housekeeping proteins such as actin vary during development and Ponceau staining does not rely on a single protein for normalization or loading control (Romero-Calvo *et al*, 2010). Blocking was

conducted using 5% milk powder (SUCOFIN) dissolved in TBS/T buffer (10 mM Tris-HCl pH 8.0, 150 mM NaCl, 0.05% Tween 20). Detection was performed using the Enhanced ChemiLuminescence method (Tesfaigzi *et al*, 1994). The signal intensity was recorded and quantified with the Fusion-SL7 system and the Bio1D software (PEQLAB BIOTECHNOLOGIE GMBH, Erlangen, D).

2.5.2 Antibodies

Membranes were probed with primary antibodies such as calmodulin-binding protein antibody (04-932, MILLIPORE, Billerica, MA, USA), phosphoserine/threonine antibody (ab17464, ABCAM, Cambridge, UK), GFP antibody (sc-9996, SANTA CRUZ BIOTECHNOLOGY, Santa Cruz, CA, USA), tubulin antibody (T0926, SIGMA-ALDRICH), cullinA, cullinC or Nedd8 antibody (GENSCRIPT, Piscataway, NJ, USA). As secondary antibodies horseradish peroxidase-coupled rabbit antibody (G21234, INVITROGEN) or mouse antibody (115-035-003, JACKSON IMMUNORESEARCH, Newmarket, UK) was used.

2.5.3 Co-purification methods

2.5.3.1 Tandem affinity purification (TAP)-tag purification

Proteins extracted from ground mycelia were incubated with 400 µl IgG-agarose (GE HEALTHCARE, München, D) for 2 h on a rotating platform at 4°C. The suspension was filtered with a PolyPrep column (BIO-RAD LABORATORIES GMBH, München, D). The remaining beads were washed twice with 10 ml IPP300 (25 mM Tris-HCl pH 8.0, 300 mM NaCl, 0.1% NP-40, 2 mM DTT), once with 10 ml IPP150 (25 mM Tris-HCl pH 8.0, 150 mM NaCl, 0.1% NP-40, 2 mM DTT), and once with 10 ml tobacco etch virus (TEV) cleavage buffer (25 mM Tris-HCl pH 8.0, 150 mM NaCl, 0.1% NP-40, 0.5 mM EDTA, 1 mM DTT). Columns were closed and 300 units of TEV protease in 1 ml of TEV cleavage buffer was added and incubated on a rotating platform overnight at 4°C. Cleaved proteins were eluted into a fresh PolyPrep column containing 300 µl calmodulin affinity resin (AGILENT TECHNOLOGIES GMBH, Waldbronn, D), equilibrated with 5 ml of calmodulin binding

buffer (CBB: 25 mM Tris-HCl pH 8.0, 150 mM NaCl, 1 mM Mg acetate, 1 mM imidazole, 2 mM CaCl_2 , 10 mM β -mercaptoethanol). The elution step was repeated once with 1 ml of TEV cleavage buffer and 6 ml CBB as well as 6 μl of 1 M CaCl_2 , were added to the solution. The solution was incubated on a rotating platform for 2 h at 4°C. The beads were washed twice with 1 ml of CBB containing 0.1% NP-40 and once with 1 ml of CBB containing 0.02% NP-40. Bound proteins were eluted three times with 1 ml of calmodulin elution buffer (CEB: 25 mM Tris-HCl pH 8.0, 150 mM NaCl, 0.02% NP-40, 1 mM Mg-acetate, 1 mM imidazole, 20 mM EGTA, 10 mM β -mercaptoethanol). The addition of trichloroacetic acid (TCA) to a concentration of 25% resulted in protein precipitation overnight at 4°C. The precipitate was collected by centrifugation with 16.000 rcf for 1 h at 4°C, washed with ice-cold acetone/0.05 M HCl and with acetone. Precipitated proteins were dried in a vacuum exhausted centrifuge. Proteins were resuspended in 30 μl 3x sample buffer and separated by SDS-PAGE followed either by protein staining, western hybridization or LC-MS/MS analysis.

2.5.3.2 GFP-Trap purification

For GFP-Trap purification 100-250 μl GFP-Trap beads (CHROMOTEK GMBH, Martinsried, D) were washed twice with 2.5 ml cold B* buffer (100 mM Tris-HCl pH 7.5, 300 mM NaCl, 10% glycerol, 2 mM EDTA pH 8.0, 0.02% NP-40). Protein extracts were mixed with beads and incubated on a rotating platform at 4°C for 2 h. The suspension was poured into a Bio-Rad PolyPrep column (BIO-RAD LABORATORIES GMBH, München, D). Beads were washed twice with cold W300 buffer (10 mM Tris-HCl pH 7.5, 300 mM NaCl, 0.5 mM EDTA). Subsequently, beads were washed twice with W500 buffer (10 mM Tris-HCl pH 7.5, 500 mM NaCl, 0.5 mM EDTA). Proteins bound to the beads were eluted three times by adding 150 μl 0.2 M glycine pH 2.5 for 30 secs under constant mixing followed by neutralization with 9.5 μl 1 M Tris pH 10.4. Samples were used for SDS-PAGE followed by protein staining, western hybridization or LC-MS/MS analysis. All buffers contained 2 mM DTT and Complete protease inhibitor cocktail (ROCHE, Basel, CH). For identification of DenA phosphorylation sites a phosphatase inhibitor mixture (1 mM NaF, 0.5 mM Na_3VO_4 , 8 mM β -glycerolphosphate disodium pentahydrate) was added.

2.5.4 Protein staining

After protein separation by SDS-PAGE, Coomassie staining was performed with Coomassie brilliant Blue solution (40% v/v ethanol, 10% v/v acetic acid, 1 g Coomassie brilliant blue R250 (SERVA)). Gels were covered with Coomassie solution and incubated at room temperature for 30 min under constant agitation. Destaining was performed with 12.5% v/v isopropanol, 10% v/v acetic acid at room temperature.

A more sensitive staining was achieved by using colloidal blue solution. After electrophoresis, gels were covered with fixation solution (40% v/v ethanol, 10% v/v acetic acid) for one hour. After two 10 minutes washing steps with water, the gels were incubated over night in colloidal solution (0.1% w/v Coomassie brilliant Blue G250 (SERVA), 5% w/v aluminum sulfate-14-18-hydrate, 10% v/v methanol, 2% v/v ortho-phosphoric acid). Destaining was performed using the fixation solution.

2.5.5 Tryptic in-gel digestion of proteins (Shevchenko *et al*, 2006)

Proteins were stained with Coomassie brilliant Blue. Respective bands were excised and cut into small pieces. These were treated with acetonitrile and incubated for 10 min at RT. After removing the solution, gel slices were dried in a vacuum exhausted centrifuge and subsequently covered with 10 mM DTT solution in 100 mM NH_4HCO_3 and incubated for 1 h at 56°C. DTT solution was replaced by 150 μl of 55 mM idoacetamid in 100 mM NH_4HCO_3 and incubated in the dark for 45 min at RT. The solution was replaced by 150 μl of 100 mM NH_4HCO_3 , incubated at RT for 10 min and replaced by 150 μl acetonitrile. After repeating the latter two steps, gel slices were dried in a vacuum exhausted centrifuge. Trypsin digestion buffer (1:20 sequencing grade modified trypsin (V5111, PROMEGA GMBH, Mannheim, D) in 50 mM NH_4HCO_3) was added and incubated for 45 min on ice. Gel pieces were covered with 50 mM NH_4HCO_3 followed by overnight incubation at 37°C. Samples were centrifuged at 11.000 rcf for 1 min at RT and the supernatant was collected in a new tube. Gel slices were covered with 20 mM NH_4HCO_3 , incubated at RT for 10 min and replaced by 50% acetonitrile/5% formic acid. Samples were incubated at RT for 25 min and the supernatant was collected after 1 min centrifugation. Both extraction steps were repeated twice. The achieved solution was evaporated in a vacuum exhausted centrifuge. Precipitated proteins were dissolved in 20 μl 95% H_2O /5% acetonitrile/0.1% formic acid and analyzed with LC-MS/MS.

2.5.6 Identification of proteins and phosphorylation sites by tandem mass spectrometry

Liquid chromatography coupled either to a LCQ DecaXP mass spectrometer or an Orbitrap Velos Pro™ Hybrid Ion Trap-Orbitrap mass spectrometer (THERMO SCIENTIFIC GMBH, Schwerte, D) was employed for protein and phospho peptide identification, respectively. 1 to 6 µl of peptide containing sample solution were trapped and washed with 100% solvent A (98% water, 2% acetonitrile, 0.07% trifluoroacetic acid) on an Acclaim® PepMap 100 pre-column (#164564, 100 µm x 2 cm, C18, 3 µm, 100 Å, THERMO SCIENTIFIC GMBH, Schwerte, D) with a flow rate of 25 µl/min for 6 min. An Acclaim® PepMap RSLC column (#164540, 75 µm or 50 cm, C18, 3 µm, 100 Å, THERMO SCIENTIFIC GMBH, Schwerte, D) was used for analytical peptide separation by reverse phase chromatography. This was performed by typically applying a gradient from 98% solvent A (water, 0.1% formic acid) and 2% solvent B (80% acetonitrile, 20% water, 0.1% formic acid) to 42% solvent B within 95 min and to 65% solvent B within the next 26 min at a flow rate of 300 nl/min (solvents and acids from THERMO SCIENTIFIC GMBH, Schwerte, D). On-line ionization of chromatographically eluting peptides was performed with the nanoelectrospray (nESI) using the Nanospray Flex Ion Source (THERMO SCIENTIFIC GMBH, Schwerte, D) at 2.4 kV followed by a continuous transfer into the mass spectrometer. Full scans of the mass range of 300-1850 m/z were applied with the Orbitrap-FT analyzer at a resolution of 30,000 with parallel data-dependent top ten MS2 collision-induced dissociation (CID) fragmentation within the LTQ Velos Pro linear ion trap. CID fragmentation was used to analyze phospho peptide samples by applying the multistage activation (MSA) method as well as higher energy collisional dissociation (HCD) fragmentation in independent runs. When HCD fragmentation was performed, data-dependent top five MS2 fragmentation was used and fragment ions were analyzed in the orbitrap. The software XCalibur 2.2 was used for LC-MS method programming and data acquisition. The evaluation of phosphorylation site probabilities was performed by using phosphoRS and for identification of proteins MS/MS2 data were analyzed against the *A. nidulans* genome database (Cerqueira *et al*, 2014) using the Sequest and Mascot search engine and the Proteome Discoverer Software version 1.4 (Olsen & Mann, 2004; Olsen *et al*, 2006). Trypsin was used for sample digestion and a maximum of two missed cleavage sites was considered. For identification of DenA phosphorylation sites phosphopeptide enrichment with TiO₂

columns (GLYGEN CORPORATION, Columbia, MD, USA) was performed prior to LC-MS/MS analysis. Carbamidomethyl at cysteines was set as fixed modification, whereas oxidation of methionines and phosphorylation of serines, threonines, and tyrosines were considered as variable modifications. Mass tolerances of precursors and fragment ions were 10 ppm and 0.6 Da, respectively. False discovery rates were calculated with the Proteome Discoverer using the revert-decoy mode. The filter for valid peptide sequence matches was set to 0.01.

2.5.7 Phos-tag Acrylamide

For determining the phosphorylation status of DenA the Phos-tag based Mobility Shift Detection of Phosphorylated Proteins (WAKO CHEMICALS GMBH, Neuss, D) was used. All solutions required were prepared according to manufacture's instructions. 100 µl of Phos-tag AAL-107 dissolved in methanol and water was directly added to SDS-gels. After electrophoresis the proteins were fixed in the gel by soaking in fixation solution (50% H₂O, 40% v/v methanol, 10% v/v acetic acid) for 10 min with gentle agitation. Proteins were stained using Coomassie colloidal Blue solution for 2 h at RT and washed in destaining solution.

2.5.8 Computational methods

The acquisition of gene and protein accession numbers as well as BLAST searches were performed at the National Center for Biotechnology Information (Geer *et al*, 2010). Protein information was provided by CADRE (Mabey Gilsenan *et al*, 2012) or AspGD (Cerqueira *et al*, 2014). Multiple sequence alignment was performed using MultAlign (Corpet, 1988).

2.6 Fungal physiology and cell biology

2.6.1 Stress-Test

For applying stress conditions 0.04 mM menadione or 0.015% SDS was added to the agar. 5000 spores of each strain were point-inoculated on solid agar plates. Strains were incubated for four days at 37°C at constant white light exposure.

2.6.2 Microscopy

A. nidulans colonies were visualized with an OLYMPUS CS30 digital camera combined with an OLYMPUS SZX-ILLB2-200 binocular. Pictures were processed with the cellSens software (OLYMPUS DEUTSCHLAND GMBH, Hamburg, D). For fluorescence microscopy 500-2000 spores of each strain were inoculated in an 8-well borosilicate coverglass system (THERMO SCIENTIFIC GMBH, Schwerte, D) containing 400 µl liquid minimal medium and incubated at 37°C for 14-24 h. Microscopy was performed with a ZEISS Axio Observer Z.1 system with ZEISS PlanAPOCHROMAT 63x/1.4oil (CARL ZEISS AG, Oberkochen, D). Pictures and movies were obtained with a QuantEM:512SC (PHOTOMETRICS, Tucson, AZ, USA) or a Coolsnap HQ² (PHOTOMETRICS, Tucson, AZ, USA) camera and the SlideBook 5.0 imaging software (INTELLIGENT IMAGING INNOVATIONS INC., Göttingen, D). Membranes were stained with 1 mM FM4-64 (INVITROGEN) and mitochondria with 50 nM MitoTracker Red CMXRos (INVITROGEN). Nuclei were visualized with ectopically integrated *h2A::rfp*. Exposure times for GFP: 1000 ms, RFP: 100 ms, DIC: 100 ms and in BiFC experiments exposure times were YFP: 1000 ms, RFP: 100 ms, DIC: 100 ms.

2.6.3 Quantification methods

Radial growth tests were performed by point-inoculation of 5000 spores. Plates were incubated at 37°C for six days and colony diameter was measured each day.

Quantification of conidiospores was performed by point-inoculation of 5000 spores. Plates were incubated at 37°C for three days and distinct regions of the colony were excised with the end of a 0.2 ml tip, vortexed for 30 min in 0.5 ml of saline. Spores were counted using a THOMA counting chamber or a Coulter Z2 particle count and size analyzer (BECKMANN COULTER GMBH, Krefeld, D).

To quantify septa within vegetative hyphae, hyphal membranes were stained (including septa) with 1 mM FM4-64 (INVITROGEN). The amount of formed septa was counted and the average septa distance was calculated.

Pixel density values for quantification of the western hybridization signals were quantified using the Bio1D software (PEQLAB BIOTECHNOLOGIE GMBH, Erlangen, D).

3 Results

3.1 Deneddylase deficient *A. nidulans* strains accumulate neddylated cullins

Cycles of neddylation and deneddylation regulate various substrates, including cullin-RING ligases, which target proteins for ubiquitin-dependent degradation. The two deneddylases CSN and DenA/DEN1 possess different functions regarding deneddylation specificity. In *A. nidulans* deletion of CSN or DenA encoding genes lead to impaired deneddylation, which results in accumulation of different subsets of neddylated proteins (Christmann *et al*, 2013; Beckmann *et al*, 2015). This suggests that the substrate specificity for both deneddylases is not identical. Whether overlapping substrates exist that become deneddylated by both deneddylases, was studied in more detail. For this purpose, the neddylation level of CSN specific substrates namely fungal CUL1 (CulA) or CUL3 (CulC) was analyzed in different deneddylase deficient strains. A strain impaired in CSN activity was represented by a *csnE* deletion strain, which lacks the catalytic active CSN subunit. This mutant was compared to wild type, *denA* deletion strain and to a *csnE/denA* double deletion strain. Western hybridizations with protein crude extracts of vegetative grown strains were performed using CulA or CulC antibodies. In wild type a slight signal at a molecular weight corresponding to 100 kDa represented the cullin variant that is modified with Nedd8 (Figure 11A & 11B). A prominent lower migrating signal displayed the respective unneddylated cullin version. In wild type around $75\% \pm 5\%$ of overall CulA and $92\% \pm 1\%$ of CulC were present in their unneddylated form (Figure 11A & 11B, lower panels). In general, all deletion strains revealed an increase in neddylated cullins, independent of the analyzed cullin. The most dominant signal of neddylated CulA or CulC was achieved upon *csnE* deletion, which resulted, depending on the respective cullin, in a two to seven fold increase of the neddylation intensity when compared to wild type. Deletion of *denA* resulted only in a slight enhanced amount of neddylated cullins. In contrast to the single deletion strains, in the *csnE/denA* double mutant almost no signal was detected for the unmodified cullins, but instead a slower migrating signal appeared. This cullin version with an increased molecular weight was exclusively detected in the double deletion strain and suggests the existence of cullins, which are modified with multiple Nedd8 molecules (marked with asterisks in Figure 11A & 11B).

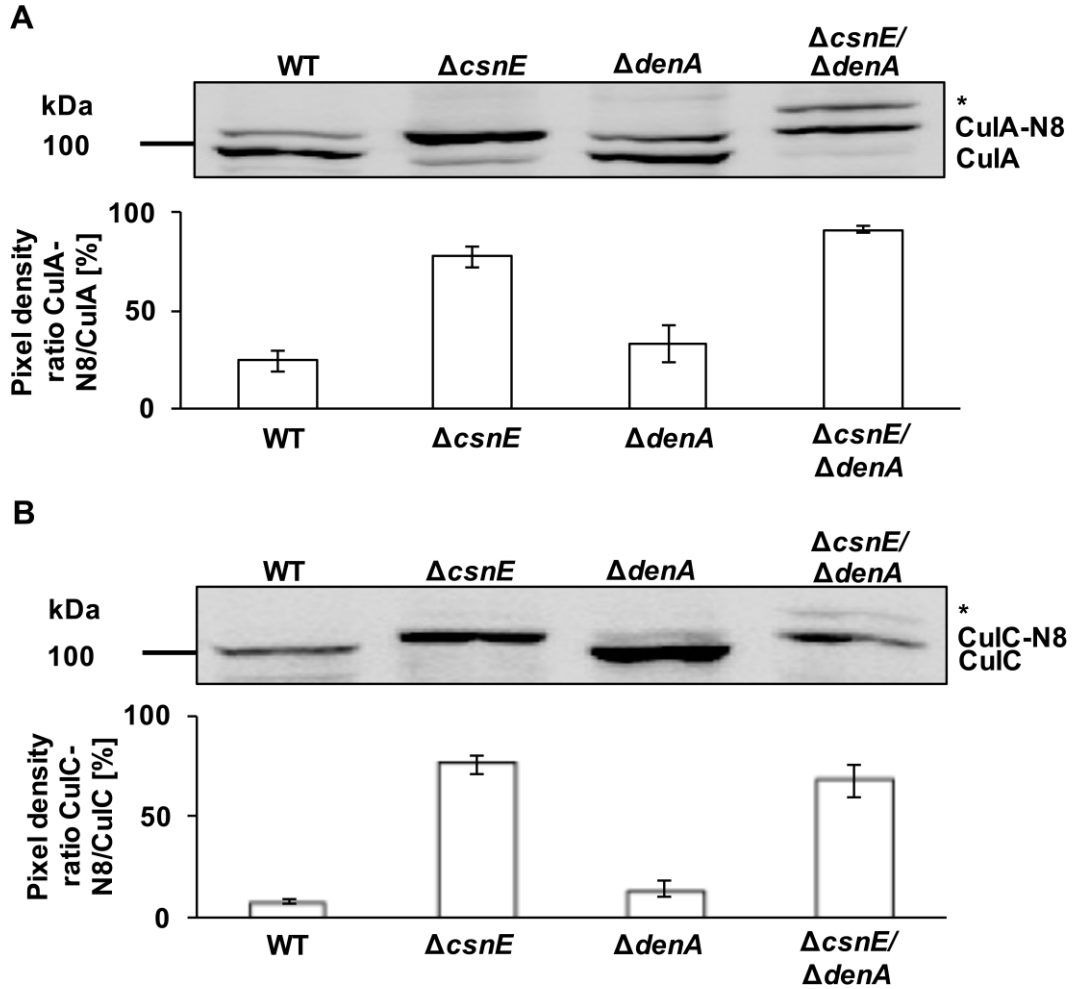


Figure 11: Influence of CSN and DenA on CulA or CulC deneddylation.

Western hybridizations of wild type (WT) and deneddylase deficient strains. Protein crude extracts from vegetative grown mycelia of WT, $\Delta csnE$, $\Delta denA$ and $csnE/denA$ double deletion strains were compared. Cullin versions of CulA (A) or CulC (B) were visualized using cullinA or cullinC antibody, respectively. Detected bands represent unneddylated cullins (CulA/CulC), mononeddylated cullins (CulA-N8/CulC-N8) and multineeddylated cullins (marked with asterisks). The ratio of neddylated CulA and CulC to the respective deneddylated protein versions was calculated (lower panels). Three independent experiments were used to generate these data. The mean values with standard deviations are shown.

These results corroborate that the CSN complex is the main deneddylating enzyme for mononeddylated cullins, whereas DenA possesses only a slight affinity towards these neddylated substrates. Cullins with higher molecular weight accumulated in a strain defective in both deneddylases. As these cullin variants were absent in the deneddylase single deletion strains and appeared only in the $denA/csnE$ double deletion strain, both fungal deneddylases are presumably able to process multineeddylated cullins to yield a mononeddylated variant.

3.2 Accumulation of neddylation proteins caused by an impaired CSN complex can be reduced by elevated *denA* expression

The deneddylases DenA/DEN1 and CSN deconjugate Nedd8 from modified substrates, where neddylation cullins represent the main targets of the CSN (Enchev *et al*, 2012; 2015). It was analyzed whether increased DenA amount affects neddylation proteins that accumulate in strains with defects in the CSN deneddylase activity. The focus was on the overall protein neddylation intensities in strains with different genetic backgrounds. Of special interest was a *csnG* deletion strain, which is impaired in the main CSN interaction partner of DenA as well as on a *csnE* mutant strain, lacking the deneddylase subunit that possesses activity towards neddylation cullins.

To increase the cellular amount of DenA, its encoding gene under control of an inducible promoter was ectopically integrated into wild type, *csnG* or *csnE* mutant strains. Expression levels of *denA* in vegetative hyphae were verified by qRT-PCR (data not shown). Transformants with similar elevated *denA* expression were selected to assure a reliable comparison between all tested strains. To study the impact of elevated DenA levels on neddylation substrates, which accumulate due to impaired CSN activity, protein crude extracts of vegetative grown wild type, overexpression *denA* (OE *denA*), $\Delta csnG$, $\Delta csnG$ /OE *denA*, $\Delta csnE$ and $\Delta csnE$ /OE *denA* strains were compared by western hybridization using Nedd8 antibody. In wild type and in the OE *denA* strain an intense signal corresponding to neddylation cullins could be detected at a molecular weight of around 100 kDa (Figure 12A). In strains deleted for *csnG* and *csnE* an increase of overall neddylation proteins was observed. The accumulation of neddylation proteins included cullins as well as putative non-cullin proteins with a wide variety of smaller molecular weights. In strains deleted for *csnG* or *csnE* the intensity of neddylation proteins, was 2.5 fold of the value that was detected for wild type or OE *denA* strains (Figure 12B). Overexpression of *denA* in a *csnE* mutant ($\Delta csnE$ /OE *denA*) did not affect the neddylation pattern as similar intensities were observed in the presence or absence of OE *denA*. In contrast, elevated DenA amount in a *csnG* deficient strain ($\Delta csnG$ /OE *denA*) reduced neddylation proteins, meaning that the overall neddylation profile of $\Delta csnG$ /OE *denA* strain was similar to the pattern that was detected in wild type.

These data indicate that increased levels of DenA can partially counteract the accumulation of neddylation proteins caused by an impaired CSN complex.

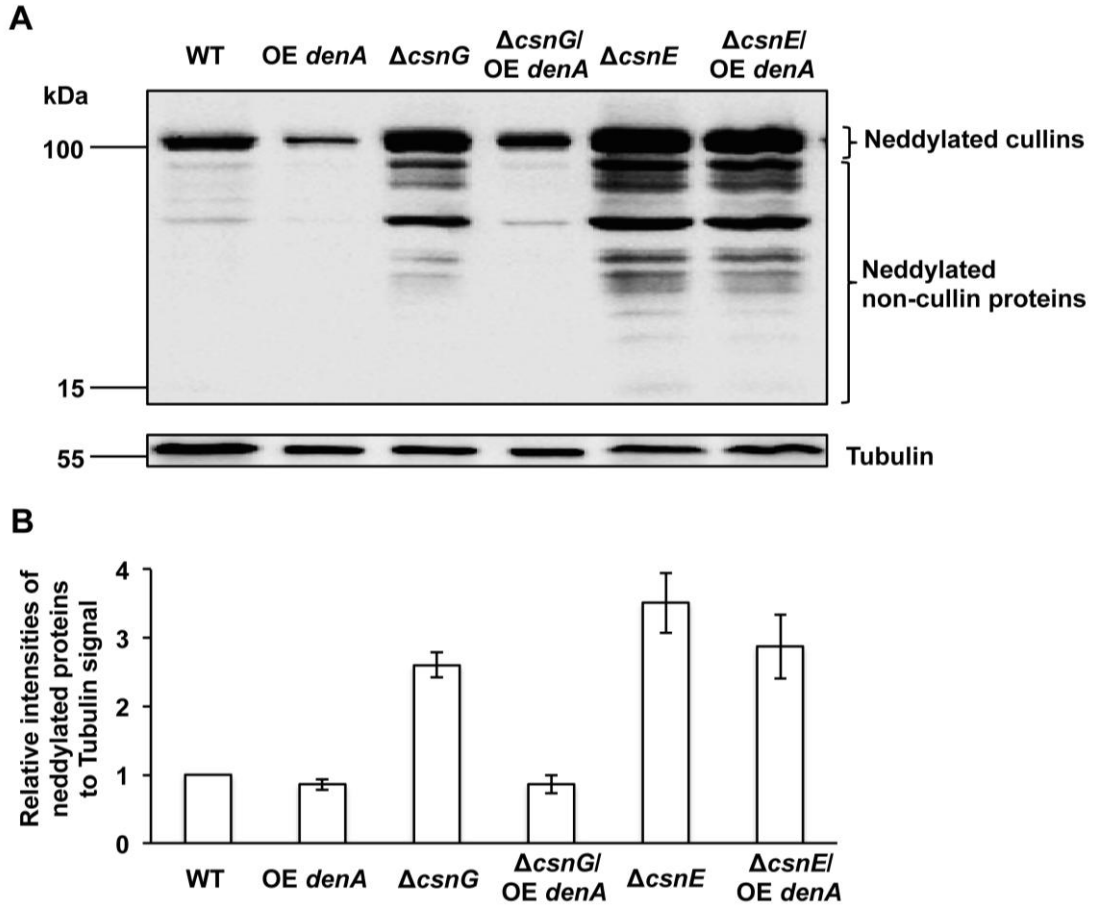


Figure 12: Changes in deneddylase activity and its consequences for the cellular pool of neddylated proteins.

(A) Western analyses of wild type (WT) compared to mutant strains with altered deneddylase activity (increased *denA* (OE *denA*), decreased COP9 signalosome (Δ *csnG*, Δ *csnE*) and combinations of defective CSN and increased *denA* (Δ *csnG*/OE *denA*, Δ *csnE*/OE *denA*)). Protein crude extracts from vegetative grown mycelia were probed with Nedd8 antibody and the membrane was re-probed with Tubulin antibody as loading control. Neddylated cullins correspond to \approx 100 kDa and faster migrating bands are summarized as neddylated non-cullin proteins. (B) Semi-quantitative analyses of Nedd8 signal intensity of the same strains as shown in (A). Normalization of respective signals was achieved by quantification to Tubulin signals. Three independent experiments were used to generate these data. The mean values with standard deviations are shown.

3.3 High copy of *denA* affects the ratio of neddylated to deneddylated cullins in *csnG* but not in *csnE* deletion strain

The effect of increased DenA amount on neddylation levels of CSN specific substrates, represented by CulA or CulC, was analyzed in *csn* deficient strains. Protein crude extracts of vegetative grown wild type, overexpression *denA* (OE *denA*), Δ *csnG*, Δ *csnG*/OE *denA*, Δ *csnE* and Δ *csnE*/OE *denA* strains were compared.

Western hybridizations using corresponding antibodies revealed that in wild type cells most of the cullins were unneddylated, resulting in less than 20% of the total cellular protein of CulA or CulC being neddylated (Figure 13A & 13B).

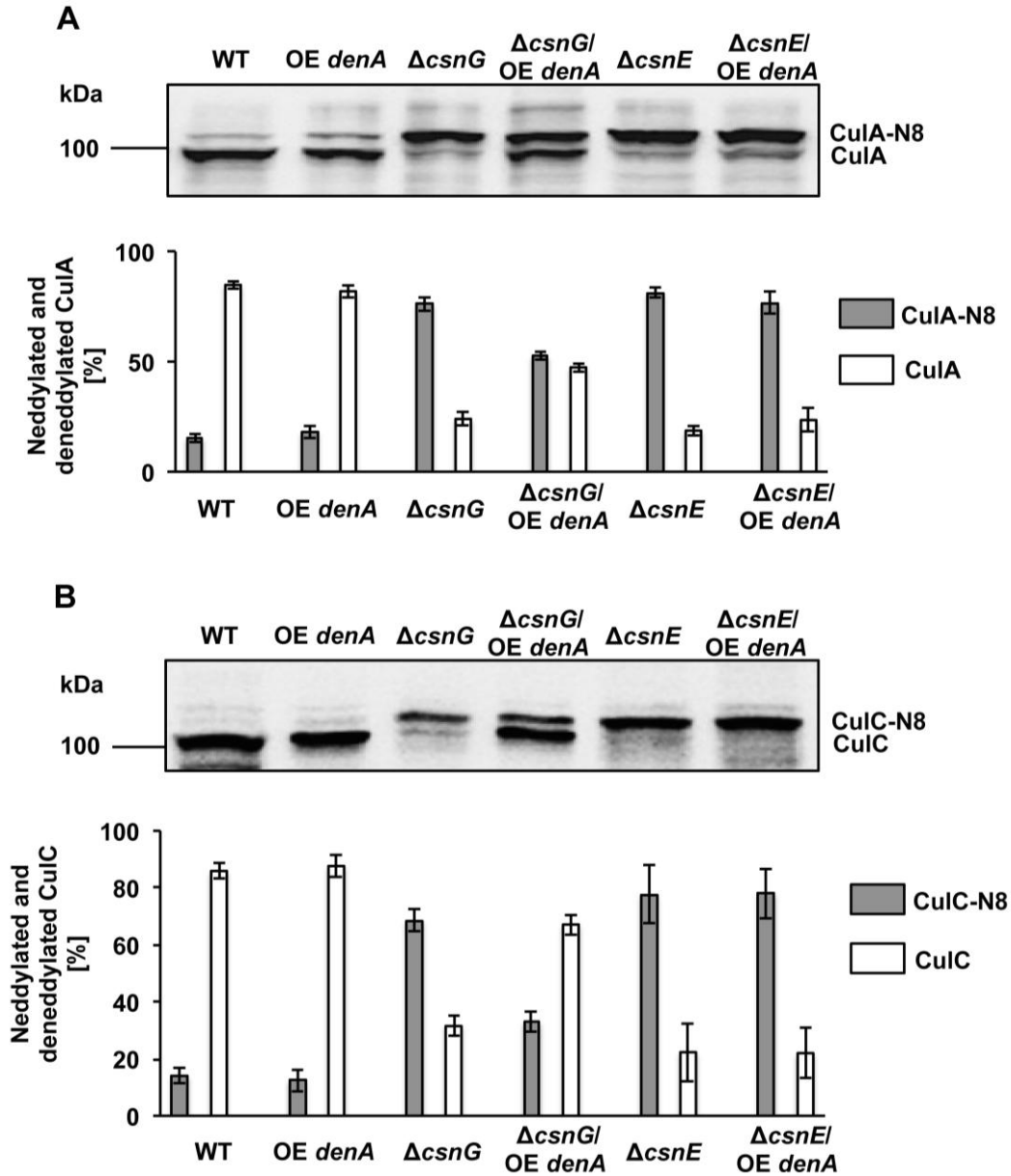


Figure 13: Changes in deneddylase activity and its consequences for the cellular pool of neddylated CulA or CulC.

Western analyses of *A. nidulans* wild type (WT) compared to mutant strains with altered deneddylase activity either achieved by overexpression of *denA* (OE *denA*), deletion of CSN subunit encoding genes ($\Delta csnG$, $\Delta csnE$) or combinations of defective CSN and increased *denA* expression ($\Delta csnG$ /OE *denA*, $\Delta csnE$ /OE *denA*). Protein crude extracts from vegetative grown mycelia were probed with cullinA (A) or cullinC (B) antibody. The ratio of neddylated CulA (CulA-N8) and neddylated CulC (CulC-N8) to deneddylated protein versions (CulA/CulC) was determined (lower panels). Three independent experiments were used to generate these data. The mean values with standard deviations are shown.

Increased DenA amount did not affect the ratio of neddylated versus unneddylated cullins in wild type background. Deletion of either *csnG* or *csnE* reversed this ratio and resulted in a drastic increase of neddylated cullins. In both of the *csn* deletion strains 70% of total cullins were neddylated and only 30% were unneddylated cullins, corroborating the dominant impact of a functional CSN complex on cullin deneddylation. However, there were distinct effects when *denA* was overexpressed in different *csn* mutant strains. By overexpressing *denA* in a $\Delta csnE$ strain ($\Delta csnE/OE\ denA$) no influence on the cullin neddylation level was observed, which is in agreement with the overall neddylation pattern seen in figure 12A & 12B. In contrast, high levels of DenA in a *csnG* deletion strain ($\Delta csnG/OE\ denA$) changed the cullin neddylation pattern towards a higher ratio of unneddylated cullins (50% for CulA or 70% for CulC).

These findings imply that in the absence of CsnG high levels of DenA can compensate the lack of a functional CSN complex, regarding its deneddyase activity towards CSN-specific substrates, which are modified with Nedd8.

3.4 Increased *denA* expression can partially rescue asexual development in CSN deficient strain

Deletion of *csn* genes in mammals and other higher eukaryotes such as plants and insects results in embryonic lethality (Wei & Deng, 1999; Freilich *et al*, 1999; Tomoda *et al*, 2004). In contrast, *csn* deletion strains of *A. nidulans* are viable and display a pleiotropic phenotype (Busch *et al*, 2003; 2007; Nahlik *et al*, 2010; Beckmann *et al*, 2015). Deletion of *csnG* or *csnE* in *A. nidulans* is not only restricted to cause accumulation of neddylated proteins. These mutants reveal a loss of sexual development, reduced asexual spore formation and an impaired secondary metabolism, which is indicated by an accumulation of reddish orcinol derivatives within hyphae and the surrounding medium (Nahlik *et al*, 2010; Beckmann *et al*, 2015). It was studied whether the compensatory effect of DenA in *csnG* deletion strain is reflected in fungal developmental phenotypes. To analyze whether overexpressed DenA is capable to counteract developmental defects caused by an impaired CSN, asexual development of wild type, *csn* deletion strains and respective mutants with overexpressed *denA* were studied (Figure 14).

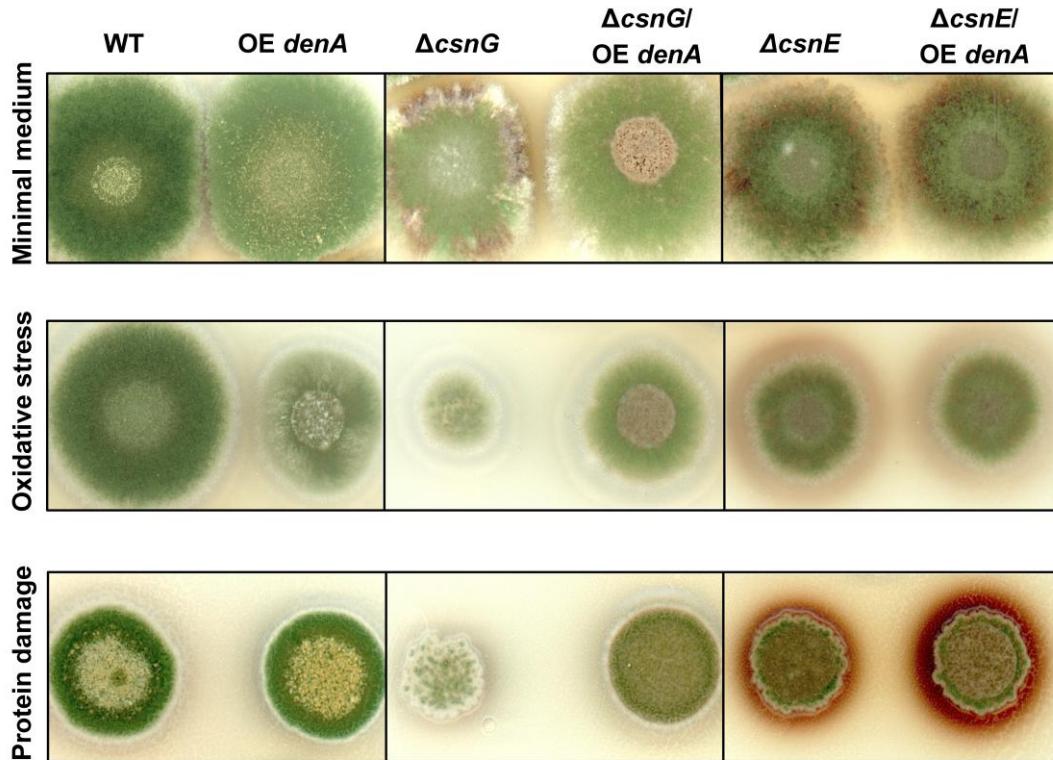


Figure 14: Impact of altered deneddylase activity on asexual development and stress response.

Equal amount of spores of wild type (WT) and strains with altered deneddylase activity represented by overexpression of *denA* (OE *denA*), *csn* deletion strains (Δ *csnG*, Δ *csnE*) and combinations of increased *denA* expression and impaired *csn* activity (Δ *csnG*/OE *denA*, Δ *csnE*/OE *denA*) were analyzed. These strains were point-inoculated and grown for four days under asexual development inducing conditions. Respective strains are either shown on minimal medium (upper panel) or stress inducing media (oxidative stress with Menadione, middle panel; protein damage with SDS, lower panel).

When grown on minimal medium increased *denA* expression in wild type background had no significant consequence on asexual development in comparison to wild type (Figure 14, upper panel). However, high DenA levels in the *csnG* mutant slightly reduced the secreted reddish dye compared to Δ *csnG* with normal *denA* expression. This indicates that elevated *denA* expression causes a reduced secretion of orcinol derivatives in *csnG* deletion strain. A similar effect was not observed when *denA* was overexpressed in Δ *csnE* strain. When grown in the presence of stress inducing agents such as menadione, causing oxidative stress, or SDS, causing protein damage, the Δ *csnG*/OE *denA* strain revealed a healthier asexual colony compared to *csnG* mutant (Figure 14, middle and lower panels). The colonies were more similar to

wild type than to respective deletion strains in respect to colony size and conidiospore production indicated by an enhanced green pigmentation. The block of sexual development in respective *csn* deletion strains was unaffected upon *denA* overexpression (data not shown) suggesting a specific impact of DenA on substrates involved in asexual development.

Taken together, these results imply that DenA can partially compensate the lack of its main CSN interaction partner CsnG but not of CsnE. In addition to the deneddylation activity of DenA against non-cullin proteins, these data suggest an auxiliary function of DenA in the absence of an intact CSN complex regarding deneddylation of nuclear CSN targets as cullins, which probably have a specific impact on asexual development and stress response.

3.5 Three PCI domain containing CSN subunits as well as the two MPN subunits destabilize DenA in the nucleus

CsnG was reported to be a binding partner of DenA and their physical interaction in the nucleus results in DenA degradation (Christmann *et al.*, 2013). It was unknown whether CsnG is the only COP9 signalosome subunit causing destabilization of DenA. Therefore, it was analyzed whether among all CSN subunits CsnG exclusively causes destabilization of DenA. The deneddylase DenA was C-terminally tagged with GFP and the respective fusion construct (*denA-gfp*) was expressed at its native locus under the endogenous promoter in wild type background and in single *csn* deletion strains. DenA-GFP protein amounts were analyzed during vegetative growth and at different time points during illumination, which induces asexual development in wild type. Western hybridization was performed using GFP-antibody and Ponceau staining was applied as loading control. The DenA-GFP fusion product was expressed and stable during vegetative growth in wild type as well as in *csnA*, *csnB* or *csnD* deletion backgrounds (Figure 15A, upper panels). When asexual conditions were induced by illumination DenA-GFP was degraded in these strains and was no longer visible after 48 h or 72 h. Free GFP, which is a stable remnant from degradation of the DenA fusion protein, accumulated during development in all tested strains.

RESULTS

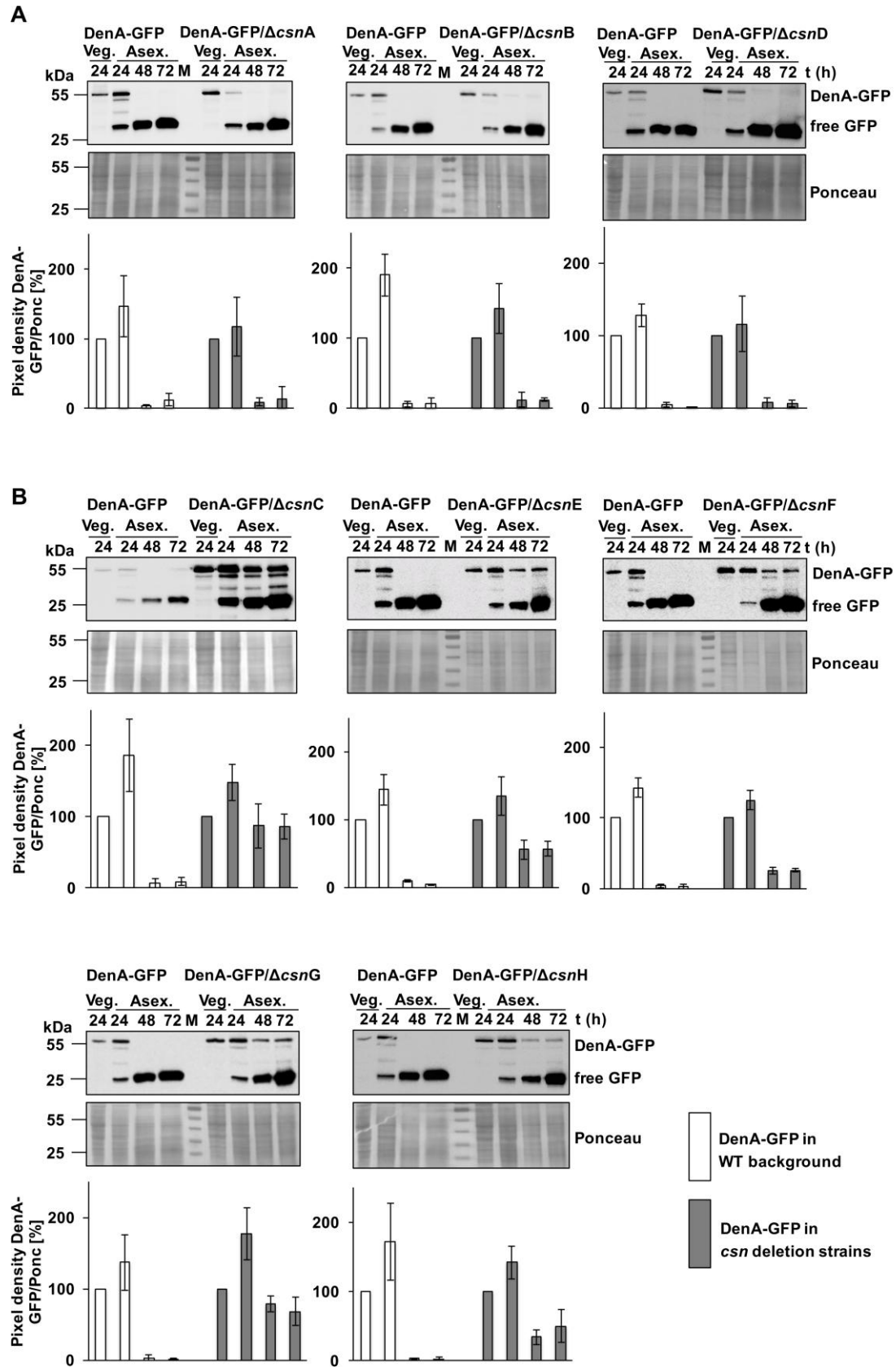


Figure 15: Protein amount of DenA-GFP in various *csn* deletion strains during development.

DenA is stable during vegetative growth but not during illumination corresponding to advanced wild type asexual development. **(A)** Protein level of DenA-GFP (54.5 kDa) is monitored in presence (*csnA*, *csnB*, *csnD*) or absence (Δ *csnA*, Δ *csnB*, Δ *csnD*) of indicated CSN subunit encoding genes by western hybridization with GFP-antibody. Protein extracts from indicated time points (in hours) of vegetative (Veg.) or illumination induced development (Asex.) were analyzed. The signal of free GFP (25 kDa) corresponds to DenA degradation. Ponceau staining was used as loading control (below). **(B)** Western hybridization with GFP-antibody on protein crude extracts of DenA-GFP in wild type in comparison to Δ *csnC*, Δ *csnE*, Δ *csnF*, Δ *csnG* or Δ *csnH* strains. Deletion of *csnC*, *csnE*, *csnF*, *csnG* and *csnH* stabilize DenA during illumination induced asexual development. The ratio of DenA-GFP and Ponceau was calculated (lower panels). Three independent experiments were used to generate these data. The mean values with standard deviations are shown. M: molecular weight marker.

In contrast, deletion of *csnC*, *csnE*, *csnF*, *csnG* or *csnH* resulted in a different effect on DenA stability. In all these strains the level of the DenA-GFP fusion protein decreased during development, but was still detectable after 72 h (Figure 15B, upper panels). This effect was most dominant in *csnC* and *csnG* deletion strains, in which around 80%, respectively 70% of the fusion product was still present at late time points of illumination (Figure 15B lower panels).

These data suggest that DenA is stable during vegetative growth and converts into an unstable protein after the induction of asexual development. Degradation of nuclear DenA requires the five intact subunits CsnC, E, F, G and H. A fully assembled COP9 signalosome seems to be not required for this developmental control of DenA stability, because the subunits CsnA, B or D are dispensable for the DenA turnover control.

3.6 DenA stability regulated by distinct phosphorylation events is required for asexual development

3.6.1 DenA is phosphorylated

Posttranslational modifications of proteins (PTMs) can affect their activity, localization, stability and interaction with other proteins (Seo & Lee, 2004; Duan & Walther, 2015). As DenA was stable during vegetative growth but became unstable during asexual development, it was studied whether DenA degradation is linked to

changes in PTMs. Previous studies demonstrated that CSN associated proteins become phosphorylated in a CSN mediated kinase reaction, which has an impact on their stability (Naumann *et al*, 1999; Bech-Otschir *et al*, 2001; Harari-Steinberg & Chamovitz, 2004; Choi *et al*, 2015). The question was addressed whether DenA is phosphorylated and if there are differences in DenA phosphorylation pattern during vegetative growth and asexual development. To enrich DenA in a highly specific manner the two-step tandem-affinity purification (TAP) was applied. DenA was C-terminally fused to the TAP-tag consisting of the calmodulin-binding protein (CBP), a tobacco etch virus protease (TEV) cleavage site and proteinA (Figure 16A).

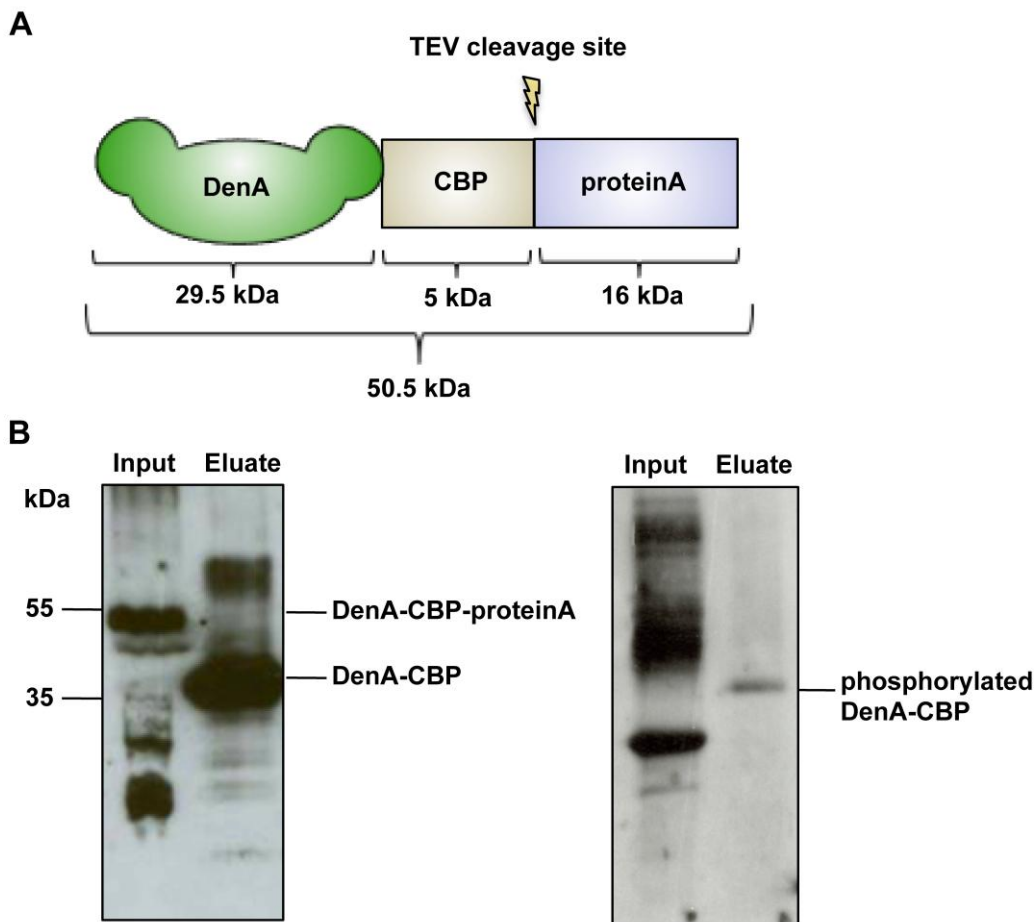


Figure 16: Enrichment of phosphorylated DenA from vegetative cultures.

(A) Illustration of C-terminally tagged DenA-CBP-proteinA fusion construct (total 50.5 kDa) for TAP purification. TEV cleavage site is indicated. (B) DenA-CBP-proteinA in the input fraction and enriched vegetative DenA-CBP (34.5 kDa) after TEV cleavage and elution were visualized by western hybridization with calmodulin-binding protein antibody (left column). Reprobing the membrane with serine/threonine phosphorylation specific antibody visualized phosphorylated DenA-CBP (right column).

The DenA-CBP-proteinA fusion construct was integrated at the native *denA* locus where it was under control of the endogenous *denA* promoter. The entire fusion protein with a molecular weight of 50.5 kDa was enriched from vegetative cultures. After cleavage with the TEV protease the molecular weight of the fusion product was reduced to 34.5 kDa. The presence of the remaining and enriched DenA-CBP was monitored by western hybridization using CBP-antibody (Figure 16B). Treatment of the membrane with serine/threonine phosphorylation specific antibody revealed several phosphorylated proteins in the input fraction and generated a single signal at the expected size of DenA-CBP in the elution sample. These data indicate that DenA is phosphorylated during vegetative conditions.

3.6.2 DenA possesses an additional phosphorylation at position S253 during asexual development

To analyze whether the conversion of a stable vegetative DenA to an unstable protein during asexual development is caused by differences in the DenA phosphorylation pattern, modifications of DenA during both conditions were compared. Instead of TAP-tag a GFP-tag fusion was used, which enables a more efficient purification method. A strain with a *denA-gfp* fusion construct (Figure 17A) under control of the endogenous *denA* promoter was used to enrich DenA-GFP by GFP-affinity purification. DenA-GFP was extracted from 24 h vegetative grown and 24 h asexually developed mycelium and DenA phosphorylation during the transition from vegetative growth to asexual development was examined. A strain with ectopically integrated GFP, driven by a constitutively active promoter, served as control (OE *gfp*). Phos-tag acrylamide gels were used to visualize DenA-GFP variants, which differ in the rate of modified phosphorylation sites. These gels displayed different mobility shifts supporting distinct phosphorylation variants for vegetative and asexually enriched DenA-GFP (Figure 17B). The control strain revealed that overexpressed GFP was not phosphorylated as it showed a pronounced single band during vegetative growth as well as after the induction of development. DenA-GFP was differentially phosphorylated during the analyzed conditions. Two vegetative in comparison to three asexual DenA-GFP versions indicated that there are developmental-specific changes in DenA phosphorylation after the induction of asexual development.

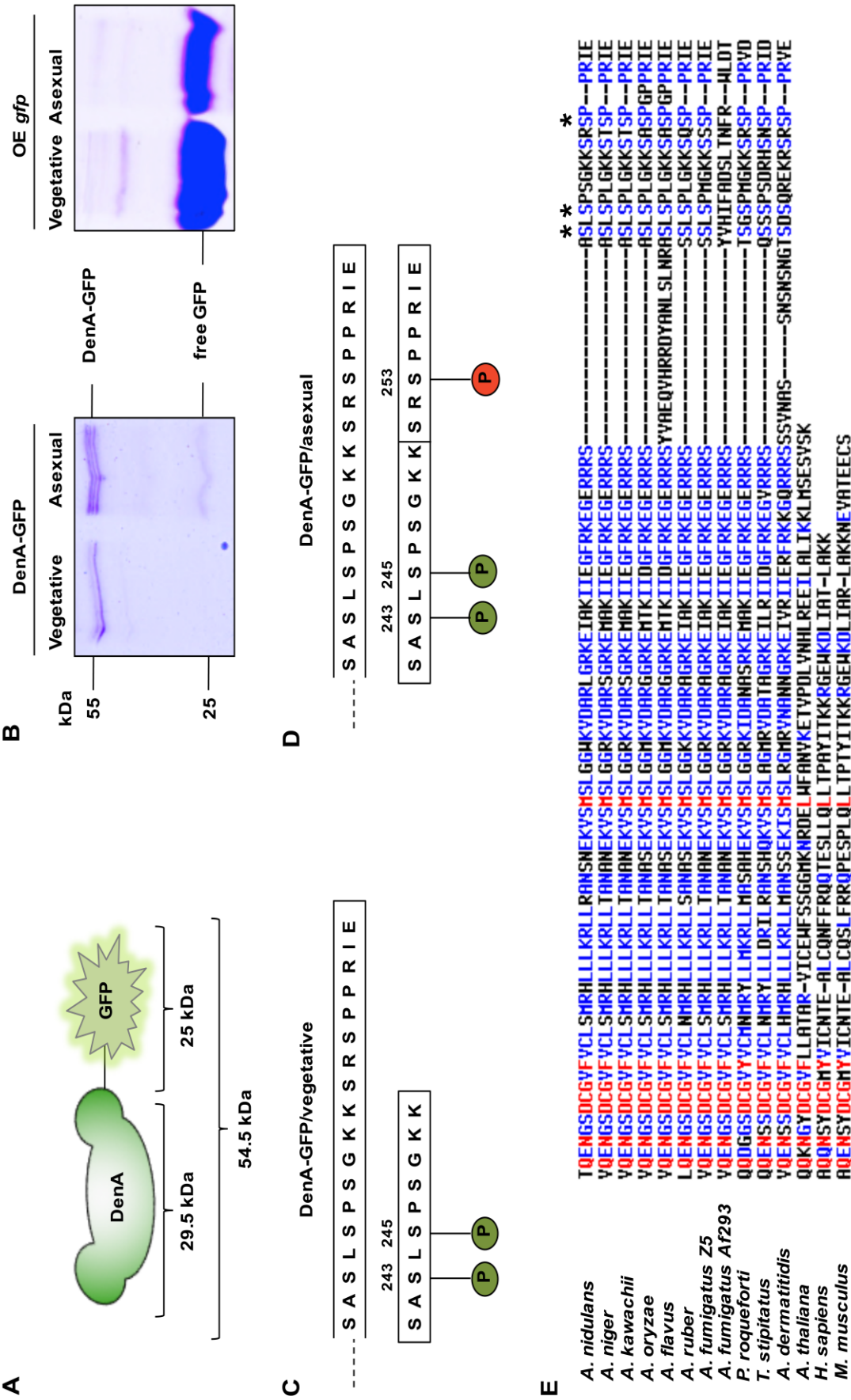


Figure 17: Identification of DenA phosphorylation sites.

(A) Illustration of C-terminally tagged DenA-GFP (54.5 kDa) for GFP-Trap. (B) Colloidal blue stained Phos-tag gel with DenA-GFP extracted from 24 h vegetative and 24 h asexually grown cultures (left column). Strain overexpressing GFP (OE *gfp*) served as control (right column). (C) Deduced amino acid sequence of DenA C-terminus. LC-MS/MS analyses identified one peptide with two phosphorylated serines at position S243 and S245 of DenA during vegetative growth and (D) two peptides with three phosphorylated DenA serines S243, S245 and S253 during asexual development. (E) Multiple alignments of DenA C-termini of *A. nidulans*, *A. niger*, *A. kawachii*, *A. oryzae*, *A. flavus*, *A. ruber*, *A. fumigatus* Z5, *A. fumigatus* Af293, *Penicillium roqueforti*, *Talaromyces stipitatus*, *Ajellomyces dermatitidis*, *Arabidopsis thaliana*, *Homo sapiens* and *Mus musculus*. Identified phosphorylation sites are marked with asterisks. Red: high (90%), blue: low (50%) consensus values (Corpet, 1988).

DenA-GFP purified during vegetative and asexual conditions was analyzed by LC-MS/MS to reveal the amount as well as the exact localization of respective phosphorylation sites. Stable DenA isolated from vegetative cultures possessed two phosphorylated serines (S243, S245), whereas DenA enriched during asexual development carried an additional phosphate residue at serine S253 (Figure 17C & 17D). Analyses of the identified DenA phosphorylation sites using a computational prediction tool (Huang *et al*, 2005b) led to the identification of the cyclin dependent cell cycle kinase Cdc2 as a potential kinase responsible for the phosphorylation of DenA at its C-terminally located serines S245 and S253.

Multiple alignments of DenA C-termini from different species revealed a partial conservation of identified phosphorylation sites within the fungal kingdom. The modified serines are found in a wide range of laboratory (*A. nidulans*, *A. ruber*, *Talaromyces stipitatus*) industrial (*A. niger*, *A. kawachii*, *A. oryzae*, *Penicillium roqueforti*) and clinical (*A. flavus*, *A. fumigatus* Z5, *Ajellomyces dermatitidis*) relevant fungal strains (Figure 17E, phosphorylated serines are marked with asterisks). They are absent in other important *Aspergilli* such as *A. clavatus*, *A. fumigatus* Af293, *A. terreus* and are neither present in plants nor animals.

These data demonstrate that DenA is differentially phosphorylated at the C-terminal end during vegetative growth and development. Stable DenA from vegetative growth possesses two phosphorylated residues at positions S243 and S245. The transition from stable vegetative DenA to an unstable DenA protein during asexual development coincides with the appearance of an additional developmental-specific phosphate group at position S253 of the 258 amino acids long protein.

3.6.3 Phosphorylation of DenA S253 destabilizes the protein during fungal development

The role of the additional S253 phosphorylation site of DenA was analyzed to determine whether it is relevant for the destabilization of the DenA protein during asexual development. The S253 codon was either exchanged for the negatively charged aspartic acid (DenA^{S253D}) mimicking constant phosphorylation at this site or for neutral alanine (DenA^{S253A}), which cannot be phosphorylated. These *denA* variants were fused C-terminally to GFP and integrated at the endogenous *denA* locus. Proteins from vegetative and asexually developed mycelium were extracted at various time points and used for western hybridization applying GFP antibody. Wild type DenA-GFP was present in vegetative growth, decreased during early stages of asexual development and was undetectable after 72 h. The simulated phosphorylated DenA^{S253D} variant was unstable and already undetectable after 40 h of asexual development, indicating a premature degradation of the protein (Figure 18A). In contrast, the amount of DenA^{S253A}, mimicking a dephosphorylated protein at this site, was present throughout the entire asexual development suggesting that the protein is even more stable than wild type DenA, which is degraded after 72 hours of asexual development (Figure 18B). This suggests that DenA stability is controlled by phosphorylation during asexual development.

The next step was to analyze the function of S243 and S245 in the destabilization of DenA through the adjacent S253 phosphorylation site after the induction of asexual development. A DenA variant was constructed where all three phosphorylated serine residues (S243, S245, S253) were exchanged for aspartic acid to introduce negative charges. The triple aspartic acid variant DenA^{S243D-S245D-S253D}-GFP mimics a constant phosphorylated version of DenA. DenA^{S243D-S245D-S253D}-GFP remained stable even 72 hours after the induction of asexual development (Figure 18C). This is in contrast to the DenA wild type version, which was stable during initial asexual development but became degraded after 72 hours. It is also different from the DenA S253D variant, which was already unstable after 40 hours of asexual development. The triple aspartic acid version is reminiscent of the S253A variant, which was also stabilized during development. These results suggest that phosphorylation of S243 and S245 stabilize DenA within the fungal cell during development, whereas S253 phosphorylation has a destabilizing function.

To analyze whether the stabilization function of phosphorylated S243/S245 can be verified, all three serine residues were exchanged for alanine. The triple alanine DenA^{S243A-S245A-S253A}-GFP version that cannot be phosphorylated at these sites, was as unstable as the A253D variant and was undetectable after 40 h of asexual development (Figure 18D).

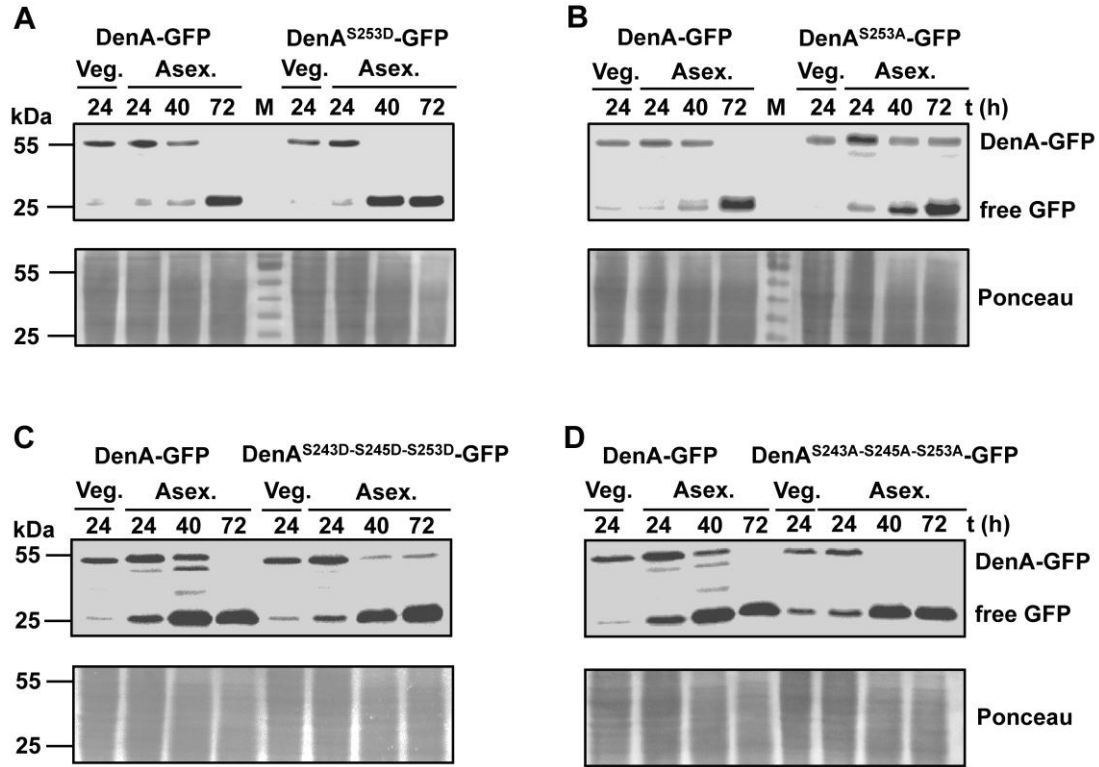


Figure 18: Influence of amino acid substituted DenA phosphorylation sites on its protein stability.

Western hybridization with equal amounts of protein extracts of DenA-GFP (54.5 kDa) compared to (A) DenA^{S253D}-GFP carrying a negative charge reminiscent of phosphorylated protein, (B) DenA^{S253A}-GFP which cannot be phosphorylated, (C) DenA^{S243D-S245D-S253D}-GFP with three negative charges similar to a triple phosphorylated protein and (D) the corresponding DenA^{S243A-S245A-S253A}-GFP which cannot be phosphorylated. Samples were taken from vegetative hyphae (Veg.) and at indicated time points (in hours) of illumination, which induces asexual development (Asex.). Membranes were treated with GFP-antibody to visualize the fusion protein and free GFP (25 kDa). Ponceau staining was used as loading control. M: molecular weight marker.

These data indicate that DenA protein level is controlled by stabilizing and destabilizing modifications at the C-terminus of the protein. Phosphorylation of at positions S243/S245 has a protective function for DenA protein stability during asexual development, whereas phosphorylation of S253 promotes DenA degradation.

3.6.4 DenA stability control is required for asexual development

An *A. nidulans* strain deleted for *denA* is impaired in asexual development during limited pyrimidine supply (Christmann *et al*, 2013). It was analyzed whether the triple amino acid substituted DenA variants, DenA^{S243A-S245A-S253A} and DenA^{S243D-S245D-S253D}, which are different in protein stability, affect fungal development. Respective constructs, under control of an inducible promoter, were ectopically integrated in the *denA* deletion strain. It was revealed that the DenA^{S243A-S245A-S253A} variant, which is prematurely destabilized during asexual development in wild type background, displayed the same reduction in asexual development during pyrimidine limitation as observed for the *denA* deletion phenotype (Figure 19A & 19B). This indicates that a constantly unphosphorylated DenA is insufficient to complement the *denA* deletion phenotype. In contrast, the DenA^{S243D-S245D-S253D} strain, in which DenA is stabilized throughout development, formed a colony similar to wild type.

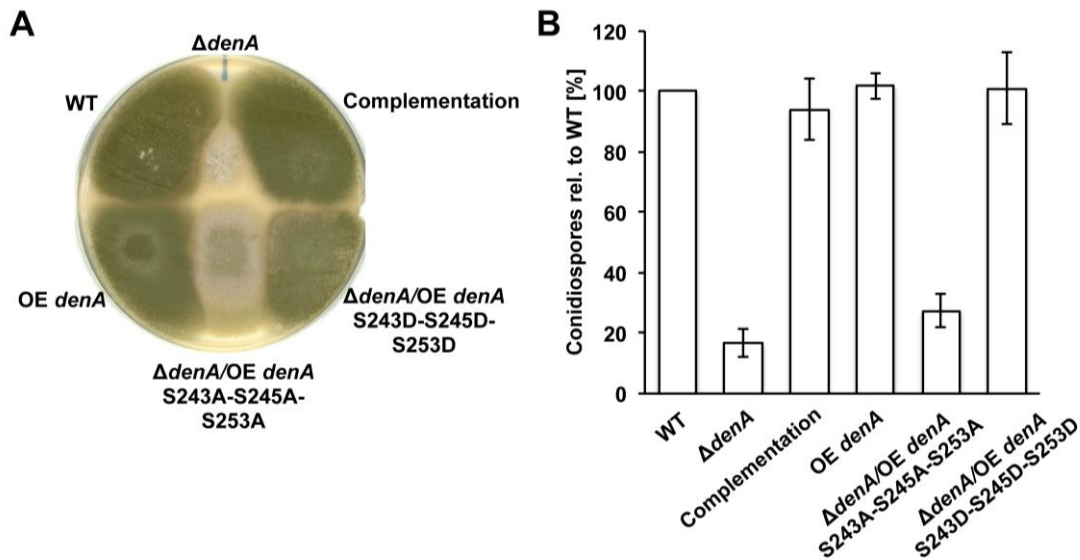


Figure 19: Influence of amino acid substituted DenA phosphorylation sites on asexual development.

(A) Phenotypically characterization of strains with mutated DenA. Equal amount of spores of wild type (WT), *denA* deletion strain ($\Delta denA$), complementation strain, *denA* under control of an inducible promoter (OE *denA*) and respective DenA variants with mutated phosphorylation sites in *denA* deletion background ($\Delta denA$ /OE *denA*^{S243A-S245A-S253A}) / ($\Delta denA$ /OE *denA*^{S243D-S245D-S253D}) were incubated under limited pyrimidine supply during asexual development inducing conditions. The phenotype of the DenA variant carrying alanines instead of the phosphorylated serine residues is reminiscent of the *denA* deletion phenotype regarding colony size and conidiation. **(B)** Quantifications of conidiospores from the same strains as shown in (A). Experiments were performed in triplicates and the mean values with standard deviations are shown.

This finding suggests that DenA has to be present and phosphorylated in the initial phase (until 40 hours) of development where it is required for efficient asexual spore formation.

3.7 Characterization of the phosphatase DipA

3.7.1 AN10946 encodes a DenA interacting phosphatase (DipA) including a conserved metallophosphatase domain

In a previous study putative DenA interacting proteins were identified by co-purification experiments with DenA either tagged with TAP or GFP (Christmann, 2012). Among them were proteins with specific roles in ribosome biogenesis, nuclear migration, and transport processes such as nuclear import/export and cytoplasmatic shuttling. Since our data revealed that DenA stability is regulated by phosphorylation of specific serine residues the focus was on a co-purified candidate that was a so far uncharacterized putative serine/threonine phosphatase. This enzyme, encoded by AN10946 was named DenA interacting phosphatase (DipA). As the biological function of the DipA protein and respective substrates for dephosphorylation are unknown in *A. nidulans* and related species, it was of interest to analyze in which cellular processes DipA is involved in and whether DipA contributes to DenA stability, phospho-regulation or localization.

The *dipA* gene locus is located on chromosome IV and encodes a transcript of four exons interrupted by three introns with a length of 2590 bp (Figure 20A). The mRNA has a total length of 2212 bp including the coding sequence, which is flanked by an upstream-untranslated region (5'UTR). After translation the resulting DipA protein contains 704 aa and has a predicted molecular mass of 74.5 kDa. BLAST search analyses revealed that DipA is conserved within fungal kingdom but is absent in higher eukaryotes such as plants or mammals. The highest amino acid sequence similarity was found in other *Aspergilli*. The industrial relevant strains *A. niger* and *A. oryzae* possess candidates that share 83% and 79% aa identity, respectively to DipA. Similar amino acid sequences were also present in *P. roqueforti* (75%), in the model organism *N. crassa* (59%), in the plant pathogen *Ustilago maydis* (51%) and in *S. pombe*, which shares 51% aa identity to DipA.

Multiple alignments of MPP consensus sequence (pfam12850; (Aravind & Koonin, 1998)) with other organisms revealed that the MPP domain of DipA is conserved within the fungal kingdom (Figure 20B). The most conserved residues are two aspartates (D51 and D76) and one histidine (H73) (marked with asterisks). Two high abundant asparagine residues could also be identified at positions N55 and N60. As these latter amino acids were not conserved throughout all sequences displayed in figure 20B, they were not further considered.

The finding that the serine/threonine phosphatase DipA is a putative DenA interaction partner strengthens our suggestion that DenA is regulated by phosphorylation and dephosphorylation of specific serine residues. The metallophosphatase domain of DipA supports that the protein might be a catalytically active phosphatase and that the three highly conserved amino acid residues D51, H73 and D76 represent parts of the catalytic core of DipA.

3.7.2 DipA is required for asexual development

The three highly conserved amino acids aspartate at positions D51 and D76 and histidine H73 form the predicted catalytic core of the phosphatase DipA. These residues were mutated to validate this prediction and to analyze if there is an impact of the DipA phosphatase domain on fungal development. The two aspartates D51 and D76 as well as the histidine H73 were substituted for alanine. The resulting *dipA** strain was used for phenotypical analysis. Equal amount of spores were point-inoculated and incubated under asexual development inducing conditions. The *dipA** strain was viable but revealed an aberrant phenotype when compared to wild type. The respective colony of the mutated DipA strain displayed a smaller size and green pigmentation was reduced indicating decreased asexual development (Figure 21A). A brownish dye surrounded the colony suggesting an impaired secondary metabolism. A *dipA* deletion strain was generated to explore the function of entire DipA in fungal cells. The comparison between *dipA** mutant strain and *dipA* deletion strain allows to differentiate between DipA function as a phosphatase and DipA function as a protein. Deletion of the *dipA* coding region resulted in a viable strain that demonstrated similar defects in asexual development concerning colony size and secondary metabolism as it was observed for *dipA** strain. Reintegration of *dipA* at the endogenous locus in *dipA* deletion strain complemented the phenotype. The colony

diameters of asexually incubated *dipA** and $\Delta dipA$ strains were measured daily for a period of six days. When compared to wild type or complementation strain it was observed that the colony size was reduced by half when DipA was mutated (*dipA**) or deleted ($\Delta dipA$) (Figure 21B).

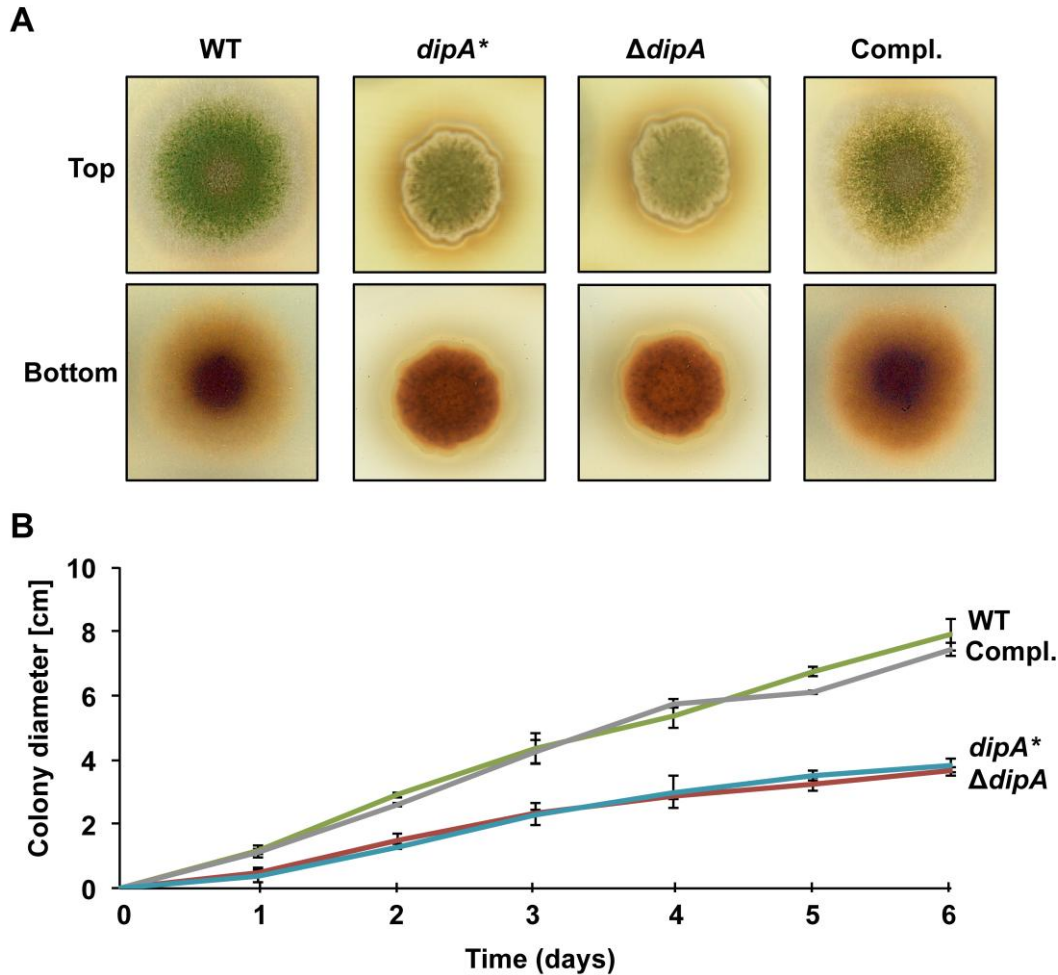


Figure 21: Asexual colony formation of wild type, *dipA* mutant and *dipA* complementation strains.

(A) Top and bottom view of wild type (WT), *dipA** (codon exchange of catalytic core), *dipA* deletion ($\Delta dipA$) and complementation (Compl.) strains. Strains were point-inoculated with the same amount of spores and incubated for three days under asexual development inducing conditions. (B) Spores of the same strains as shown in (A) were point-inoculated and the diameter of respective colonies was measured for six days. The mean values with standard deviations derived from three independent experiments are shown.

These results imply that the observed phenotype of the *dipA** strain is caused by a malfunctioning DipA protein suggesting that at least one if not all of the mutated amino acids D51, H73 and D76 belong to the catalytic core of the phosphatase DipA.

The colony morphology and development of the *dipA* deletion and *dipA** strains was analyzed in more detail to gain additional information about cellular processes influenced by DipA. It is known that development of *A. nidulans* is triggered by abiotic factors such as light. Illumination represses sexual development and promotes the asexual cycle (Pöggeler *et al*, 2006; Bayram *et al*, 2010; Yu, 2010). The asexually incubated colonies of *dipA** and *dipA* deletion strain formed hardly any asexual conidiophores (co) after seven days but instead mature sexual fruiting bodies (cleistothecia, cl) were observed (Figure 22A). The *dipA* complementation strain was similar to wild type. Quantification of asexually conidiospores displayed a significant reduction when the *dipA* locus was altered. In contrast to wild type and complementation strain the *dipA** and $\Delta dipA$ strains formed around 60% less conidiospores (Figure 22B).

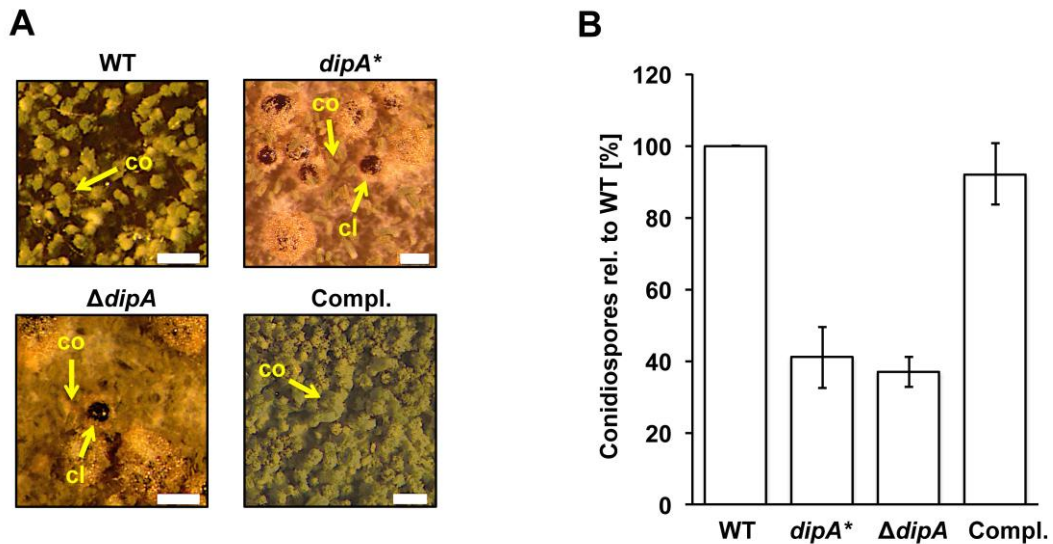


Figure 22: Impaired development of strains lacking a functional DipA.

(A) Binocular images taken from wild type (WT), *dipA** (codon exchange of catalytic core), *dipA* deletion ($\Delta dipA$) and complementation (Compl.) strains. Asexual structures (conidiophores, co) and sexual fruiting bodies (cleistothecia, cl) are shown after seven days. Scale bar: 100 μ m. (B) Quantification of conidiospores after three days. Mean values with standard deviations from three independent experiments are shown.

These data suggest that the phosphatase DipA is important for conidiophore development and might be involved in the control of light-dependent repression of sexual development, because the *dipA** as well as the *dipA* deletion strains were unresponsive to light.

3.7.3 DipA controls intervals of septa positioning

Hyphal growth as well as the formation of conidiospores require proper cell divisions (Mouriño-Pérez & Riquelme, 2013). The asexual conidiophore forms conidiospores in a manner that is reminiscent of the process of septation.

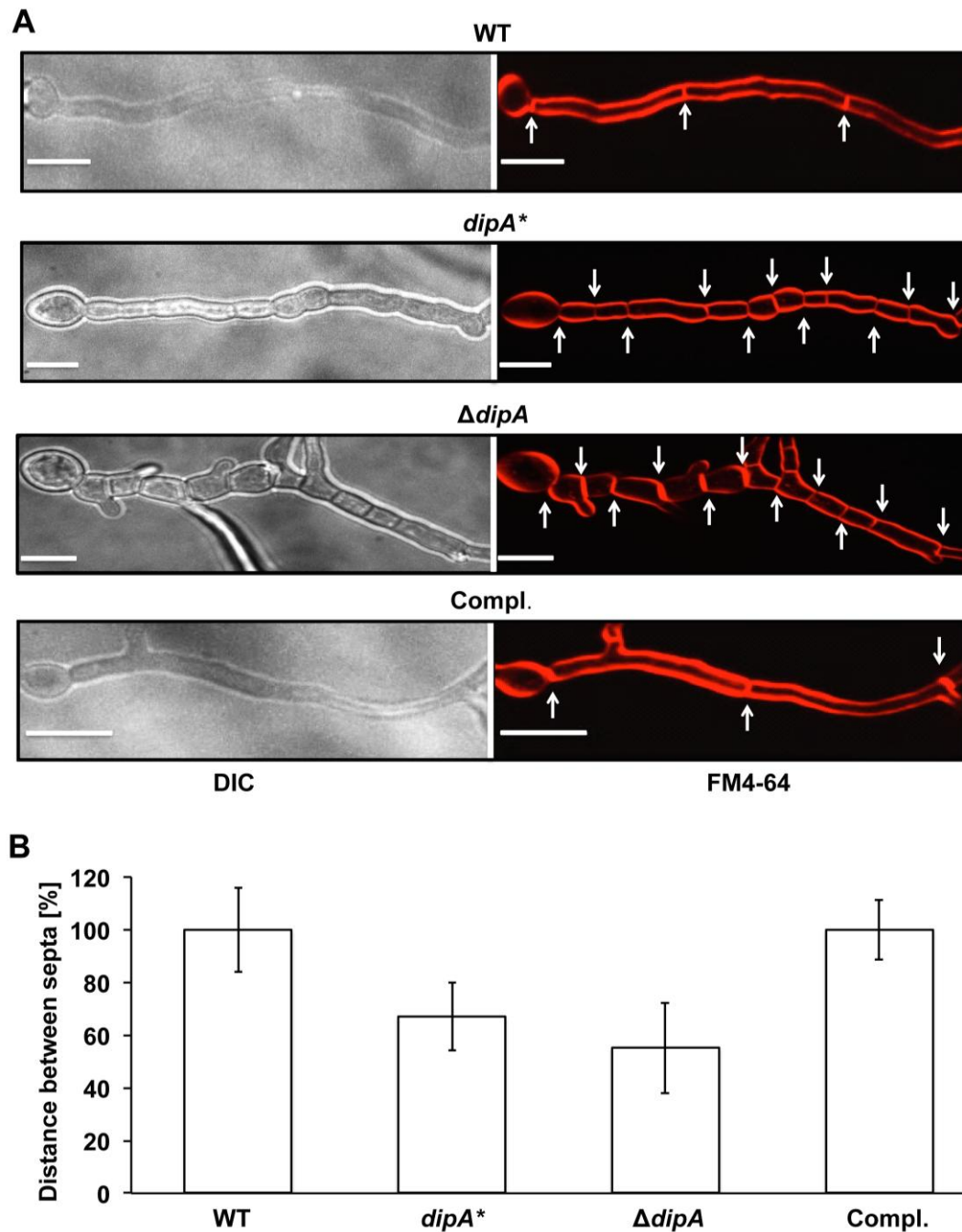


Figure 23: Hyphal morphology of *dipA* deletion strain.

(A) Fluorescence microscopy of wild type (WT), *dipA** (DipA strain with mutated catalytic core), *dipA* deletion ($\Delta dipA$) and complementation (Compl.) strains. Membranes/septa were stained with FM4-64. White arrows are highlighting septa. Scale bar: 5 μ m. (B) Diagram illustrates distances between septa. WT was set to 100%. Data derived from 70 hyphae of each strain. Shown are the mean values with standard deviations.

Hyphal morphology was studied to analyze whether impaired growth and reduced conidia formation are caused by altered septa positioning in the *dipA*^{*} and *dipA* deletion strains. Fluorescence microscopy of vegetative hyphae revealed that *dipA*^{*} and *dipA* deletion strains display an increased septa formation when compared to wild type and *dipA* complementation strain (Figure 23A). In the *dipA*^{*} and *dipA* deletion strains the average distance between two septa was reduced to $67 \pm 13\%$ and $55 \pm 17\%$ respectively, when compared to wild type or complementation strain (Figure 23B). Some hyphal units, given as compartments flanked by one septum on either side, were observed with sizes reduced to 5 μm or less, which was never seen in respective parental strains. These results indicate an involvement of the phosphatase DipA in the coordination of septa positioning.

3.7.4 DipA is present in the cytoplasm, at septa and is undetectable during late asexual development

Since DipA controls processes such as septation and development, it was of interest to analyze its cellular distribution and its protein half-life during development. DipA was fused at its C-terminus to GFP and the construct was integrated at the endogenous *dipA* locus of the *dipA* deletion strain. The observed phenotypes caused by deletion of *dipA* shown in chapter 3.7.2 and 3.7.3, were complemented indicating that the GFP fusion protein is fully functional. Analysis of the subcellular localization of DipA-GFP by fluorescence microscopy of vegetative hyphae, with stained nuclei and membranes including septa, revealed several distinct DipA-GFP signals with different intensities. DipA was most dominantly localized in the cytoplasm and at septa, but not inside nuclei (Figure 24A). Time lapse experiments displayed a dynamic shuttling of the phosphatase through the cell. DipA-GFP moved bi-directionally between septa and nuclei (Figure 24B).

To study DipA-GFP protein levels, western hybridization applying GFP-antibody and Ponceau staining as loading control was performed. Mycelium was harvested 24 h after vegetative growth and at different time points of asexual development. DipA-GFP was present in vegetative hyphae where it represented a stable protein (Figure 24C). Protein amount of DipA-GFP decreased constantly within 48 h of asexual differentiation resulting in an undetectable protein level during advanced asexual development. Stable free GFP accumulated over time, indicating a

constant degradation of DipA. DipA protein level correlated with DenA stability, which decreased within a similar time frame of asexual differentiation (Figure 24D).

These results imply that DipA shows a similar protein half-life during development when compared to DenA, which supports a correlation between both proteins. In addition, it is demonstrated that DipA is absent from nuclei, but present in the cytoplasm. The appearance close to septa strengthens the hypothesis that DipA has a direct influence on septa formation.

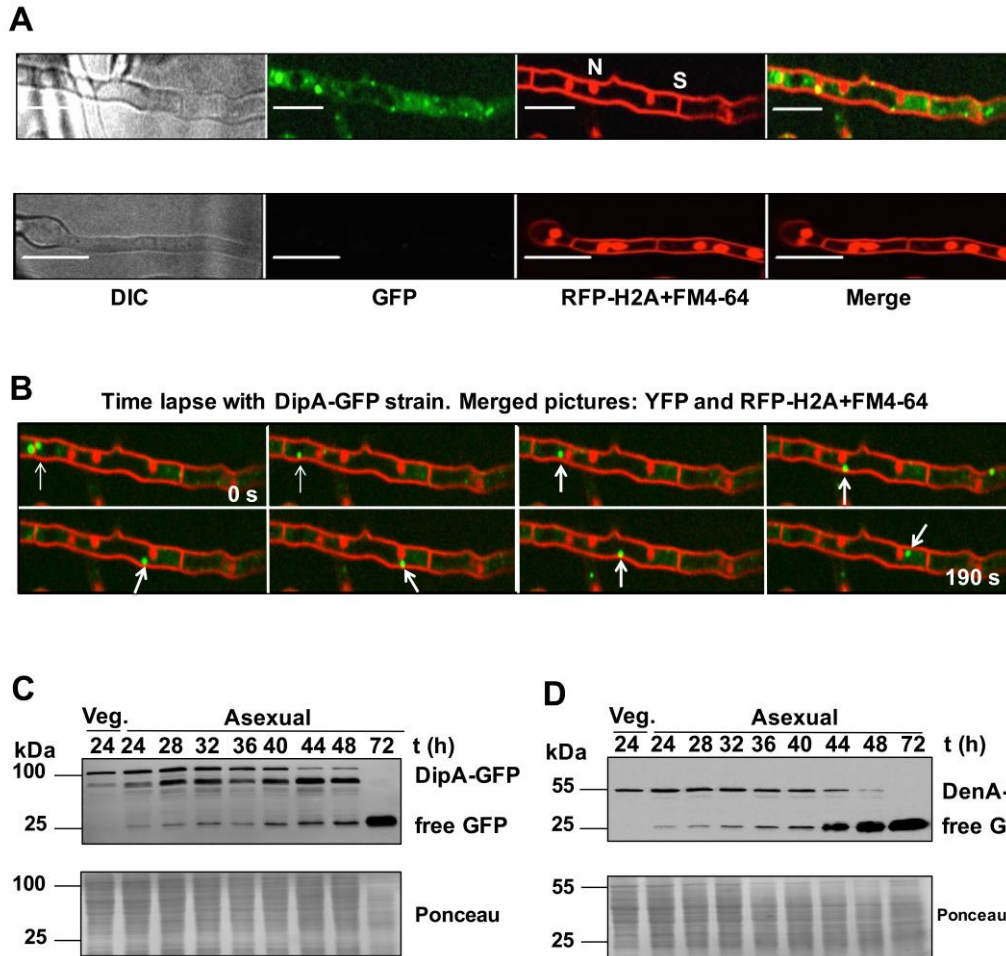


Figure 24: Protein localization and occurrence of DipA.

(A) GFP was C-terminally fused to DipA and localization was followed by fluorescence microscopy. Several distinct spots were visible in the cytoplasm and at septa. Nuclei are marked with N and septa with S. Nuclei were visualized with expressed *rfp::h2A*. As control wild type hyphae were used. Scale bar: 5 μ m. (B) Time lapse observations over 190 seconds. Shuttling of DipA-GFP is highlighted and followed by white arrows. (C) Western hybridizations of DipA-GFP and (D) DenA-GFP. Samples were taken from vegetative cultures (Veg.) and during different time points (in hours) of asexual development. SDS gels were loaded with equal amounts of protein crude extracts. Membranes were treated with GFP-antibody and as loading control staining with Ponceau was applied. Protein molecular weight of DipA-GFP was 99.5 kDa, DenA-GFP was 54.5 kDa and free GFP was 25 kDa.

3.8 DenA and DipA physically interact in the cytoplasm and at septa

Previously it was reported that nuclear DenA interacts with CsnG which results in DenA degradation (Christmann *et al*, 2013). Beside the nuclear subpopulation, DenA is localized in the cytoplasm and there predominantly at septa (Figure 25A).

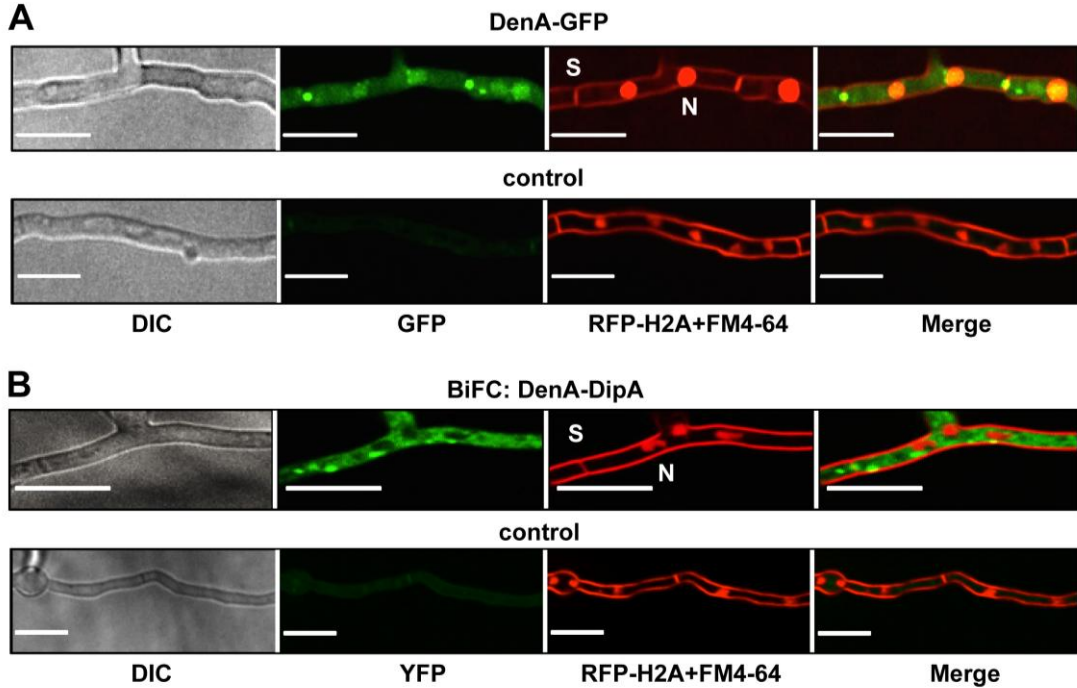


Figure 25: Cytoplasmatic interaction between DenA and DipA.

In vivo localization of DenA and DenA-DipA interaction complex. (A) Fluorescence microscopy of DenA-GFP subpopulations within vegetative hyphae located the protein in the nucleus (N), in the cytoplasm and there with a specific enrichment at septa (S). Control: wild type without GFP. (B) Bimolecular fluorescence studies (BiFC) of DenA (*denA::nyfp*) and DipA (*dipA::cyfp*) showed restricted interaction in the cytoplasm, at septa (S) and close to, but not inside nuclei (N). Control: strain expressing *denA::nyfp* and *cyfp*. Nuclei are marked with N and septa with S. Nuclei were visualized with expressed *rfp::h2A* and membranes were stained with FM4-64, scale bar: 5 μ m.

As DipA was found in co-purification experiments to be a putative DenA binding partner it was analyzed where both proteins interact *in vivo*. To identify the respective DenA subpopulation that interacts with DipA, bimolecular fluorescence complementation (BiFC) studies were performed. DenA was fused through its C-terminus to the N-terminal part of YFP (*denA::nyfp*) and DipA C-terminus was attached to the C-terminal half of YFP (*dipA::cyfp*). To exclude unspecific interactions a control strain was used that only expressed the *denA* fusion protein

(*denA::nyfp*) and single *cyfp*. Interactions in hyphae were followed by fluorescence microscopy. Several distinct fluorescence spots within hyphae were observed, representing the physical interaction between DenA and DipA (Figure 25B). These DenA-DipA binding complexes were located at septa, in the cytoplasm and in close proximity to, but not inside nuclei. Thus, the localization of DenA-DipA correlates with the distribution of DipA as shown in chapter 3.7.4. The BiFC results suggest that the phosphatase DipA is a physical binding partner of the cytoplasmic/septatic DenA subpopulation.

3.8.1 The DenA-DipA interaction complex is dynamically transported

As DenA is localized in different cellular compartments, it was of interest to analyze whether the interaction with DipA contributes to DenA dispersion. Therefore, DenA localization was studied in the *dipA* deletion strain. Fluorescence microscopy experiments revealed that DenA-GFP was present in the nucleus, in the cytoplasm and at septa, although the amount of these internal cross walls was significantly increased in the *dipA* deletion strain (Figure 26A). This suggests that the overall distribution of DenA within the cell was unaffected by deletion of *dipA*.

To determine whether the interaction between DenA and DipA depends on the phosphorylation status of DenA, the BiFC strain was used and the three identified phosphorylated serine residues S243, S245 and S253 of DenA were mutated either to alanine (mimics constant unphosphorylation at these sites) or to aspartic acid (simulated constant phosphorylation). Although fluorescence signals were less intense, they could be detected in both cases (data not shown). This indicates that the DenA-DipA interaction is independent of the phosphorylation status of DenA.

DenA was co-purified with the phosphatase DipA but also with proteins that are involved in transport processes (Christmann, 2012). Time lapse fluorescence microscopy experiments were performed to unveil whether the DenA-DipA dimer shuttles. The BiFC DenA-DipA strain without artificial amino acid substitutions was used. Several distinct DenA-DipA interaction spots, which were dynamically moving through the cytoplasm, were observed. The two proteins shuttled in both directions between nuclei and septa (Figure 26B) in a similar way as it was observed for DipA-GFP (chapter 3.7.4). Moreover, by staining the mitochondria, the DenA-DipA movement seemed to be associated to these widespread filaments (Figure 26C).

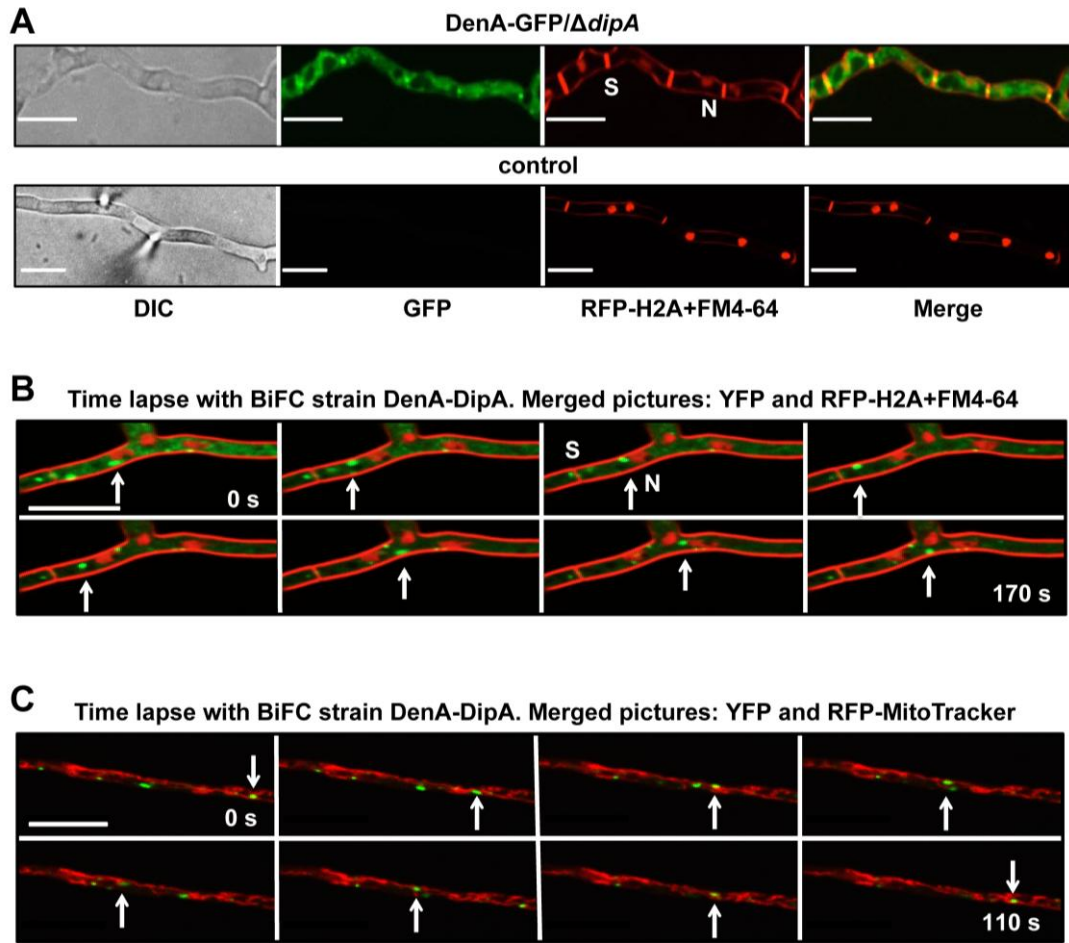


Figure 26: Dynamic co-transport of DenA-DipA interaction complex.

(A) Overall cellular distribution of DenA was not affected by the absence of DipA. In the $\Delta dipA$ strain DenA-GFP was present inside nuclei (N), in the cytoplasm and predominantly at septa (S). As control wild type hyphae were used. (B) Time lapse experiment over 170 seconds using the DenA-DipA bimolecular fluorescence strain (*denA::nyfp-dipA::cyfp*) revealed dynamic transport processes of interacting DenA-DipA between nuclei and septa. The shuttling was bi-directional. A single interaction complex is highlighted and followed by white arrows. Nuclei are marked with N and septa with S. (C) Time lapse experiment over 110 seconds using the DenA-DipA bimolecular fluorescence strain (*denA::nyfp-dipA::cyfp*) with stained mitochondria (red). The bi-directional transport of a single DenA-DipA interaction complex is highlighted and followed by white arrows. Expressed *rfp::h2A* decorates nuclei, membranes were stained with FM4-64 and mitochondria with MitoTracker. Scale bar: 5 μ m.

These results show that DipA interacts with DenA in the cytoplasm and at septa where they are part of a dynamic shuttling complex, which approaches nuclei and mitochondria. The ratio of DenA at its different locations is independent of DipA, but the observation of a bi-directional transport indicates an interrelation between DenA subpopulations.

3.9 Stability of DenA is increased in *dipA* deletion strain

The phosphatase DipA interacts with DenA and DenA phosphorylation regulates the stability of the deneddylase. DenA-GFP protein levels in the absence of the phosphatase were compared to wild type strain with an intact DipA to analyze the impact of DipA on DenA protein amount. Mycelium of respective strains was harvested during vegetative growth and after different time points of illumination, which induces asexual development in wild type. Protein crude extracts were analyzed by western hybridization using GFP antibody and Ponceau staining as loading control (Figure 27). DenA-GFP with an intact DipA in wild type background was present at 24 h of vegetative growth but was undetectable after 48 h of illumination. In contrast, in a *dipA* deletion strain the DenA-GFP fusion protein was still detectable after advanced asexual development. The respective signal intensity decreased after the transition from 24 h to 48 h but remained detectable up to 72 h. A constant increase of free GFP was visible in both strains.

These results indicate that DipA promotes degradation of DenA. Since their interaction occurred in the cytoplasm it is likely that DipA destabilizes the cytoplasmatic DenA subpopulation.

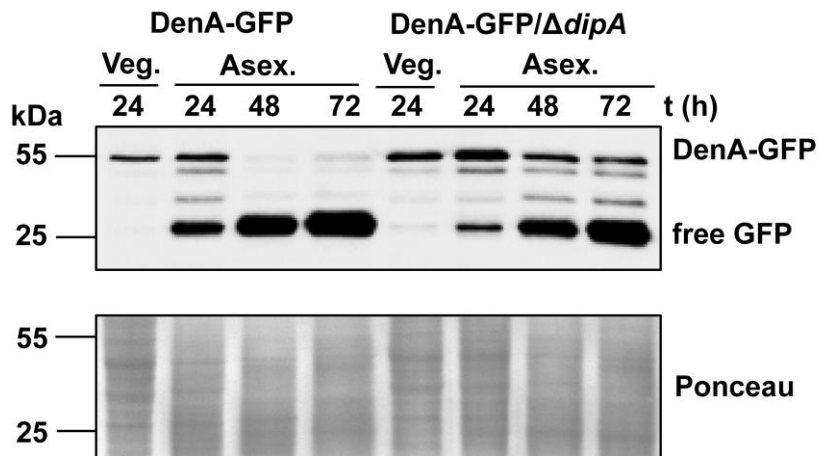


Figure 27: DenA protein level in *dipA* deletion strain.

Western hybridization of DenA-GFP in wild type background and $\Delta dipA$ strain. Samples were taken during vegetative growth (Veg.) and after different time points (in hours) of illumination, inducing asexual development in wild type (Asex.). DenA-GFP in wild type was undetectable during advanced asexual development, whereas free GFP increased constantly over time. In contrast, in $\Delta dipA$ strain DenA-GFP was detectable after 72 h of light incubation. SDS gel was loaded with equal amounts of protein crude extracts. Membrane was treated with GFP-antibody and as loading control staining with Ponceau was applied. Protein molecular weight of DenA-GFP was 54.5 kDa and of free GFP 25 kDa.

3.10 DipA and CsnG affect stability of DenA in a similar manner

It was shown that DipA interacts with DenA in the cytoplasm (chapter 3.8), whereas CsnG interacts with DenA in the nucleus (Christmann *et al*, 2013). Both interactions result in DenA degradation. As described in chapter 3.7.2 the *dipA* deletion strain produced sexual fruiting bodies after seven days of incubation during asexual conditions. In contrast, $\Delta csnG$ strain is unable to produce mature sexual fruiting bodies, even at circumstances that promote sexual differentiation (Beckmann *et al*, 2015). A strain deleted for the two proteins that interact and destabilize different DenA subpopulations was generated to analyze the combined impact on development and stability. Respective strains were incubated under conditions, which induce asexual development. Single *dipA* and *csnG* deletion showed a reduced colony size and secretion of brownish compounds to the surrounding medium. The generated *dipA/csnG* double deletion strain exhibited additive effects of the single deletion phenotypes (Figure 28). The growth defect as well as the accumulation of brownish compounds in the surrounding medium were increased in the double deletion when compared to either single deletion strain.

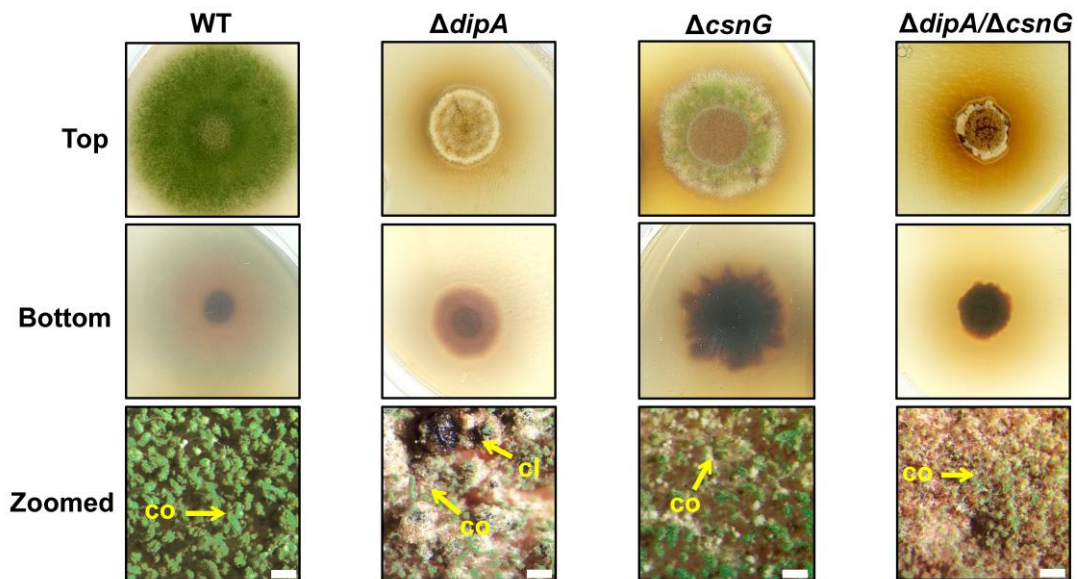


Figure 28: Effect of *dipA/csnG* double deletion on development.

Top and bottom view of illuminated wild type colony (WT) developing asexual spores and *dipA*, *csnG* and combined *dipA/csnG* deletion strains under the same condition. Same amounts of spores were point-inoculated and incubated for three days with illumination. Lower panel (zoomed) shows binocular images of asexual structures (conidiophores, co) and the sexual fruiting bodies (cleistothecia, cl) after seven days. Scale bar: 100 μ m.

DipA as well as CsnG target DenA for degradation. The effect of the *dipA/csnG* double deletion strain on DenA stability was studied, to analyze whether additional effects can be observed. Mycelium of the *dipA/csnG* double deletion strain was harvested from vegetative cultures and at different time points of asexual development inducing conditions. Western hybridization was performed using GFP-antibody and Ponceau staining as loading control.

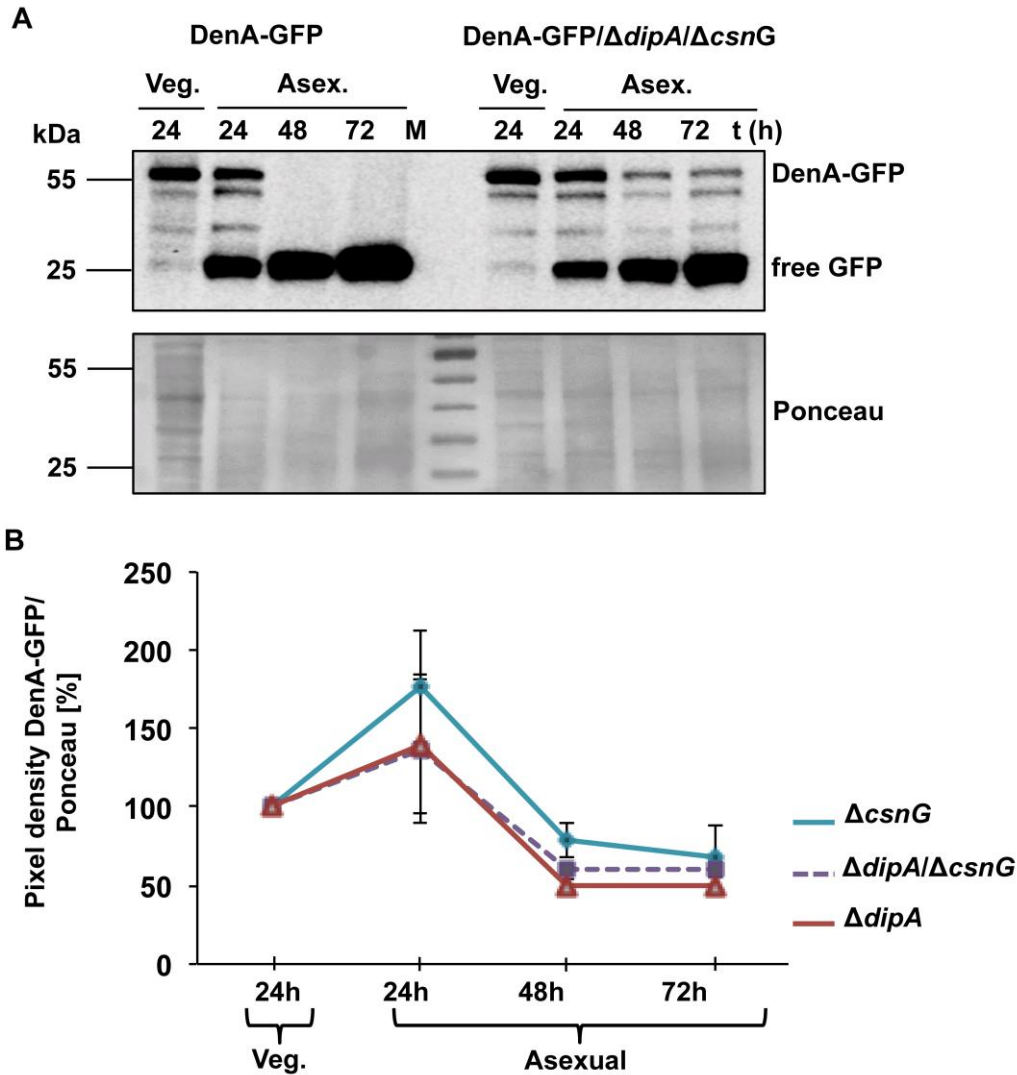


Figure 29: Effect of *dipA/csnG* double deletion on DenA stability.

(A) DenA-GFP protein stability in wild type background and in *dipA/csnG* double deletion strain during vegetative growth (Veg.) and after different time points (in hours) of illumination (Asex.). SDS gels were loaded with equal amounts of protein crude extract. Membranes were treated with GFP-antibody and as loading control staining with Ponceau was applied. Protein molecular weight of DenA-GFP was 54.5 kDa and of free GFP 25 kDa. M: molecular weight marker. (B) Diagram of DenA-GFP protein levels in *csnG* deletion strain, *dipA* deletion strain and *dipA/csnG* double deletion strain at the same time points as shown in (A). The GFP/Ponceau pixel ratio and the standard deviation are shown from three independent experiments.

It was revealed that DenA-GFP was stabilized in the *dipA/csnG* double deletion strain (Figure 29A). The effect was similar as it was observed for single deletions of *dipA* and *csnG*. In the *dipA/csnG* double deletion strain about 60% of DenA-GFP remained detectable after 72 h (Figure 29B). In *csnG* deletion strain around 70% and in *dipA* deletion strain 50% of DenA-GFP was detectable after 72 h of illumination when compared to vegetative growth. Since the *dipA/csnG* double deletion strain could not further increase the amount of stabilized DenA in comparison to the single deletions of *dipA* and *csnG*, these results suggest that DipA and CsnG act independently on asexual development, probably by influencing different metabolic pathways. Although their interaction with DenA occurs at different locations both proteins reduce DenA amount to the same extent, which supports a complex interrelation between DenA subpopulations.

4 Discussion

The focus of many studies investigating deneddylases is the COP9 signalosome with its various impacts on cellular processes (Wei *et al*, 2008; Stratmann & Gusmaroli, 2012; Meir *et al*, 2015). In contrast, not much attention was paid to the cellular function of DenA/DEN1. The emphasis of this thesis was to analyze the contribution of the fungal deneddylase DenA to asexual development by studying the role of its interacting proteins and their influence on DenA stability, localization and function. The main finding of this thesis is that a precise regulation of DenA is required to support asexual development. Stability of DenA is controlled by its interacting partners, the deneddylase COP9 signalosome and the phosphatase DipA, at different subcellular compartments and in a phosphorylation dependent manner. A dynamic succession of stabilizing and destabilizing phosphorylation events at distinct C-terminal serine residues of DenA is involved in the decision to promote asexual spore formation while sexual development is reduced. This temporally ordered process of phosphorylation and dephosphorylation occurs around the transition from vegetative growth to asexual development. Thus, a molecular feature for developmental competence was discovered that depends on the deneddylase DenA and the phosphatase DipA.

4.1 The two deneddylases COP9 signalosome and DenA share cullins as common substrates

The deconjugation process of Nedd8 is catalyzed by the two deneddylases CSN and DenA/DEN1. Both deneddylases differ in their substrate specificity. Mononeddylated cullins are the main substrate of the CSN, whereas modified non-cullin proteins are only of minor interest. In contrast, DenA/DEN1 shows activity towards neddylated cullins *in vitro* (Wu *et al*, 2003; Zhou & Watts, 2005) but catalyzes primarily deneddylation of non-cullin proteins (Su *et al*, 2013; Christmann *et al*, 2013; Mergner *et al*, 2015; Enchev *et al*, 2015). As *A. nidulans* represents an organism that can survive without either of the two deneddylases it is especially suited to dissect the impact of each deneddylase on cullin deneddylation *in vivo*. By comparing cullin neddylation levels in *csnE* and *denA* deletion strains this study corroborates that CSN

has the most pronounced effect towards cullins modified with Nedd8. The impact of DenA on these substrates was only marginal. Interestingly, analyses of a *csnE/denA* double deletion strain revealed a second, slower migrating band above the mononeddylated cullins (Figure 11). The higher molecular weight implies that the detected cullins are modified with several Nedd8 molecules. This assumption is in agreement with a previous study, where western hybridization using a Nedd8 antibody revealed an additional band of unknown origin, which was migrating slower than the mononeddylated cullins (Christmann *et al*, 2013). Increased molecular weight of cullins caused by neddylation can either be achieved by the attachment of multiple mono-Nedd8 molecules to several internal cullin lysine residues or by the formation of Nedd8 chains. Similar to ubiquitin, it was reported that Nedd8 can form poly-Nedd8 chains by conjugating to its own lysine residues (Xirodimas *et al*, 2008; Jones *et al*, 2008). It was shown that higher molecular weight bands of mammalian CulA/CUL1 disappeared by using methylated Nedd8 which is defective for chain formation (Ohki *et al*, 2009). Based on these results, the slower migrating bands observed in the double deneddylase deficient strain, probably represent cullins modified with poly-Nedd8 chains rather than multiple mono-Nedd8 molecules. However, the exact amount of Nedd8 molecules participating in such a chain is still elusive and requires further research.

Polyneddylated cullins were absent in the single deneddylase deletion strains and exclusively detected in the double deletion strain. This observation indicates that polyneddylated cullin variants are deneddylated by DenA as well as by CSN. In previous studies a common substrate of both deneddylases could not be identified. Mammalian DenA/DEN1 was able to deconjugate polyneddylated CulA/CUL1 *in vitro*, but no activity of the CSN complex towards these substrates was observed. It was speculated that both deneddylases differ in the way they identify their substrates (Wu *et al*, 2003; Pan *et al*, 2004). DenA/DEN1 was suggested to recognize a Nedd8 molecule on polyneddylated cullins that is located at the distal end of the Nedd8 chain. In contrast, the CSN was thought to act specifically on cullins modified with a mono-Nedd8 molecule by identifying the interface of Nedd8 with both cullin and Rbx1 (Pan *et al*, 2004). Based on the results that polyneddylated cullins accumulated in *A. nidulans* only when both deneddylases were missing indicates that fungal CSN can recognize polyneddylated cullins similarly to DenA. Thus, both deneddylases do not only have different but also overlapping substrates (Figure 30).

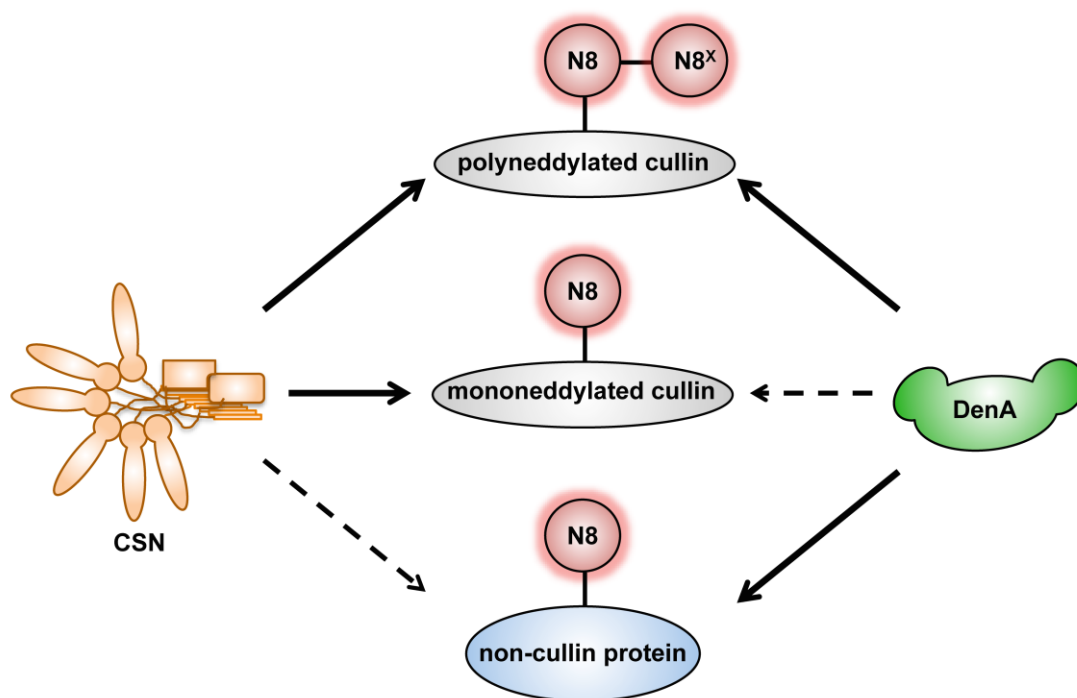


Figure 30: Substrate specificity of the fungal deneddylases CSN and DenA.

The model displays the preferences of the two deneddylases to different neddylated proteins. Mononeeddylated cullins represent the central substrate of the CSN complex, whereas non-cullin proteins are not in the main focus of this deneddylase. In contrast, mononeeddylated cullins are not of interest for DenA, which acts primarily towards neddylated non-cullin proteins. CSN and DenA do not only have different but also overlapping functions in *A. nidulans*. Both enzymes act towards cullins modified with poly-Nedd8 chains to yield the mononeeddylated variant. The exact amount of Nedd8 (N8) molecules participating in such a chain is currently unknown, indicated by $N8^X$.

The physiological function of poly-Nedd8 chains is still elusive, but Nedd8 polymers were observed on histones in response to DNA damage suggesting a role in DNA repair and stress response (Ma *et al*, 2013). The formation of Nedd8 chains on cullins might alter cullin-RING ligase activity. An *A. nidulans* strain without the deneddylases DenA and CSN grows predominantly vegetative and is highly impaired in multicellular development (Christmann *et al*, 2013). This indicates that polyneddylation of cullins is prevented by either of the deneddylases to assure proper CRL activity and coordinated cell differentiation.

Taking into account that mammalian CSN was unable to deneddylate polyneddylated cullins *in vitro* (Wu *et al*, 2003), it can be speculated that the recombinant CSN, which was used in the study of Wu and colleagues, is not fully active. Since several CSN subunits are known to be phosphorylated (Uhle *et al*, 2003;

Fang *et al*, 2008; Chung & Deliaire, 2015), it is possible that phosphorylation of its subunits might be essential for CSN to acquire full activity *in vivo*. Alternatively, the substrate specificity of CSN might have changed during 1.5 Billion years of evolution from fungi to human. This means that CSN of higher eukaryotes could have lost the capability to act towards Nedd8 chains and that DenA/DEN1 may represent the sole enzyme of higher eukaryotes with activity towards these substrates. It will be interesting to examine whether this hypothesis holds true for other model organisms.

4.2 DenA provides an auxiliary function to support deneddylation and development in the absence of a functioning CSN complex

The affinity of DenA/DEN1 towards mononeddylated cullins, which represent main targets of the CSN, is marginal *in vivo*. Only when levels of mammalian DenA/DEN1 were increased *in vitro*, the respective CulA/CUL1 was deneddylated (Wu *et al*, 2003; Mergner *et al*, 2015). In addition, it was reported that high isopeptidase activity of fungal DenA/DEN1 might work partially on other ubiquitin-like proteins *in vivo* as it compensates some developmental defects caused by deleting the gene for a SUMO isopeptidase (Harting *et al*, 2013). In the present study it was revealed that in *A. nidulans* high abundant fungal DenA partially counteracts and neutralizes the accumulation of neddylated proteins caused by a defective CSN (Figure 12 & 13). Among these substrates were putative non-cullin proteins of many different molecular weights as well as the cullins CulA and CulC. This observation indicates that fungal DenA can deneddylate CSN related substrates to the same extent as the CSN itself and supports the assumption that both deneddylases of *A. nidulans* have common substrates (Figure 30). In addition to the deneddylation activity of DenA towards neddylated non-cullin proteins and cullins modified with poly-Nedd8 chains, DenA is capable to target mononeddylated cullin versions *in vivo* when it is present in high amounts. The compensatory effect of high abundant DenA on cullin deneddylation was most pronounced on CulC when compared to CulA (Figure 13). Previous studies reported that CulC/CUL3 of metazoans and higher plants control different developmental processes and stress responses such as embryogenesis, cytokinesis and hypoxia (Kurz *et al*, 2002; Singer *et al*, 1999; Figueroa *et al*, 2005; Genschik *et al*, 2013). By reducing the neddylated CulC variant, elevated concentration of DenA presumably affects CulC-associated substrates, enabling them

to promote proper cell differentiation and stress responses. This assumption is supported by the compensatory effect that was seen when *denA* is overexpressed, which counteracted impaired asexual development caused by a defective CSN, especially under stress conditions (Figure 14).

Increased deneddylation as well as promotion of asexual development was only observed by overexpressing *denA* in a *csnG* deletion strain but not in a *csnE* mutant strain (Figure 12 - 14). In both deletion strains an active CSN complex cannot be assembled (Pick *et al*, 2012; Beckmann *et al*, 2015) suggesting that an inactive CSN is not automatically mediating the auxiliary function of DenA. The differences observed for the two *csn* deletion strains on DenA function can be either caused by positive or negative effects. DenA was unable to compensate CSN associated functions in a *csnE* deletion strain. This indicates that CsnE might be required to support the auxiliary function of DenA in a strain that is impaired in CSN deneddylation. This could be achieved by forming a joint deneddylase, consisting of DenA and CsnE, with concerted deneddylase activity (Figure 31A). This hypothesis is supported by the fact that CsnE/CSN5 of *A. nidulans* as well as of *S. pombe* interact with DenA or Nep1, respectively (Zhou & Watts, 2005; Christmann *et al*, 2013). Since CsnE/CSN5 is only active when incorporated into the CSN complex (Beckmann *et al*, 2015), it is likely that the putative super-deneddylase also includes other CSN subunits, except of CsnG, which might have stabilizing functions.

Beside this positive effect on DenA activity mediated by a CSN subunit, a second possibility rises when taking into account that DenA was only able to compensate CSN associated functions when *csnG* was missing. CsnG might negatively regulate cellular function of DenA. Among all CSN subunits, CsnG represents the main physical DenA interaction partner in *A. nidulans* (Christmann *et al*, 2013). This interaction could have an inhibitory effect on the isopeptidase activity of DenA. CsnG might inhibit activity of DenA by binding and/or blocking its active site (Figure 31B). An inhibitory effect caused by CSN was previously observed for mammalian CsnF/CSN6 which binds and blocks the catalytic core of avian leucosis virus (ALV) integrase, representing a key enzyme in retroviral life cycle (Wang *et al*, 2014). One possibility to distinguish between these positive and negative effects mediated by CsnE or CsnG, respectively, would be to analyze deneddylation activity of overexpressed *denA* in a *csnG/csnE* double deletion strain. This approach would

deliver interesting starting points to further clarify the impact of these CSN subunits on DenA activity.

The capability of DenA to overtake some CSN related functions in a *csnG* deficient strain occurs only when *denA* levels are elevated. No compensatory effect of DenA was visible in a respective deletion strain with regular *denA* expression. This suggests that additional mechanisms might exist that influence DenA function. These could be represented by e.g. other factors with negative impact on DenA activity, but whose inhibitory function is equalized when DenA levels are increased. Therefore, an additional mechanism might explain the compensatory effect that was observed when high levels of DenA were present in a *csnG* deletion strain. Recent research revealed that a seven subunit pre-CSN complex, including CsnG, assembles prior to the incorporation of CsnE to form the CSN holocomplex (Beckmann *et al*, 2015). In mammals a CsnE/CSN5 free CSN subcomplex cannot deneddylate but still bind CRLs, which primarily involves CsnB/CSN2 and the cullin C-terminal domain as well as the CsnA/CSN1-CsnC/CSN3 region and the CRL substrate recognition unit. The neddylation of cullin is stabilized by the CSN-CRL interaction, even when CsnE/CSN5 is absent (Enchev *et al*, 2012; Dubiel *et al*, 2015). Thus, the binding of the seven subunit pre-CSN complex to neddylation site might prevent recognition/binding of the neddylation site by DenA (Figure 31C). In case of *csnG* deletion, the CSN pre-complex cannot be formed, meaning that probably only some CSN subunits are loosely attached to the CRL. This might bring DenA in a situation where it competes with the remaining CSN subunits for binding to the neddylation site. The competitive situation between CSN subunits and DenA might shift towards DenA when DenA levels are increased. Finally, DenA is capable to recognize/bind the modified cullins resulting in their deneddylation.

Misregulated neddylation and CSN activity are involved in neurodegenerative disorders, cardiac disease and cancer (Lee *et al*, 2011; Chen *et al*, 2012b; Kandala *et al*, 2014). Targeting neddylation has become a promising task for the treatment of these diseases (Marsh, 2015). Therefore, the finding of a compensatory function of DenA under conditions in which the CSN complex is not active might play an important role in future research, especially for studies that aim to downregulate CSN activity by therapeutic drugs.

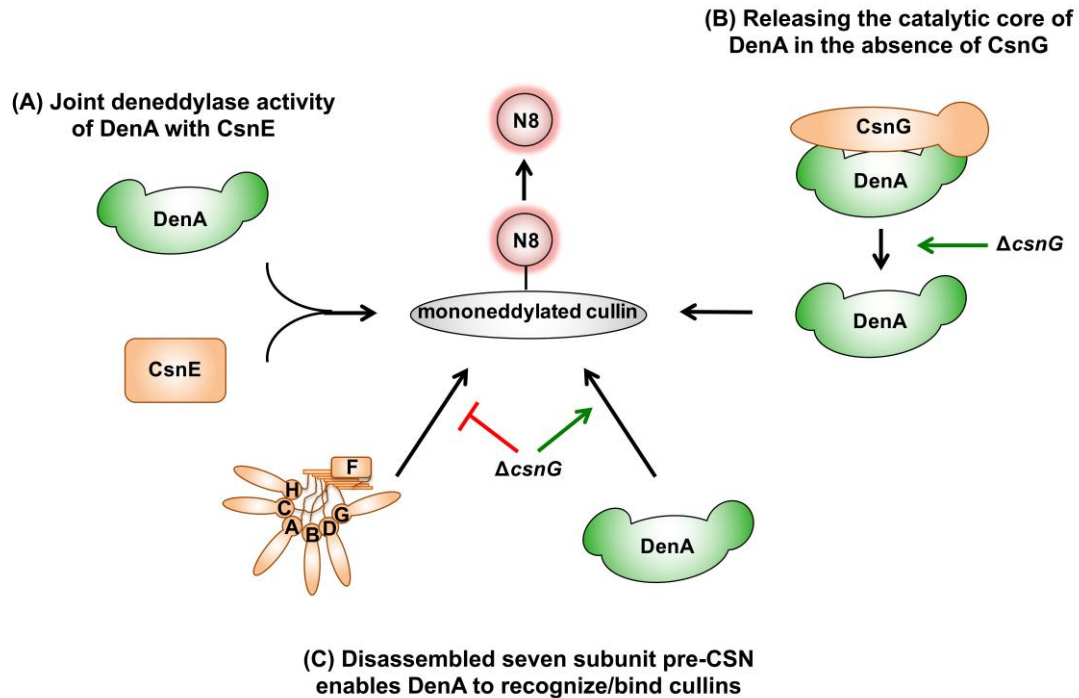


Figure 31: Model for auxiliary DenA function to compensate CSN associated defects.

Hypotheses how high abundant DenA compensates impaired activity of CSN when cells lack *csnG* but CsnE is present. **(A)** DenA requires the presence of CsnE, but not of CsnG, to form a new complex with concerted deneddylation activity. **(B)** The DenA-CsnG interaction blocks the catalytic core of DenA under normal conditions. If CsnG is missing, DenA activity would be increased resulting in the deneddylation of cullins. **(C)** A seven subunit pre-CSN complex, including CsnG but not CsnE, inhibits recognition and/or binding of DenA to neddylation cullins. The pre-CSN complex cannot be formed when CsnG is missing, which enables high abundant DenA to approach and deneddylation cullins.

4.3 The presence of five neighboring CSN subunits targets nuclear DenA for degradation

The two deneddylases DenA/DEN1 and COP9 signalosome remove the ubiquitin-like protein Nedd8 from modified targets and are required for development in fungi as well as in insects, plants and mammals (Serino & Deng, 2003; Tomoda *et al*, 2004; Singer *et al*, 2014; Beckmann *et al*, 2015). In *A. nidulans* the two deneddylases are involved in different developmental pathways. DenA supports asexual development, which is promoted when the fungus reaches the soil surface and perceives light signals, whereas CSN is essential for sexual development (Christmann

et al, 2013; Beckmann *et al*, 2015). Both deneddylases physically interact which is conserved from fungi to human (Christmann *et al*, 2013). The nuclear CSN-DenA interaction might be part of a developmental control which delays asexual development and supports sexual differentiation and secondary metabolism e.g. in the soil and in darkness. The impact of the interrelationship between the two deneddylases was studied by monitoring DenA protein levels in the absence of single CSN subunits. It was found that three PCI subunits (CsnC, CsnG, CsnH) and the two MPN containing proteins (CsnE, CsnF) were required to destabilize DenA, whereas the other three CSN subunits (CsnA, CsnB, CsnD) did not affect DenA stability (Figure 15). These findings indicate that both deneddylases do not only interact with each other, but that in addition five CSN subunits are responsible to trigger the amount of nuclear DenA.

Previous studies identified proteins whose stability is affected by the complete or partial loss of CSN (Wei *et al*, 2008; Choi *et al*, 2015). Among them are CSN interacting proteins such as the cyclin-dependent kinase inhibitors p57 and p27, which negatively control cell cycle progression. The stability of p57 is negatively regulated by subunit CSN6 (Chen *et al*, 2012a) whereas the influence of CSN on p27 stability is still controversial. *In vitro* data demonstrate a CSN mediated inhibition of p27 degradation (Yang *et al*, 2002), whereas transient overexpression of the five mammalian CSN subunits CSN3, CSN5, CSN6, CSN7 and CSN8 results in p27 down-regulation (Tomoda *et al*, 2002; Choi *et al*, 2015). These five mammalian CSN components correlate with the same five fungal CSN subunits, which were identified in this study as supporters of DenA degradation in *A. nidulans*. Although scientific evidences suggest that beside the eight subunit CSN holocomplex also CSN subcomplexes can be formed (Wei *et al*, 2008; Sharon *et al*, 2009; Kotiguda *et al*, 2012; Dubiel *et al*, 2015), no “mini-CSN” complex consisting of those five CSN subunits was described so far. As DenA is stabilized in distinct *csn* deletion strains it is likely that DenA degradation is not automatically induced by a disassembled CSN complex but might depend on physical interactions with respective CSN subunits. The crystal structure of the human CSN complex revealed that it is composed of two organized centers. The C-terminal α -helices of every subunit create a large bundle and the six subunits with a PCI domain form a horseshoe-like structure with their N-terminal domains (Lingaraju *et al*, 2014; Meister *et al*, 2015). According to the

subunit composition, the five CSN subunits with destabilization effect on DenA are adjacent and probably form a common surface (Figure 32). This suggests that proteins such as DenA, p57 or p27 physically interact with these CSN subunits resulting in the degradation of the interacting protein.

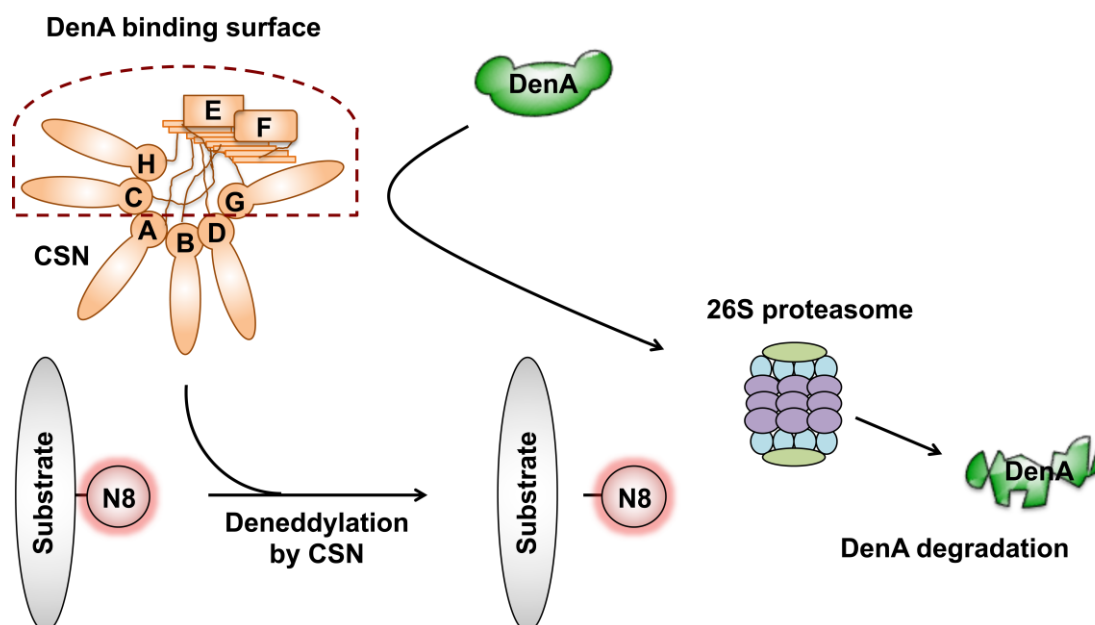


Figure 32: DenA degradation mediated by the COP9 signalosome.

The model shows the involvement of CSN in DenA degradation. The active CSN holocomplex consists of eight CSN subunits and mediates deneddylation of Nedd8 conjugates. The five DenA destabilizing CSN subunits CsnC, CsnE, CsnF, CsnG and CsnH are closely aligned, suggesting the formation of a common DenA binding surface. Interaction of DenA with this binding site targets DenA for degradation via the 26S proteasome.

Cellular proteins can be degraded via two different mechanisms. Proteins in the extracellular lumen are taken up by receptor-mediated endocytosis. Enclosed by vesicles those proteins are transported to lysosomes where they are degraded. The lysosomal destruction pathway can be further divided into phagocytosis and autophagy, but they represent a rather unspecific protein degradation system (Eskelinen & Saftig, 2009; Flannagan *et al*, 2012). To sustain fundamental biological processes a precise protein turnover is required. The non-lysosomal pathway, the ubiquitin-proteasome system, represents the major process of highly selective protein destruction of intracellular substrates (Schrader *et al*, 2009; Ciechanover, 2015). Based on the observation that human DenA/DEN1 was stabilized in a cyclohexamide

experiment by addition of the proteasome inhibitor MG132 (Christmann *et al*, 2013), it is likely to assume that the five CSN subunits with destabilization effect on DenA support degradation of DenA via the ubiquitin-proteasome system (Figure 32). This suggestion is further supported by the finding that DenA/DEN1 of *A. thaliana* is modified with ubiquitin, indicating a 26S proteasome mediated degradation (Mergner *et al*, 2015).

Increased DenA stability in a strain that lacks the gene encoding for the main interaction partner of DenA, CsnG, might correlate with the compensatory effect of high abundant DenA, which was observed in the same deletion strain. DenA might be stabilized in a *csnG* deletion strain, in order to be capable to at least partially counteract the absent CSN activity by compensating the deneddylation of CSN related targets. Such a mechanism might exist to maintain fundamental cellular processes such as development and stress response in CSN defective cells. The supporting deneddylation function of DenA under conditions where CSN is inactive may represent an aspect, which explains the necessity to encode two deneddylases. The interference of both deneddylases suggests that DenA degradation is supported by CSN under conditions where asexual development is negligible and sexual differentiation needs to be promoted by the CSN complex.

4.4 A specific choreography of changing phosphorylation events at DenA C-terminus regulates its stability and fungal development

It is known that phosphorylation and protein destruction are often coupled processes (Glickman & Ciechanover, 2002; Nguyen *et al*, 2013). Depending on the respective degron, addition of one or more phosphate groups to a protein can either stabilize the respective target (phospho-inhibited degron) or it becomes recognized by CRLs resulting in protein degradation (phosphodegron) (Ravid & Hochstrasser, 2008; Holt, 2012; Randle & Laman, 2015). DenA represents a stable protein during vegetative growth and presumably during the establishment of developmental competence but it converts into a destabilized variant later during development (Figure 15). DenA stability control correlates with fungal development and the phosphorylation of three serine residues located at its C-terminus at position S243, S245 and S253. The two phosphorylated serine residues at position S243 and S245, identified during vegetative growth, stabilize DenA (Figure 18). This implies that

respective phosphorylation sites represent phospho-inhibited degrons, which are important to prevent DenA degradation. A triple amino acid substitution of the identified serines to alanine, mimicking a constant dephosphorylated protein at these sites, caused this DenA variant to degrade earlier than wild type DenA during asexual development inducing conditions. The unphosphorylated DenA protein was unable to restore wild type phenotype in a *denA* deletion background when pyrimidine supply was limited (Figure 19). Impaired asexual development suggests that DenA has to be phosphorylated at serines S243 and S245 and stabilized, to promote asexual development (Figure 33). The formation of reproductive structures such as asexual conidiospores requires high amounts of purines and pyrimidines representing essential components of RNA and DNA (Sigoillot *et al*, 2002; 2003). As DenA is a deneddylase that acts primarily on neddylated non-cullin proteins (Christmann *et al*, 2013; Enchev *et al*, 2015; Mergner *et al*, 2015) stable DenA might be required to deneddylate so far unknown substrates as prerequisite to support the transition from vegetative growth to asexual development. The impaired asexual spore formation of strains either lacking *denA* or displaying premature DenA degradation during limited pyrimidine supply hints to putative DenA substrates linked to pyrimidine metabolism.

After vegetative hyphae reach the stage of developmental competence external stimuli induce either sexual or asexual development, depending on the environmental signals (Axelrod *et al*, 1973; Adams *et al*, 1998; Bayram & Braus, 2012; Dasgupta *et al*, 2015). Asexual spore formation is primarily induced by light and controlled by a central regulatory pathway that directs expression of transcription factors such as *brlA*, *abaA* and *wetA*, which are required for conidiophore assembly (Yu, 2010; Ruger-Herreros *et al*, 2011). DenA supports the transition from filamentous growth to asexual differentiation during the establishment and the evaluation process of developmental competence, which results in the decision to promote asexual development (Figure 33). Since DenA possesses deneddylation activity it is likely that at the beginning of asexual development its activity directly or indirectly affects this conidiation cascade, although a respective substrate is not known so far. Comparative gene expression analyses of these genes in *denA* deletion strain and wild type might lead to interesting insights about the contribution of DenA in this central asexual pathway. After developmental transition is completed, DenA is successively degraded and presumably dispensable for further asexual development.

Protein degradation is not only closely linked to ubiquitination of the substrate, but also to phosphorylation. Phosphorylation of the substrate often occurs prior ubiquitination, especially when ubiquitination results in degradation of the substrate (Nguyen *et al*, 2013; Randle & Laman, 2015). Destabilization of DenA during later stages of development depended on the presence of an additional serine at position S253, which can be phosphorylated. A negative charge provided by an aspartate residue at this position produced an unstable DenA, whereas exchange of serine to alanine at this position resulted in a stable DenA (Figure 18). This suggests that S253 represents a phosphodegron, which targets DenA for degradation. Negative charges at all three C-terminal DenA residues provided by aspartate codon exchanges instead of the original serine residues, resulted in a stable protein. This observation implies that the vegetative phosphorylation sites S243 and S245 are more dominant when compared to single phosphorylation of S253. It is assumable that DenA has to be dephosphorylated at positions S243 and S245 during asexual development before it can be destabilized by phosphorylation of the putative phosphodegron S253 at a later stage of differentiation.

The amino acid substitution experiments revealed a discrepancy between the identification of the triple phosphorylated DenA variant during conditions in which DenA was degraded and the artificially three fold phosphorylated DenA version that was stabilized. As phosphorylation and dephosphorylation are dynamic events, the DenA variant, which possesses three phosphorylated serine residues, might represent an intermediate status that is present between the transition from vegetative growth to asexual differentiation (Figure 33). The equilibrium of differentially phosphorylated DenA variants may change towards single phosphorylated DenA at position S253 during advanced asexual development resulting in its degradation. Taking into account that asexual mycelium consists of a mixture of young and older hyphae, the additional possibility raises that the peptides, which were identified during asexual development, derived from a mixture of cells that were either in the initial or advanced stage of asexual development. Proteins from these different growth phases cannot be distinguished by LC-MS/MS analyses, which might explain the finding of a triple phosphorylated and therefore stabilized DenA during conditions in which DenA degradation begins.

DenA stability is controlled by different CSN subunits as well as by phosphorylation events. One could speculate that both effects are correlating in a way

that CSN subunits regulate DenA stability by mediating phosphorylation of DenA through CSN associated kinases. The CSN interacting kinases CK2 (formerly casein kinase 2) and PKD (protein kinase D) of mammals phosphorylate CSN subunits CSN2 and CSN7 (Uhle *et al*, 2003). Other known phosphorylated CSN subunits are CSN1, CSN3, CSN6 and CSN8 (Fang *et al*, 2008; Chung & Dellaire, 2015; Meir *et al*, 2015). Phosphorylation by CSN interacting kinases is not only restricted to CSN subunits but also includes modifications of CSN-associated proteins (Harari-Steinberg & Chamovitz, 2004). For instance, the transcription factor c-Jun and the tumor suppressor p53 interact with CSN5 and are phosphorylated by CSN associated kinases. While phosphorylation stabilizes c-Jun, a CSN specific phosphorylation of p53 results in its degradation (Naumann *et al*, 1999; Bech-Otschir *et al*, 2001; Chung & Dellaire, 2015). Another candidate is the cyclin-dependent kinase inhibitor p27, which interacts with CSN5 and is phosphorylated by the cyclin-dependent kinase CDK2. This results in nuclear export and subsequent degradation of p27 (Vlach *et al*, 1997; Sheaff *et al*, 1997; Tomoda *et al*, 2002). The hypothesis that CSN associated kinases regulate DenA stability is not only supported by the physical interaction between both deneddylases (Zhou & Watts, 2005; Christmann *et al*, 2013) but also by computational prediction (Huang *et al*, 2005b) of putative kinase candidates which might be responsible for phosphorylating DenA at the identified sites. It was revealed that the fungal cyclin dependent cell cycle kinase Cdc2, which is related to the human CDK2, may represent a potential candidate responsible for the phosphorylation of DenA at serines S245 and S253 (Figure 33). These serines have opposing effects on DenA stability, suggesting that the kinase has stabilizing as well as destabilizing functions. In *A. nidulans* NimX^{Cdc2} corresponds to Cdc2 and is the only mitotic cyclin-dependent protein kinase (Osmani *et al*, 1994). Previously, it was revealed that mammalian CDK2 interacts with the CsnE/CSN5 subunit (Yoshida *et al*, 2013). CsnE might mediate phosphorylation of DenA by NimX^{Cdc2}, which would explain the absence of a kinase in our approach to identify DenA interacting proteins. As phosphorylation can alter the biological function of the modified protein (Nishi *et al*, 2011; Duan & Walther, 2015), the hypothesis of a NimX^{Cdc2} driven phosphorylation of DenA suggests that the deneddylase is misregulated in a *csnE* deletion strain. This might explain the incapability of DenA to compensate CSN related functions in a *csnE* deletion strain (Figure 12 - 14). Analyses of the third phosphorylation site S243 did not lead to a reliable kinase candidate responsible for its modification.

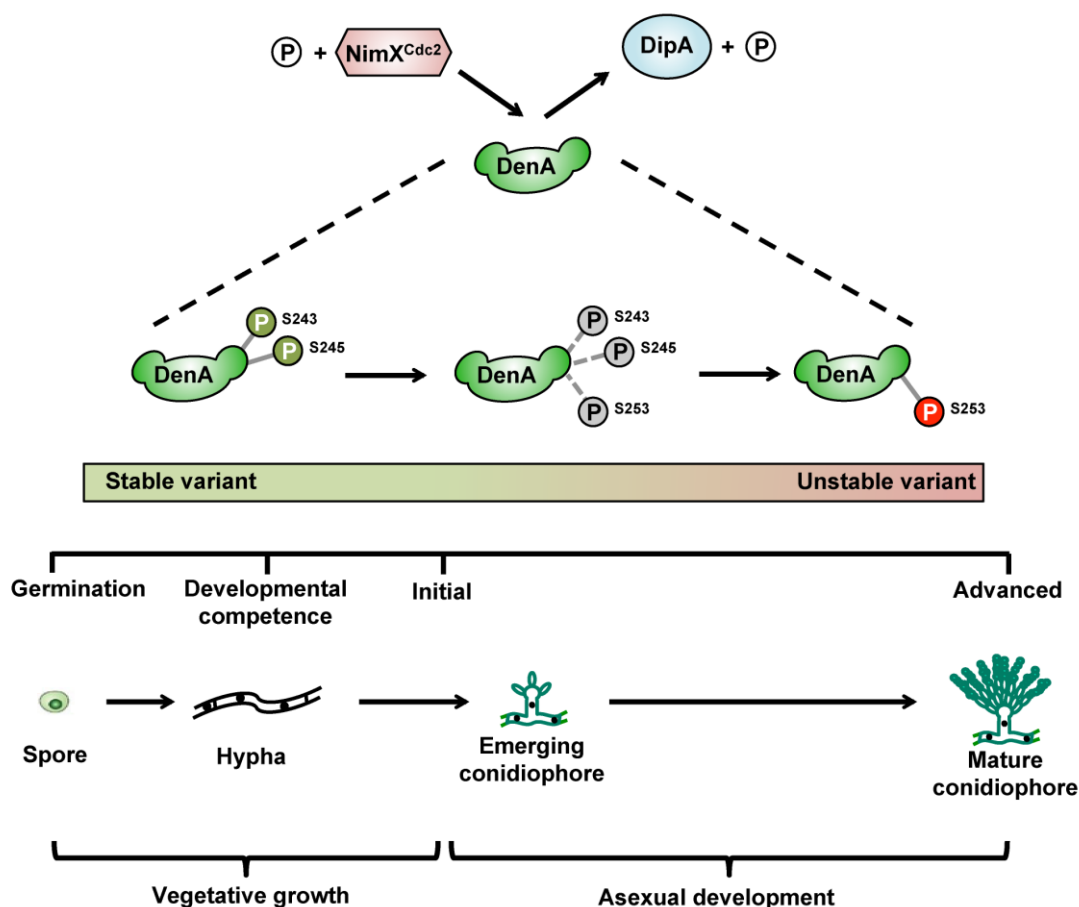


Figure 33: Phosphorylation of DenA regulates its stability and fungal development.

This model displays the effect of DenA phosphorylation on its stability and fungal development. These modifications might be catalyzed by the kinase NimX^{Cdc2} and reversed by the phosphatase DipA. A spore germinates to form a hypha that continuously grows until it reaches the stage of developmental competence. During this vegetative growth phase and early asexual development, DenA is stabilized by phosphorylation of the serine residues S243 and S245. Phosphorylated DenA is required for efficient asexual spore formation after developmental competence was achieved. The phosphorylation status of DenA changes the protein stability within continuous asexual differentiation. An additional phosphorylation at residue S253 occurs. The exact chronological order of phosphorylation and dephosphorylation events is currently unknown, therefore a putative intermediate DenA variant is represented with dashed phosphorylation lines. Advanced asexual development results in the formation of a mature conidiophore. DenA becomes dispensable so that the vegetative, stabilizing phosphorylation sites are dephosphorylated and the single phosphorylation at serine S253 causes DenA degradation.

4.5 The phosphatase DipA targets cytoplasmatic DenA for degradation

The complex phosphorylation control of DenA during fungal development is supported by the discovery of the DenA interacting phosphatase DipA. Deletion of the corresponding *dipA* gene resulted in an increased DenA stability during asexual development, which implies that DipA uses DenA as a substrate (Figure 27). The increased DenA stability in the *dipA* deletion strain, in which DenA phosphorylation status is probably misregulated, is reminiscent of the stabilized DenA variant that was generated by amino acid substitution of the identified phosphorylation sites S243, S245 and S253 mimicking a constant phosphorylated DenA protein at these sites (Figure 18). This observation suggests that DipA removes the protective C-terminal phosphates of DenA at position S243 and S245, which results in subsequent degradation of DenA, mediated by phosphorylation of S253. DipA as well as the three identified phosphorylation sites of DenA are conserved within the fungal kingdom and might represent an ancient mechanism to control the transition from filamentous growth to asexual differentiation.

Previous studies reported that different subpopulations of proteins, present in separate compartments, can display different degradation patterns (Boisvert *et al*, 2012; Larance *et al*, 2013). It was suggested that the interaction with other proteins present in the different compartments might individually influence the stability of the respective protein (Rodway *et al*, 2004; Boisvert *et al*, 2012). The localization data presented in this study imply that the interaction between DenA and CSN, which was previously found inside nuclei (Christmann *et al*, 2013), is different from the DenA-DipA interaction complex. *In vivo* analyses using bimolecular fluorescence complementation revealed that DipA interacts exclusively with the cytoplasmatic DenA subpopulation, which is enriched at septa (Figure 25 & 26). Taking into account that DenA stability is increased in a *dipA* deficient strain, it is likely that DipA destabilizes the cytoplasmatic/septatic DenA subpopulation. The localization data in combination with the results of DenA stability suggest that stability of fungal DenA is controlled by various mechanisms, including nuclear CSN and cytoplasmatic DipA (Figure 34).

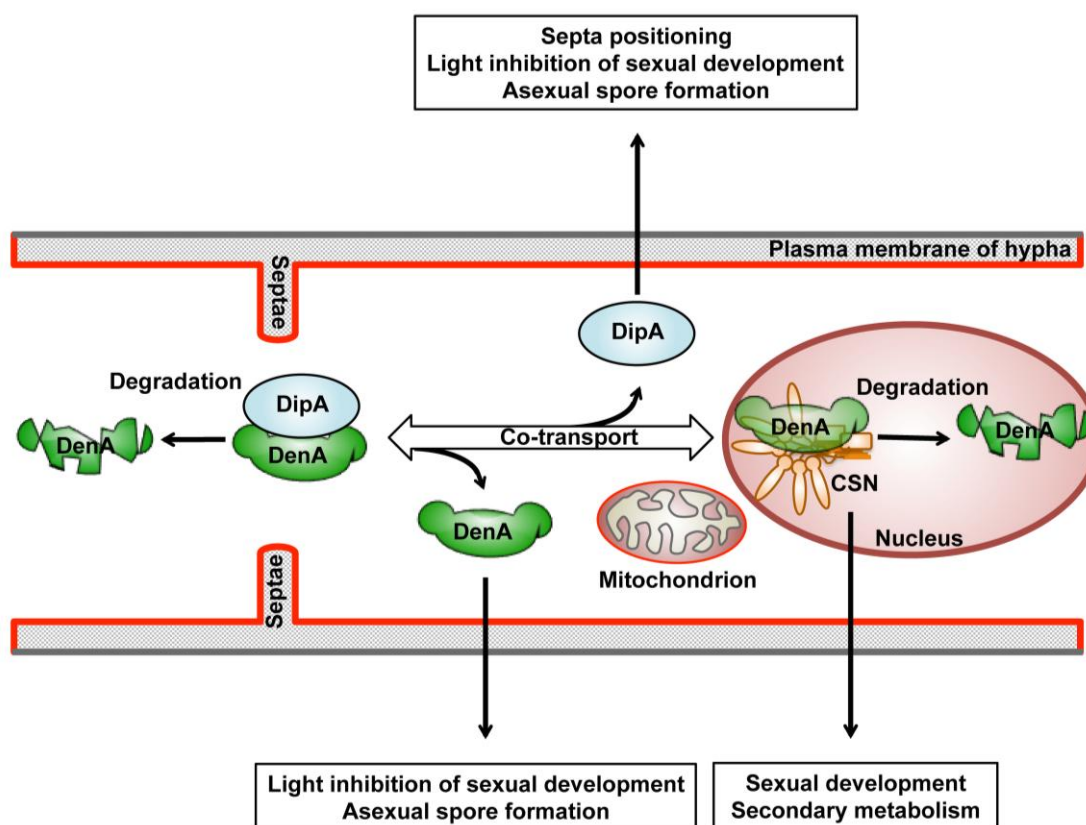


Figure 34: CSN and DipA target different subpopulations of DenA for degradation.

The model displays degradation of differently localized DenA subpopulations. DenA, which is involved in the repression of sexual development to promote asexual differentiation during illumination, is located in the nucleus, in the cytoplasm and there especially enriched at septa. The nuclear DenA subpopulation interacts with CSN subunits, which is required for sexual development and secondary metabolism. The DenA-CSN interaction targets nuclear DenA for degradation. Cytoplasmatic DenA is destabilized by the phosphatase DipA. DipA regulates septa intervals, inhibits sexual development in light and supports asexual spore formation. The DenA-DipA interaction complex shuttles in the cytoplasm between mitochondria, nuclei and septa, suggesting that both DenA turnover points are connected.

When DenA stability control mechanisms are impaired (e.g. in a *dipA/csnG* double deletion), the cellular DenA amount was similarly stabilized and enriched compared to single deletion strains (Figure 29). This suggests that both stability checkpoints are communicating with each other in a yet unknown manner. Cytoplasmatic DenA is highly dynamic and shuttles between nuclei, mitochondria and septa. Transport of various cargoes, including mitochondria, vesicles, peroxisomes or vacuoles requires the cytoskeleton including tubulins and actins

(Suelmann & Fischer, 2000; Egan *et al*, 2012; Takeshita *et al*, 2014). It is likely that association of DenA to DipA-dependent or even DipA-independent cellular transport processes might be part of the communication between different DenA stability control mechanisms in the nucleus and the cytoplasm, respectively. Other proteins could participate in the intracellular shuttling of DenA. DenA interaction is not restricted to DipA and CsnG but also includes possible transport proteins as the fungal counterpart of yeast SCP160 transporting RNA molecules within a cell (Christmann, 2012).

Often, kinase and phosphatase reactions are dynamic and transient. The observation that the DenA-DipA interaction is not a “kiss and run” event but a continuous co-transport might result from a strong binding due to the chosen BiFC method or because of low activity of DipA towards its potential substrate. It will be interesting to reveal whether the phosphorylation pattern of DenA varies depending on whether it is located in the nucleus or in the cytoplasm/septa. Amino acid substitution experiments revealed that the complex formation of DenA-DipA is independent of whether the three identified phosphorylation sites at the C-terminus of DenA are phosphorylated or unphosphorylated. This might indicate that DenA possesses additional phosphorylation sites that are controlled by DipA.

4.6 The phosphatase DipA controls cytokinesis

The DenA interacting phosphatase DipA is required for septa positioning within fungal filaments. Formation of septa is the equivalent of cytokinesis with the exception that septation leads to compartmentalization and mostly incomplete cell separation (Balasubramanian *et al*, 2004). Growing hyphae are normally partitioned into compartments separated by several septa. These internal cross walls are formed at more or less regular intervals. In this study it was found that strains lacking either a functional DipA or the entire DipA encoding gene revealed an increased amount of septa (Figure 23). This observation suggests that an active DipA phosphatase is required to control the correct septa interval. The formation of septa requires three steps (Kim *et al*, 2009; Mouriño-Pérez, 2013). Septation starts with the selection of the division site. The second step is the orderly assembly of >100 conserved proteins which are temporally and spatially coordinated to form a septum (Seiler & Justa-Schuch, 2010). Septum formation finishes with dynamic constrictions of a contractile

actomyosin ring, invagination of the plasma membrane and deposition of cell wall materials (Harris, 2001; Walther & Wendland, 2003; Mouriño-Pérez, 2013; Delgado-Álvarez *et al*, 2014). The lack of *dipA* might interfere with one or several of these processes that regulate septation. First, the cytoskeleton plays an important role during septum formation where actin appears to be the first protein to mark the future septum site (Momany & Hamer, 1997; Delgado-Álvarez *et al*, 2014; Manck *et al*, 2015). DipA localizes to septa and shuttles through hyphae where it is closely connected to ATP producing mitochondria (Figure 26). In *A. nidulans* the distribution of mitochondria depends predominantly on the actin cytoskeleton (Suelmann & Fischer, 2000), which raises the possibility that DipA supports actin to define the septation site. Second, the availability of sufficient amounts of ATP is required for motor proteins to mediate transport processes of various cargos to the site of septation. Misregulation of motor proteins results in altered septation (Liu & Morris, 2000; Taheri-Talesh *et al*, 2012; Takeshita *et al*, 2015). Increased septa formation in strains lacking *dipA* might be caused by misregulation of these cargo receptors possibly due to alterations of the cellular ATP pool. Third, in mammals, yeast and filamentous fungi, cell separation has been linked to posttranslational modifications, including phosphorylation. Septins, which represent a group of proteins that is involved in coordinating a variety of cellular processes at the site of septation, are controlled by phosphorylation (Dobbelaere *et al*, 2003; Juvvadi *et al*, 2013; Bridges & Gladfelter, 2014). The observed defects in septa formation of *dipA* mutant strains suggest an enrichment of phosphorylated substrates, such as septins, that cause the increased septation. Since DenA and DipA are co-transported in the cytoplasm and accumulate at septa it is still elusive whether these substrates are phosphorylated and/or neddylated and therefore are substrates of DipA and/or DenA, respectively. The analyzed *denA* mutant strains did not show obvious defects in septa formation in comparison to wild type, suggesting that DenA is presumably not directly involved in this phenotype.

Cytoplasmatic DipA interacts at septa with phosphorylated DenA, which might point to the kinase, which is the antagonist of DipA as another interesting player. As mentioned above, analyses of the identified DenA phosphorylation sites with a computational prediction tool (Huang *et al*, 2005b) revealed the fungal cyclin dependent cell cycle kinase NimX^{Cdc2} as potential candidate responsible for phosphorylating DenA. In *A. nidulans* the activity of NimX^{Cdc2} is strictly controlled

by the phosphatase NimT, which triggers NimX^{Cdc2} activation by dephosphorylating tyrosine15 (O'Connell *et al*, 1992). Controlled activity of NimX^{Cdc2} is required for proper septa formation in *A. nidulans* (Harris & Kraus, 1998; Osmani *et al*, 1994). Elevated NimX^{Cdc2} activity causes hyperseptated hyphae (Harris & Kraus, 1998; Aguirre, 1993). Increased septation in strains lacking *dipA* might be caused by misregulated NimX^{Cdc2}, suggesting DipA contributes to the phosphoregulation of this kinase. Since deletion of *dipA* in *A. nidulans* resulted in hyperseptation, it is also possible that putative substrates of NimX^{Cdc2}, that accumulate in their phosphorylated form in *dipA* deletion strain, cause the impaired septa formation.

4.7 The phosphatase DipA controls development

Formation of septa is essential in filamentous ascomycetes and might be prerequisite for asexual spore formation (Mouriño-Pérez & Riquelme, 2013). The asexual conidiophore forms conidiospores in a manner that is similar to diploid yeast pseudohyphae formation and reminiscent of the process of septation. At the end of a central regulatory pathway asexual spores emerge on the conidiophore by continuous budding processes that give rise to long chains of conidiospores (Adams *et al*, 1998; Yu, 2010). Reduced asexual spore formation as well as reduced growth of the *dipA* deletion strain observed in this study (Figure 21 & 22), might result from malfunctioning cell division. This is in accordance to phenotypically analyses of a plethora of phosphatase encoding genes in *A. nidulans*. Some of them are essential, others are required for normal growth or involved in mitosis, which supports the importance of phosphatase-mediated protein dephosphorylation in regulating cell cycle progression and development in fungi (Son & Osmani, 2009; Ghosh *et al*, 2014; Kück *et al*, 2015).

Additional developmental defects were observed during illumination of a *dipA* deletion strain. During asexual conditions deletion of *dipA* resulted in the formation of sexual reproductive structures combined with the accumulation of a brownish dye, which is typical for impaired fungal secondary metabolism (Figure 22). A strain carrying DipA with a mutated catalytic core was indistinguishable from a *dipA* deletion strain, demonstrating that the observed phenotypes are caused by impaired phosphatase activity. Therefore, DipA mediated dephosphorylation seems to be required for fungal light response, which normally promotes asexual development

and reduces sexual development (Adams *et al*, 1998; Bayram *et al*, 2008a; Purschwitz *et al*, 2008). As development and secondary metabolism are often coordinated in fungi (Bayram & Braus, 2012; Brakhage, 2013; Gerke & Braus, 2014), DipA might represent an interesting target for discovering new secondary metabolites and respective gene clusters. The complex phenotype of *dipA* deletion strain suggests that developmental programs require the dynamic DipA-DenA interaction for the local dephosphorylation and/or deneddylation of multiple, not yet identified substrates, at various cytoplasmatic locations, including septa.

Several master regulators control fungal development. The light sensor FphA is a sensor kinase with auto- or transphosphorylation activity, which represses sexual development in red light (Blumenstein *et al*, 2005; Brandt *et al*, 2008; Dasgupta *et al*, 2015). As the *dipA* deletion strain displayed a constitutive active sexual development, it can be speculated that DipA is required to integrate light signals sensed by FphA, probably by affecting its phosphorylation status (Figure 35A). Due to the cytoplasmatic localization of FphA, it was suggested that red-light photoperception occurs in the cytoplasm (Blumenstein *et al*, 2005). This corresponds to DipA localization and further supports a possible impact of the phosphatase on FphA mediated light response.

An additional possibility of how DipA may influence fungal development rises by taking into account that the central developmental regulator VeA can co-purify DipA (J. Gerke, personal communication). This suggests that both proteins are physically interacting. VeA shuttles into the nucleus in the dark, which is prerequisite to form the trimeric VeA-VelB-LaeA *velvet* complex that coordinates sexual development and secondary metabolism (Bayram *et al*, 2008b; Sarikaya-Bayram *et al*, 2015). Overexpression of the VeA encoding gene results in a constitutively active sexual development (Kim *et al*, 2002). DipA might affect sexual development by directly or indirectly repressing the nuclear translocation of VeA in the light (Figure 35B) or by mediating degradation of the cytoplasmatic VeA fraction during illumination (Figure 35C). Since VeA occurs as a phosphorylated and a non-phosphorylated form (Purschwitz *et al*, 2009), the phosphatase DipA could represent a VeA interacting protein, which regulates the function of VeA by altering its phosphorylation status. The accumulation of a brownish dye in strains lacking a functional DipA indicates an involvement of the phosphatase in the production of secondary metabolites and supports the observation that development and secondary

metabolism are often coordinated in fungi (Bayram *et al*, 2008b; Bayram & Braus, 2012; Gerke & Braus, 2014). The presented hypotheses describe putative mechanisms, in which DipA has a direct impact on proteins that regulate development. One could find evidences of a direct influence of DipA on the regulation of respective proteins by performing localization studies of e.g. VeA or FphA in a *dipA* deletion background. Also co-localization studies using BiFC strains to test physical interactions between DipA and these developmental regulators could support a direct relation between these proteins. If a direct effect of DipA on central developmental regulatory proteins cannot be confirmed, the phosphatase might act downstream. This could be caused by the repression of genes, which are required to induce the sexual life cycle in the dark but are inhibited during illumination.

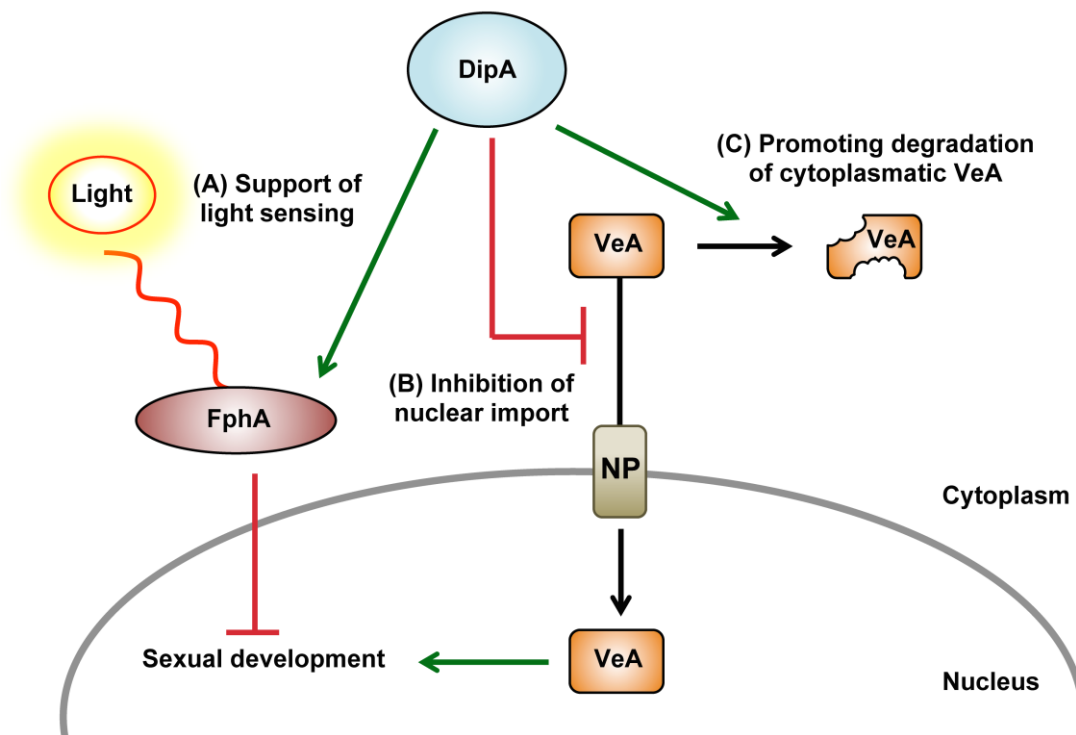


Figure 35: Putative impact of DipA on central regulators of fungal development.

The phosphatase DipA is required for proper fungal development. The model shows three possible mechanisms of how DipA might directly influence the life cycle of *A. nidulans*. (A) DipA enables FphA to sense light, which in return suppresses sexual development. (B) DipA represses nuclear entry of VeA and thereby the activation of genes regulating sexual differentiation. (C) DipA is required for degradation of the cytoplasmic subpopulation of VeA, resulting in an inactive sexual program.

In summary, this study provides comprehensive indications that DenA stability is controlled at various levels in order to allow proper asexual development. It was revealed that phosphorylation events trigger both stabilization and destabilization of DenA. Destabilizing phosphorylation of cytoplasmatic DenA might be delayed by the phosphatase DipA in the cytoplasm to overcome the initial phases of fungal differentiation during the window when the fungus establishes developmental competence and the future programs for differentiation are started. The well-orchestrated phosphorylation of DenA might include nuclear kinases, which are associated to the CSN and play an important role in DenA stability control. Whether NimX^{Cdc2} represents the potential kinase of DenA remains to be studied.

4.8 Future outlook

DenA stability is regulated by phosphorylation and dephosphorylation events. Finding the kinase which is the antagonist of DipA is a challenging task. But it would improve our understanding of the phosphorylation dependent stability control of DenA and its impact on Nedd8 controlled processes and cell differentiation. First one could test via BiFC whether NimX^{Cdc2} physically interacts with DenA. When this result is negative, one could analyze DenA interacting proteins in more detail. As kinases were absent in previous DenA-GFP purification experiments (Christmann, 2012), one could analyze the neighboring proteins of DenA with the BioID method (proximity-dependent biotin identification, Roux *et al*, 2013). This allows to label and identify proteins that physically interact with DenA as well as proteins that are in close proximity. This approach might answer, whether phosphorylation of DenA is mediated by CSN associated kinases.

Beside the importance to identify the kinase responsible for DenA, it would be attractive to study whether nuclear and cytoplasmatic DenA reveal differences regarding their phosphorylation pattern and/or deneddylation activity/specificity. The regulated nuclear import/export process of proteins depends on nuclear localization and export signals, which are distinct stretches of residues within a protein (Lange *et al*, 2007; Kosugi *et al*, 2008). The identification of such sequences within DenA and the subsequent deletion of these particular regions might allow to trap the deneddylase in a certain compartment. Thus, one could distinguish between the two different DenA subpopulations and analyze their distinct impact on cellular processes.

DenA physically interacts with both the COP9 signalosome as well as the phosphatase DipA. It would be appealing to analyze whether the deneddylation activity of DenA is influenced by their binding. *In vitro* deneddylation experiments with functional DenA, in the presence or absence of DipA or combinations with different CSN subunits, might lead to insights about activity control of DenA by its interacting proteins.

DipA represents an enzyme, which is dynamically co-transported with DenA and deletion of the corresponding gene results in several phenotypes affecting stability of DenA, septation and development. Further understanding of this phosphatase is missing. It will be attractive to reveal proteins that form a complex with this phosphatase. These proteins could be central developmental regulators such as FphA, VeA and septins. The identification of putative substrates of DipA will help to understand the biological function of this phosphatase in more detail. To address this the already existing DipA-GFP strain grown during different developmental conditions could be used for GFP-Trap experiments, which are followed by LC-MC/MS analyses.

DipA is a fungal specific phosphatase, which is absent in higher eukaryotes. Fungal pathogens require proper septation and cell shape for invasion of the host tissue (Bridges & Gladfelter, 2014). DipA is an interesting target to control fungal growth including pathogens, which control host infection through the cell cycle (Saunders *et al*, 2010; Dagdas *et al*, 2012; Bridges & Gladfelter, 2014). The influence of DipA on cytokinesis may help to shed new light into cell differentiation in plants and mammals and may extend the possibilities to manipulate pathways involved in cell cycle control and virulence.

Literature

- Adams TH, Wieser JK & Yu JH (1998) Asexual sporulation in *Aspergillus nidulans*. *Microbiol Mol Biol Rev.* **62**: 35–54
- Aguirre J (1993) Spatial and temporal controls of the *Aspergillus brlA* developmental regulatory gene. *Mol Microbiol.* **8**: 211–218
- Aramayo R, Adams TH & Timberlake WE (1989) A large cluster of highly expressed genes is dispensable for growth and development in *Aspergillus nidulans*. *Genetics* **122**: 65–71
- Aravind L & Koonin EV (1998) Phosphoesterase domains associated with DNA polymerases of diverse origins. *Nucleic Acids Res.* **26**: 3746–3752
- Arnason T & Ellison MJ (1994) Stress resistance in *Saccharomyces cerevisiae* is strongly correlated with assembly of a novel type of multiubiquitin chain. *Mol Cell Biol.* **14**: 7876–7883
- Arst HN Jr & Cove DJ (1973) Nitrogen metabolite repression in *Aspergillus nidulans*. *Mol Gen Genet.* **126**: 111–141
- Axelrod DE, Gealt M & Pastushok M (1973) Gene control of developmental competence in *Aspergillus nidulans*. *Dev Biol.* **34**: 9–15
- Balasubramanian MK, Bi E & Glotzer M (2004) Comparative analysis of cytokinesis in budding yeast, fission yeast and animal cells. *Curr Biol.* **14**: R806–18
- Barr FA, Elliott PR & Gruneberg U (2011) Protein phosphatases and the regulation of mitosis. *J Cell Sci.* **124**: 2323–2334
- Bayram Ö & Braus GH (2012) Coordination of secondary metabolism and development in fungi: the velvet family of regulatory proteins. *FEMS Microbiol Rev.* **36**: 1–24
- Bayram Ö, Bayram ÖS, Ahmed YL, Maruyama J, Valerius O, Rizzoli SO, Ficner R, Irniger S & Braus GH (2012) The *Aspergillus nidulans* MAPK module AnSte11-Ste50-Ste7-Fus3 controls development and secondary metabolism. *PLoS Genet.* **8**: e1002816
- Bayram Ö, Biesemann C, Krappmann S, Galland P & Braus GH (2008a) More than a repair enzyme: *Aspergillus nidulans* photolyase-like CryA is a regulator of sexual development. *Mol Biol Cell* **19**: 3254–3262
- Bayram Ö, Braus GH, Fischer R & Rodríguez-Romero J (2010) Spotlight on *Aspergillus nidulans* photosensory systems. *Fungal Genet Biol.* **47**: 900–908
- Bayram Ö, Krappmann S, Ni M, Bok JW, Helmstaedt K, Valerius O, Braus-Stromeyer S, Kwon NJ, Keller NP, Yu JH & Braus GH (2008b) VelB/VeA/LaeA complex coordinates light signal with fungal development and secondary

- metabolism. *Science* **320**: 1504–1506
- Bech-Otschir D, Kraft R, Huang X, Henklein P, Kapelari B, Pollmann C & Dubiel W (2001) COP9 signalosome-specific phosphorylation targets p53 to degradation by the ubiquitin system. *EMBO J.* **20**: 1630–1639
- Beckmann EA, Köhler AM, Meister C, Christmann M, Draht OW, Rakebrandt N, Valerius O & Braus GH (2015) Integration of the catalytic subunit activates deneddylase activity *in vivo* as final step in fungal COP9 signalosome assembly. *Mol Microbiol.* **97**: 110–124
- Bennett EJ, Rush J, Gygi SP & Harper JW (2010) Dynamics of cullin-RING ubiquitin ligase network revealed by systematic quantitative proteomics. *Cell* **143**: 951–965
- Bennett JW (1998) Mycotechnology: the role of fungi in biotechnology. *J Biotechnol.* **66**: 101–107
- Bertani G (1951) Studies on lysogenesis. I. The mode of phage liberation by lysogenic *Escherichia coli*. *J Bacteriol.* **62**: 293–300
- Bleichrodt RJ, Hulsman M, Wösten HA & Reinders MJ (2015) Switching from a unicellular to multicellular organization in an *Aspergillus niger* hypha. *MBio* **6**: e00111
- Bleichrodt RJ, van Veluw GJ, Recter B, Maruyama J, Kitamoto K & Wösten HA (2012) Hyphal heterogeneity in *Aspergillus oryzae* is the result of dynamic closure of septa by Woronin bodies. *Mol Microbiol.* **86**: 1334–1344
- Blumenstein A, Vienken K, Tasler R, Purschwitz J, Veith D, Frankenberg-Dinkel N & Fischer R (2005) The *Aspergillus nidulans* phytochrome FphA represses sexual development in red light. *Curr Biol.* **15**: 1833–1838
- Boisvert FM, Ahmad Y, Gierliński M, Charrière F, Lamont D, Scott M, Barton G & Lamond AI (2012) A quantitative spatial proteomics analysis of proteome turnover in human cells. *Mol Cell Proteomics* **11**: M111.011429
- Bornstein G & Grossman C (2015) COP9-Signalosome deneddylase activity is enhanced by simultaneous neddylation: insights into the regulation of an enzymatic protein complex. *Cell Div.* **10**:5
- Boylan MT, Mirabito PM, Willett CE, Zimmerman CR & Timberlake WE (1987) Isolation and physical characterization of three essential conidiation genes from *Aspergillus nidulans*. *Mol Cell Biol.* **7**: 3113–3118
- Bradford MM (1976) A rapid and sensitive method for the quantitation of microgram quantities of protein utilizing the principle of protein-dye binding. *Anal Biochem.* **72**: 248–254
- Brakhage AA (2013) Regulation of fungal secondary metabolism. *Nat Rev Micro* **11**: 21–32

- Brandt S, von Stetten D, Günther M, Hildebrandt P & Frankenberg-Dinkel N (2008) The fungal phytochrome FphA from *Aspergillus nidulans*. *J Biol Chem.* **283**: 34605–34614
- Bridges AA & Gladfelter AS (2014) Fungal pathogens are platforms for discovering novel and conserved septin properties. *Curr Opin Microbiol.* **20**: 42–48
- Brown JS & Jackson SP (2015) Ubiquitylation, neddylation and the DNA damage response. *Open Biol* **5**: 150018
- Busch S, Eckert SE, Krappmann S & Braus GH (2003) The COP9 signalosome is an essential regulator of development in the filamentous fungus *Aspergillus nidulans*. *Mol Microbiol.* **49**: 717–730
- Busch S, Schwier EU, Nahlik K, Bayram Ö, Helmstaedt K, Draht OW, Krappmann S, Valerius O, Lipscomb WN & Braus GH (2007) An eight-subunit COP9 signalosome with an intact JAMM motif is required for fungal fruit body formation. *Proc Natl Acad Sci USA.* **104**: 8089–8094
- Butt TR, Khan MI, Marsh J, Ecker DJ & Crooke ST (1988) Ubiquitin-metallothionein fusion protein expression in yeast. A genetic approach for analysis of ubiquitin functions. *J Biol Chem.* **263**: 16364–16371
- Carlucci A & D'Angiolella V (2015) It is not all about BRCA: Cullin-Ring ubiquitin Ligases in ovarian cancer. *Br J Cancer* **112**: 9–13
- Casselton L & Zolan M (2002) The art and design of genetic screens: filamentous fungi. *Nat Rev Genet.* **3**: 683–697
- Cerqueira GC, Arnaud MB, Inglis DO, Skrzypek MS, Binkley G, Simison M, Miyasato SR, Binkley J, Orvis J, Shah P, Wymore F, Sherlock G & Wortman JR (2014) The *Aspergillus* Genome Database: multispecies curation and incorporation of RNA-Seq data to improve structural gene annotations. *Nucleic Acids Res.* **42**: D705–710
- Chamovitz DA (2009) Revisiting the COP9 signalosome as a transcriptional regulator. *EMBO Rep.* **10**: 352–358
- Chan Y, Yoon J, Wu JT, Kim HJ, Pan KT, Yim J & Chien CT (2008) DEN1 deneddylates non-cullin proteins *in vivo*. *J Cell Sci.* **121**: 3218–3223
- Chen B, Zhao R, Su CH, Linan M, Tseng C, Phan L, Fang L, Yang HY, Yang H, Wang W, Xu X, Jiang N, Cai S, Jin F, Yeung SC & Lee MH (2012a) CDK inhibitor p57 (Kip2) is negatively regulated by COP9 signalosome subunit 6. *Cell Cycle* **11**: 4633–4641
- Chen CH, Dunlap JC & Loros JJ (2010) *Neurospora* illuminates fungal photoreception. *Fungal Genet. Biol.* **47**: 922–929
- Chen Y, Neve RL & Liu H (2012b) Neddylation dysfunction in Alzheimer's disease. *J Cell Mol Med.* **16**: 2583–2591

- Cheng HC, Qi RZ, Paudel H & Zhu HJ (2011) Regulation and function of protein kinases and phosphatases. *Enzyme Res.* **2011**: 794089
- Choi HH, Guma S, Fang L, Phan L, Ivan C, Baggerly K, Sood A & Lee MH (2015) Regulating the stability and localization of CDK inhibitor p27(Kip1) via CSN6-COP1 axis. *Cell Cycle* **14**: 2265–2273
- Christmann M (2012) Deneddylation and fungal development - Regulation of Nedd8 protein modification by DenA and the COP9 signalosome. Georg-August University Göttingen. Available at: <http://ediss.uni-goettingen.de/handle/11858/00-1735-0000-000D-EF70-1>
- Christmann M, Schmalzer T, Gordon C, Huang X, Bayram Ö, Schinke J, Stumpf S, Dubiel W & Braus GH (2013) Control of multicellular development by the physically interacting deneddylases DEN1/DenA and COP9 signalosome. *PLoS Genet.* **9**: e1003275
- Chung D & Dellaire G (2015) The Role of the COP9 Signalosome and Neddylolation in DNA Damage Signaling and Repair. *Biomolecules* **5**: 2388–2416
- Ciechanover A (1994) The ubiquitin-proteasome proteolytic pathway. *Cell* **79**: 13–21
- Ciechanover A (2015) The unravelling of the ubiquitin system. *Nat Rev Mol Cell Biol.* **16**: 322–324
- Ciechanover A, Elias S, Heller H, Ferber S & Hershko A (1980) Characterization of the heat-stable polypeptide of the ATP-dependent proteolytic system from reticulocytes. *J Biol Chem.* **255**: 7525–7528
- Ciechanover A, Orian A & Schwartz AL (2000) Ubiquitin-mediated proteolysis: biological regulation via destruction. *Bioessays* **22**: 442–451
- Clutterbuck AJ (1969a) A mutational analysis of conidial development in *Aspergillus nidulans*. *Genetics* **63**: 317–327
- Clutterbuck AJ (1969b) Cell volume per nucleus in haploid and diploid strains of *Aspergillus nidulans*. *J Gen Microbiol.* **55**: 291–299
- Collinge AJ & Markham P (1985) Woronin bodies rapidly plug septal pores of severed *Penicillium chrysogenum* hyphae. *Exp Mycol.* **9**: 80–85
- Cope GA & Deshaies RJ (2003) COP9 signalosome: a multifunctional regulator of SCF and other cullin-based ubiquitin ligases. *Cell* **114**: 663–671
- Cope GA & Deshaies RJ (2006) Targeted silencing of Jab1/Csn5 in human cells downregulates SCF activity through reduction of F-box protein levels. *BMC Biochem.* **7**: 1
- Cope GA, Suh GS, Aravind L, Schwarz SE, Zipursky SL, Koonin EV & Deshaies RJ (2002) Role of predicted metalloprotease motif of Jab1/Csn5 in cleavage of Nedd8 from Cul1. *Science* **298**: 608–611

- Corpet F (1988) Multiple sequence alignment with hierarchical clustering. *Nucleic Acids Res.* **16**: 10881–10890
- Dagdas YF, Yoshino K, Dagdas G, Ryder LS, Bielska E, Steinberg G & Talbot NJ (2012) Septin-mediated plant cell invasion by the rice blast fungus, *Magnaporthe oryzae*. *Science* **336**: 1590–1595
- Dasgupta A, Fuller KK, Dunlap JC & Loros JJ (2015) Seeing the world differently: variability in the photosensory mechanisms of two model fungi. *Environ Microbiol.* doi: 10.1111/1462-2920.13055. [Epub ahead of print].
- Dean R, van Kan JA, Pretorius ZA, Hammond-Kosack KE, Di Pietro A, Spanu PD, Rudd JJ, Dickman M, Kahmann R, Ellis J & Foster GD (2012) The Top 10 fungal pathogens in molecular plant pathology. *Mol Plant Pathol.* **13**: 414–430
- Delgado-Álvarez DL, Bartnicki-García S, Seiler S & Mouriño-Pérez RR (2014) Septum development in *Neurospora crassa*: the septal actomyosin tangle. *PLoS One* **9**: e96744
- Denning DW & Bromley MJ (2015) Infectious Disease. How to bolster the antifungal pipeline. *Science* **347**: 1414–1416
- Deribe YL, Pawson T & Dikic I (2010) Post-translational modifications in signal integration. *Nat Struct Mol Biol.* **17**: 666–672
- Deshaias RJ & Joazeiro CA (2009) RING domain E3 ubiquitin ligases. *Annu Rev Biochem.* **78**: 399–434
- Dhingra S, Andes D & Calvo AM (2012) VeA regulates conidiation, gliotoxin production, and protease activity in the opportunistic human pathogen *Aspergillus fumigatus*. *Eukaryot Cell* **11**: 1531–1543
- Dobbelaere J, Gentry MS, Hallberg RL & Barral Y (2003) Phosphorylation-dependent regulation of septin dynamics during the cell cycle. *Dev Cell* **4**: 345–357
- Doronkin S, Djagaeva I & Beckendorf SK (2003) The COP9 signalosome promotes degradation of Cyclin E during early *Drosophila* oogenesis. *Dev Cell* **4**: 699–710
- Duan G & Walther D (2015) The roles of post-translational modifications in the context of protein interaction networks. *PLoS Comput Biol* **11**: e1004049
- Dubiel D, Rockel B, Naumann M & Dubiel W (2015) Diversity of COP9 signalosome structures and functional consequences. *FEBS Lett.* **589**: 2507–2513
- Dubiel W (2009) Resolving the CSN and CAND1 paradoxes. *Mol Cell* **35**: 547–549
- Duda DM, Borg LA, Scott DC, Hunt HW, Hammel M & Schulman BA (2008) Structural insights into NEDD8 activation of cullin-RING ligases: conformational control of conjugation. *Cell* **134**: 995–1006

- Egan MJ, McClintock MA & Reck-Peterson SL (2012) Microtubule-based transport in filamentous fungi. *Curr Opin Microbiol.* **15**: 637–645
- Enchev RI, Schreiber A, Beuron F & Morris EP (2010) Structural insights into the COP9 signalosome and its common architecture with the 26S proteasome lid and eIF3. *Structure* **18**: 518–527
- Enchev RI, Schulman BA & Peter M (2015) Protein neddylation: beyond cullin-RING ligases. *Nat Rev Mol Cell Biol.* **16**: 30–44
- Enchev RI, Scott DC, da Fonseca PC, Schreiber A, Monda JK, Schulman BA, Peter M & Morris EP (2012) Structural basis for a reciprocal regulation between SCF and CSN. *Cell Rep* **2**: 616–627
- Erickson RH & Kim YS (1990) Digestion and absorption of dietary protein. *Annu Rev Med.* **41**: 133–139
- Eskelinen EL & Saftig P (2009) Autophagy: a lysosomal degradation pathway with a central role in health and disease. *Biochim Biophys Acta* **1793**: 664–673
- Fajardo-Somera RA, Jöhnk B, Bayram Ö, Valerius O, Braus GH & Riquelme M (2015) Dissecting the function of the different chitin synthases in vegetative growth and sexual development in *Neurospora crassa*. *Fungal Genet Biol.* **75**: 30–45
- Fang L, Wang X, Yamoah K, Chen PL, Pan ZQ & Huang L (2008) Characterization of the human COP9 signalosome complex using affinity purification and mass spectrometry. *J Proteome Res.* **7**: 4914–4925
- Figueroa P, Gusmaroli G, Serino G, Habashi J, Ma L, Shen Y, Feng S, Bostick M, Callis J, Hellmann H & Deng XW (2005) Arabidopsis has two redundant Cullin3 proteins that are essential for embryo development and that interact with RBX1 and BTB proteins to form multisubunit E3 ubiquitin ligase complexes *in vivo*. *Plant Cell* **17**: 1180–1195
- Finley D, Sadis S, Monia BP, Boucher P, Ecker DJ, Crooke ST & Chau V (1994) Inhibition of proteolysis and cell-cycle progression in a multiubiquitination-deficient yeast mutant. *Mol Cell Biol.* **14**: 5501–5509
- Fischer EH & Krebs EG (1955) Conversion of phosphorylase b to phosphorylase a in muscle extracts. *J Biol Chem.* **216**: 121–132
- Flannagan RS, Jaumouillé V & Grinstein S (2012) The cell biology of phagocytosis. *Annu Rev Pathol* **7**: 61–98
- Freilich S, Oron E, Kapp Y, Nevo-Caspi Y, Orgad S, Segal D & Chamovitz DA (1999) The COP9 signalosome is essential for development of *Drosophila melanogaster*. *Curr Biol.* **9**: 1187–1190
- Frickel EM, Quesada V, Muething L, Gubbels MJ, Spooner E, Ploegh H & Artavanis-Tsakonas K (2007) Apicomplexan UCHL3 retains dual specificity for ubiquitin and Nedd8 throughout evolution. *Cell Microbiol.* **9**: 1601–1610

- Gagne JM, Downes BP, Shiu SH, Durski AM & Vierstra RD (2002) The F-box subunit of the SCF E3 complex is encoded by a diverse superfamily of genes in Arabidopsis. *Proc Natl Acad Sci. USA*. **99**: 11519–11524
- Galagan JE, Calvo SE, Cuomo C, Ma LJ, Wortman JR, Batzoglou S, Lee SI, Baştürkmen M, Spevak CC, Clutterbuck J, Kapitonov V, Jurka J, Scazzocchio C, Farman M, Butler J, Purcell S, Harris S, Braus GH, Draht O, Busch S, D'Enfert C, Bouchier C, Goldman GH, Bell-Pedersen D, Griffiths-Jones S, Doonan JH, Yu J, Vienken K, Pain A, Freitag M, Selker EU, Archer DB, Peñalva MA, Oakley BR, Momany M, Tanaka T, Kumagai T, Asai K, Machida M, Nierman WC, Denning DW, Caddick M, Hynes M, Paoletti M, Fischer R, Miller B, Dyer P, Sachs MS, Osmani SA & Birren BW (2005) Sequencing of *Aspergillus nidulans* and comparative analysis with *A. fumigatus* and *A. oryzae*. *Nature* **438**: 1105–1115
- Gan-Erdene T, Nagamalleswari K, Yin L, Wu K, Pan ZQ & Wilkinson KD (2003) Identification and characterization of DEN1, a deneddylase of the ULP family. *J Biol Chem*. **278**: 28892–28900
- Geer LY, Marchler-Bauer A, Geer RC, Han L, He J, He S, Liu C, Shi W & Bryant SH (2010) The NCBI BioSystems database. *Nucleic Acids Res*. **38**: D492–496
- Genschik P, Sumara I & Lechner E (2013) The emerging family of CULLIN3-RING ubiquitin ligases (CRL3s): cellular functions and disease implications. *EMBO J*. **32**: 2307–2320
- Gerke J & Braus GH (2014) Manipulation of fungal development as source of novel secondary metabolites for biotechnology. *Appl Microbiol Biotechnol*. **98**: 8443–8455
- Gerke J, Bayram Ö & Braus GH (2012) Fungal S-adenosylmethionine synthetase and the control of development and secondary metabolism in *Aspergillus nidulans*. *Fungal Genet. Biol*. **49**: 443–454
- Ghosh A, Servin JA, Park G & Borkovich KA (2014) Global analysis of serine/threonine and tyrosine protein phosphatase catalytic subunit genes in *Neurospora crassa* reveals interplay between phosphatases and the p38 mitogen-activated protein kinase. *G3 (Bethesda)* **4**: 349–365
- Glickman MH & Ciechanover A (2002) The ubiquitin-proteasome proteolytic pathway: destruction for the sake of construction. *Physiol Rev* **82**: 373–428
- Glickman MH, Rubin DM, Coux O, Wefes I, Pfeifer G, Cjeka Z, Baumeister W, Fried VA & Finley D (1998) A subcomplex of the proteasome regulatory particle required for ubiquitin-conjugate degradation and related to the COP9-signalosome and eIF3. *Cell* **94**: 615–623
- Goldberg J, Huang HB, Kwon YG, Greengard P, Nairn AC & Kuriyan J (1995) Three-dimensional structure of the catalytic subunit of protein serine/threonine phosphatase-1. *Nature* **376**: 745–753

- Goldenberg SJ, Cascio TC, Shumway SD, Garbutt KC, Liu J, Xiong Y & Zheng N (2004) Structure of the Cand1-Cul1-Roc1 complex reveals regulatory mechanisms for the assembly of the multisubunit cullin-dependent ubiquitin ligases. *Cell* **119**: 517–528
- Goldstein G, Scheid M, Hammerling U, Schlesinger DH, Niall HD & Boyse EA (1975) Isolation of a polypeptide that has lymphocyte-differentiating properties and is probably represented universally in living cells. *Proc Natl Acad Sci USA*. **72**: 11–15
- Grou CP, Pinto MP, Mendes AV, Domingues P & Azevedo JE (2015) The *de novo* synthesis of ubiquitin: identification of deubiquitinases acting on ubiquitin precursors. *Sci Rep* **5**: 12836
- Ha BH & Kim EE (2008) Structures of proteases for ubiquitin and ubiquitin-like modifiers. *BMB Rep* **41**: 435–443
- Harari-Steinberg O & Chamovitz DA (2004) The COP9 signalosome: mediating between kinase signaling and protein degradation. *Curr Protein Pept Sci* **5**: 185–189
- Harris SD (2001) Septum formation in *Aspergillus nidulans*. *Curr Opin Microbiol.* **4**: 736–739
- Harris SD (1999) Morphogenesis is coordinated with nuclear division in germinating *Aspergillus nidulans* conidiospores. *Microbiology* **145**: 2747–2756
- Harris SD (2009) The Spitzenkörper: a signalling hub for the control of fungal development? *Mol Microbiol.* **73**: 733–736
- Harris SD & Kraus PR (1998) Regulation of septum formation in *Aspergillus nidulans* by a DNA damage checkpoint pathway. *Genetics* **148**: 1055–1067
- Harting R, Bayram Ö, Laubinger K, Valerius O & Braus GH (2013) Interplay of the fungal sumoylation network for control of multicellular development. *Mol Microbiol.* **90**: 1125–1145
- Hermann TE, Kurtz MB & Champe SP (1983) Laccase localized in hulle cells and cleistothecial primordia of *Aspergillus nidulans*. *J Bacteriol.* **154**: 955–964
- Herrmann J, Lerman LO & Lerman A (2007) Ubiquitin and ubiquitin-like proteins in protein regulation. *Circ Res.* **100**: 1276–1291
- Hershko A & Ciechanover A (1992) The ubiquitin system for protein degradation. *Annu Rev Biochem.* **61**: 761–807
- Hershko A, Ciechanover A, Heller H, Haas AL & Rose IA (1980) Proposed role of ATP in protein breakdown: conjugation of protein with multiple chains of the polypeptide of ATP-dependent proteolysis. *Proc Natl Acad Sci USA.* **77**: 1783–1786

- Hetfeld BK, Helfrich A, Kapelari B, Scheel H, Hofmann K, Guterman A, Glickman M, Schade R, Kloetzel PM & Dubiel W (2005) The zinc finger of the CSN-associated deubiquitinating enzyme USP15 is essential to rescue the E3 ligase Rbx1. *Curr Biol.* **15**: 1217–1221
- Hicke L (2001) Protein regulation by monoubiquitin. *Nat Rev Mol Cell Biol.* **2**: 195–201
- Hinnebusch AG (2006) eIF3: a versatile scaffold for translation initiation complexes. *Trends Biochem Sci.* **31**: 553–562
- Hochstrasser M (2009) Origin and function of ubiquitin-like proteins. *Nature* **458**: 422–429
- Holt LJ (2012) Regulatory modules: Coupling protein stability to phosphoregulation during cell division. *FEBS Lett.* **586**: 2773–2777
- Howard BH & Raistrick H (1955) Studies in the biochemistry of micro-organisms. 94. The colouring matters of species in the *Aspergillus nidulans* group. I. Asperthecin, a crystalline colouring matter of *Aspergillus quadrilineatus*. *Biochem J* **59**: 475–484
- Hu Y, Wu Y, Li Q, Zhang W & Jin C (2015) Solution structure of yeast Rpn9: insights into proteasome lid assembly. *J Biol Chem.* **290**: 6878–6889
- Hua Z & Vierstra RD (2011) The cullin-RING ubiquitin-protein ligases. *Annu Rev Plant Biol* **62**: 299–334
- Huang DT, Hunt HW, Zhuang M, Ohi MD, Holton JM & Schulman BA (2007) Basis for a ubiquitin-like protein thioester switch toggling E1-E2 affinity. *Nature* **445**: 394–398
- Huang DT, Paydar A, Zhuang M, Waddell MB, Holton JM & Schulman BA (2005a) Structural basis for recruitment of Ubc12 by an E2 binding domain in NEDD8's E1. *Mol Cell* **17**: 341–350
- Huang DT, Walden H, Duda D & Schulman BA (2004) Ubiquitin-like protein activation. *Oncogene* **23**: 1958–1971
- Huang HD, Lee TY, Tzeng SW & Horng JT (2005b) KinasePhos: a web tool for identifying protein kinase-specific phosphorylation sites. *Nucleic Acids Res.* **33**: W226–229
- Huang X, Langelotz C, Hetfeld-Pechoc BK, Schwenk W & Dubiel W (2009) The COP9 signalosome mediates beta-catenin degradation by deneddylation and blocks adenomatous polyposis coli destruction via USP15. *J Mol Biol.* **391**: 691–702
- Hunter T (1995) Protein kinases and phosphatases: the yin and yang of protein phosphorylation and signaling. *Cell* **80**: 225–236

- Inoue H, Nojima H & Okayama H (1990) High efficiency transformation of *Escherichia coli* with plasmids. *Gene* **96**: 23–28
- Jaimes-Arroyo R, Lara-Rojas F, Bayram Ö, Valerius O, Braus GH & Aguirre J (2015) The *SrkA* Kinase Is Part of the *SakA* Mitogen-Activated Protein Kinase Interactome and Regulates Stress Responses and Development in *Aspergillus nidulans*. *Eukaryot Cell* **14**: 495–510
- Jedd G & Chua NH (2000) A new self-assembled peroxisomal vesicle required for efficient resealing of the plasma membrane. *Nat Cell Biol.* **2**: 226–231
- Jin J, Cardozo T, Lovering RC, Elledge SJ, Pagano M & Harper JW (2004) Systematic analysis and nomenclature of mammalian F-box proteins. *Genes Dev.* **18**: 2573–2580
- Jones J, Wu K, Yang Y, Guerrero C, Nillegoda N, Pan ZQ & Huang L (2008) A targeted proteomic analysis of the ubiquitin-like modifier nedd8 and associated proteins. *J Proteome Res.* **7**: 1274–1287
- Juvvadi PR, Belina D, Soderblom EJ, Moseley MA & Steinbach WJ (2013) Filamentous fungal-specific septin *AspE* is phosphorylated *in vivo* and interacts with actin, tubulin and other septins in the human pathogen *Aspergillus fumigatus*. *Biochem Biophys Res Commun.* **431**: 547–553
- Kapelari B, Bech-Otschir D, Hegerl R, Schade R, Dumdey R & Dubiel W (2000) Electron microscopy and subunit-subunit interaction studies reveal a first architecture of COP9 signalosome. *J Mol Biol.* **300**: 1169–1178
- Karve TM & Cheema AK (2011) Small changes huge impact: the role of protein posttranslational modifications in cellular homeostasis and disease. *J Amino Acids* **2011**: 207691
- Kato N, Brooks W & Calvo AM (2003) The expression of sterigmatocystin and penicillin genes in *Aspergillus nidulans* is controlled by *veA*, a gene required for sexual development. *Eukaryot Cell* **2**: 1178–1186
- Kawaguchi M, Nonaka K, Masuma R & Tomoda H (2013) New method for isolating antibiotic-producing fungi. *J Antibiot.* **66**: 17–21
- Kawakami T, Chiba T, Suzuki T, Iwai K, Yamanaka K, Minato N, Suzuki H, Shimbara N, Hidaka Y, Osaka F, Omata M & Tanaka K (2001) NEDD8 recruits E2-ubiquitin to SCF E3 ligase. *EMBO J.* **20**: 4003–4012
- Käfer E (1977) Meiotic and mitotic recombination in *Aspergillus* and its chromosomal aberrations. *Adv Genet.* **19**: 33–131
- Kandala S, Kim IM & Su H (2014) Neddylation and deneddylation in cardiac biology. *Am J Cardiovasc Dis* **4**: 140–158
- Kerscher O, Felberbaum R & Hochstrasser M (2006) Modification of proteins by ubiquitin and ubiquitin-like proteins. *Annu Rev Cell Dev Biol.* **22**: 159–180

- Kim H, Han K, Kim K, Han D, Jahng K & Chae K (2002) The *veA* gene activates sexual development in *Aspergillus nidulans*. *Fungal Genet Biol.* **37**: 72–80
- Kim JM, Zeng CJ, Nayak T, Shao R, Huang AC, Oakley BR & Liu B (2009) Timely septation requires SNAD-dependent spindle pole body localization of the septation initiation network components in the filamentous fungus *Aspergillus nidulans*. *Mol Biol Cell* **20**: 2874–2884
- Kim K, Yoon J, Yim J & Kim HJ (2015) Deneddylase 1 Regulates Deneddylase Activity of the Cop9 Signalosome in *Drosophila Melanogaster*. *Insect Sci.* doi: 10.1111/1744-7917.12274. [Epub ahead of print].
- Kipreos ET & Pagano M (2000) The F-box protein family. *Genome Biol.* **1**: 3002
- Komander D, Clague MJ & Urbé S (2009) Breaking the chains: structure and function of the deubiquitinases. *Nat Rev Mol Cell Biol.* **10**: 550–563
- Kosugi S, Hasebe M, Tomita M & Yanagawa H (2008) Nuclear export signal consensus sequences defined using a localization-based yeast selection system. *Traffic* **9**: 2053–2062
- Kotiguda GG, Weinberg D, Dessau M, Salvi C, Serino G, Chamovitz DA & Hirsch JA (2012) The organization of a CSN5-containing subcomplex of the COP9 signalosome. *J Biol Chem.* **287**: 42031–42041
- Krappmann S, Jung N, Medic B, Busch S, Prade RA & Braus GH (2006) The *Aspergillus nidulans* F-box protein GrrA links SCF activity to meiosis. *Mol Microbiol.* **61**: 76–88
- Kubodera T, Yamashita N & Nishimura A (2000) Pyrithiamine resistance gene (*ptrA*) of *Aspergillus oryzae*: cloning, characterization and application as a dominant selectable marker for transformation. *Biosci Biotechnol Biochem.* **64**: 1416–1421
- Kumar S, Yoshida Y & Noda M (1993) Cloning of a cDNA which encodes a novel ubiquitin-like protein. *Biochem Biophys Res Commun.* **195**: 393–399
- Kurz T, Chou YC, Willems AR, Meyer-Schaller N, Hecht ML, Tyers M, Peter M & Sicheri F (2008) Dcn1 functions as a scaffold-type E3 ligase for cullin neddylation. *Mol Cell* **29**: 23–35
- Kurz T, Pintard L, Willis JH, Hamill DR, Gönczy P, Peter M & Bowerman B (2002) Cytoskeletal regulation by the Nedd8 ubiquitin-like protein modification pathway. *Science* **295**: 1294–1298
- Kück U, Beier AM & Teichert I (2015) The composition and function of the striatin-interacting phosphatases and kinases (STRIPAK) complex in fungi. *Fungal Genet Biol.* doi: 10.1016/j.fgb.2015.10.001. [Epub ahead of print].
- Lammer D, Mathias N, Laplaza JM, Jiang W, Liu Y, Callis J, Goebel M & Estelle M (1998) Modification of yeast Cdc53p by the ubiquitin-related protein rub1p affects function of the SCFCdc4 complex. *Genes Dev.* **12**: 914–926

- Lange A, Mills RE, Lange CJ, Stewart M, Devine SE & Corbett AH (2007) Classical nuclear localization signals: definition, function, and interaction with importin alpha. *J Biol Chem.* **282**: 5101–5105
- Larance M, Ahmad Y, Kirkwood KJ, Ly T & Lamond AI (2013) Global subcellular characterization of protein degradation using quantitative proteomics. *Mol Cell Proteomics* **12**: 638–650
- Latgé JP (1999) *Aspergillus fumigatus* and aspergillosis. *Clin Microbiol Rev.* **12**: 310–350
- Lee EK & Diehl JA (2014) SCFs in the new millennium. *Oncogene* **33**: 2011–2018
- Lee MH, Zhao R, Phan L & Yeung SC (2011) Roles of COP9 signalosome in cancer. *Cell Cycle* **10**: 3057–3066
- Lee SB (1990) Isolation of DNA from fungal mycelia and single spores. In: PCR Protocols: A guide to methods and applications. Innis N, Gelfand D, Sninsky J & White T (eds). New York: Academic Press, pp 282–287
- Li W & Ye Y (2008) Polyubiquitin chains: functions, structures, and mechanisms. *Cell Mol Life Sci.* **65**: 2397–2406
- Liakopoulos D, Doenges G, Matuschewski K & Jentsch S (1998) A novel protein modification pathway related to the ubiquitin system. *EMBO J.* **17**: 2208–2214
- Lin C & Todo T (2005) The cryptochromes. *Genome Biol.* **6**: 220
- Lingaraju GM, Bunker RD, Cavadini S, Hess D, Hassiepen U, Renatus M, Fischer ES & Thomä NH (2014) Crystal structure of the human COP9 signalosome. *Nature* **512**: 161–165
- Linghu B, Callis J & Goebel MG (2002) Rub1p processing by Yuh1p is required for wild-type levels of Rub1p conjugation to Cdc53p. *Eukaryot Cell* **1**: 491–494
- Liu B & Morris NR (2000) A spindle pole body-associated protein, SNAD, affects septation and conidiation in *Aspergillus nidulans*. *Mol Gen Genet.* **263**: 375–387
- Liu C, Powell KA, Mundt K, Wu L, Carr AM & Caspari T (2003) Cop9/signalosome subunits and Pcu4 regulate ribonucleotide reductase by both checkpoint-dependent and -independent mechanisms. *Genes Dev.* **17**: 1130–1140
- Liu J, Furukawa M, Matsumoto T & Xiong Y (2002) NEDD8 modification of CUL1 dissociates p120(CAND1), an inhibitor of CUL1-SKP1 binding and SCF ligases. *Mol Cell* **10**: 1511–1518
- Lo Presti L, Lanver D, Schweizer G, Tanaka S, Liang L, Tollot M, Zuccaro A, Reissmann S & Kahmann R (2015) Fungal effectors and plant susceptibility. *Annu Rev Plant Biol* **66**: 513–545

- Lorick KL, Jensen JP, Fang S, Ong AM, Hatakeyama S & Weissman AM (1999) RING fingers mediate ubiquitin-conjugating enzyme (E2)-dependent ubiquitination. *Proc Natl Acad Sci USA*. **96**: 11364–11369
- Lu Y, Lee BH, King RW, Finley D & Kirschner MW (2015) Substrate degradation by the proteasome: a single-molecule kinetic analysis. *Science* **348**: 1250834
- Lyapina S, Cope G, Shevchenko A, Serino G, Tsuge T, Zhou C, Wolf DA, Wei N, Shevchenko A & Deshaies RJ (2001) Promotion of NEDD-CUL1 conjugate cleavage by COP9 signalosome. *Science* **292**: 1382–1385
- Lydeard JR, Schulman BA & Harper JW (2013) Building and remodelling Cullin-RING E3 ubiquitin ligases. *EMBO Rep*. **14**: 1050–1061
- Ma T, Chen Y, Zhang F, Yang CY, Wang S & Yu X (2013) RNF111-dependent neddylation activates DNA damage-induced ubiquitination. *Mol Cell* **49**: 897–907
- Mabey Gilsonan J, Cooley J & Bowyer P (2012) CADRE: the Central Aspergillus Data REpository 2012. *Nucleic Acids Res*. **40**: D660–666
- Manck R, Ishitsuka Y, Herrero S, Takeshita N, Nienhaus GU & Fischer R (2015) Genetic evidence for a microtubule-capture mechanism during polarised growth of *Aspergillus nidulans*. *J Cell Sci*. **128**: 3569–3582
- Mann M & Jensen ON (2003) Proteomic analysis of post-translational modifications. *Nat Biotechnol*. **21**: 255–261
- Marchler-Bauer A, Derbyshire MK, Gonzales NR, Lu S, Chitsaz F, Geer LY, Geer RC, He J, Gwadz M, Hurwitz DI, Lanczycki CJ, Lu F, Marchler GH, Song JS, Thanki N, Wang Z, Yamashita RA, Zhang D, Zheng C & Bryant SH (2015) CDD: NCBI's conserved domain database. *Nucleic Acids Res*. **43**: D222–226
- Marsh DJ (2015) Networks regulating ubiquitin and ubiquitin-like proteins promise new therapeutic targets. *Endocr Relat Cancer* **22**: E1–3
- Mayorga ME & Timberlake WE (1990) Isolation and molecular characterization of the *Aspergillus nidulans* *wA* gene. *Genetics* **126**: 73–79
- Meir M, Galanty Y, Kashani L, Blank M, Khosravi R, Fernández-Ávila MJ, Cruz-García A, Star A, Shochot L, Thomas Y, Garrett LJ, Chamovitz DA, Bodine DM, Kurz T, Huertas P, Ziv Y & Shiloh Y (2015) The COP9 signalosome is vital for timely repair of DNA double-strand breaks. *Nucleic Acids Res*. **43**: 4517–4530
- Meister C, Kolog Gulko M, Köhler AM & Braus GH (2015) The devil is in the details: comparison between COP9 signalosome (CSN) and the LID of the 26S proteasome. *Curr Genet*. doi 10.1007/s00294-015-0525-7 [Epub ahead of print].
- Mendoza HM, Shen LN, Botting C, Lewis A, Chen J, Ink B & Hay RT (2003) NEDP1, a highly conserved cysteine protease that deNEDDylates Cullins. *J Biol Chem*. **278**: 25637–25643

- Mergner J & Schwechheimer C (2014) The NEDD8 modification pathway in plants. *Front Plant Sci* **5**: 103
- Mergner J, Heinzlmeir S, Kuster B & Schwechheimer C (2015) DENEDDYLASE1 deconjugates NEDD8 from non-cullin protein substrates in *Arabidopsis thaliana*. *Plant Cell* **27**: 741–753
- Merlet J, Burger J, Gomes JE & Pintard L (2009) Regulation of cullin-RING E3 ubiquitin-ligases by neddylation and dimerization. *Cell Mol Life Sci.* **66**: 1924–1938
- Metzger MB, Hristova VA & Weissman AM (2012) HECT and RING finger families of E3 ubiquitin ligases at a glance. *J Cell Sci.* **125**: 531–537
- Millard SM & Wood SA (2006) Riding the DUBway: regulation of protein trafficking by deubiquitylating enzymes. *J Cell Biol.* **173**: 463–468
- Mims CW, Richardson EA & Timberlake WE (1988) Ultrastructural analysis of conidiophore development in the fungus *Aspergillus nidulans* using freeze-substitution. *Protoplasma* **144**: 132–141
- Mirabito PM, Adams TH & Timberlake WE (1989) Interactions of three sequentially expressed genes control temporal and spatial specificity in *Aspergillus* development. *Cell* **57**: 859–868
- Miranda M & Sorkin A (2007) Regulation of receptors and transporters by ubiquitination: new insights into surprisingly similar mechanisms. *Mol Interv.* **7**: 157–167
- Momany M (2015) Rite of passage: a bZIP transcription factor must transit the cell apex to become competent. *Mol Microbiol.* **98**: 605–606
- Momany M & Hamer JE (1997) Relationship of actin, microtubules, and crosswall synthesis during septation in *Aspergillus nidulans*. *Cell Motil Cytoskeleton* **38**: 373–384
- Momany M, Richardson EA, Van Sickle C & Jedd G (2002) Mapping Woronin body position in *Aspergillus nidulans*. *Mycologia* **94**: 260–266
- Morimoto M, Nishida T, Nagayama Y & Yasuda H (2003) Nedd8-modification of Cul1 is promoted by Roc1 as a Nedd8-E3 ligase and regulates its stability. *Biochem Biophys Res Commun.* **301**: 392–398
- Mouriño-Pérez RR (2013) Septum development in filamentous ascomycetes. *Fungal Biol Rev* **27**: 1–9
- Mouriño-Pérez RR & Riquelme M (2013) Recent advances in septum biogenesis in *Neurospora crassa*. *Adv Genet.* **83**: 99–134
- Mukhopadhyay D & Riezman H (2007) Proteasome-independent functions of ubiquitin in endocytosis and signaling. *Science* **315**: 201–205

- Mundt KE, Liu C & Carr AM (2002) Deletion mutants in COP9/signalosome subunits in fission yeast *Schizosaccharomyces pombe* display distinct phenotypes. *Mol Biol Cell* **13**: 493–502
- Nahlik K, Dumkow M, Bayram Ö, Helmstaedt K, Busch S, Valerius O, Gerke J, Hoppert M, Schwier E, Opitz L, Westermann M, Grond S, Feussner K, Goebel C, Kaefer A, Meinicke P, Feussner I & Braus GH (2010) The COP9 signalosome mediates transcriptional and metabolic response to hormones, oxidative stress protection and cell wall rearrangement during fungal development. *Mol Microbiol.* **78**: 964–979
- Naumann M, Bech-Otschir D, Huang X, Ferrell K & Dubiel W (1999) COP9 signalosome-directed c-Jun activation/stabilization is independent of JNK. *J Biol Chem.* **274**: 35297–35300
- Nayak T, Szewczyk E, Oakley CE, Osmani A, Ukil L, Murray SL, Hynes MJ, Osmani SA & Oakley BR (2006) A versatile and efficient gene-targeting system for *Aspergillus nidulans*. *Genetics* **172**: 1557–1566
- Nguyen LK, Kolch W & Kholodenko BN (2013) When ubiquitination meets phosphorylation: a systems biology perspective of EGFR/MAPK signalling. *Cell Commun Signal* **11**: 52
- Ni M & Yu JH (2007) A novel regulator couples sporogenesis and trehalose biogenesis in *Aspergillus nidulans*. *PLoS One* **2**: e970
- Nishi H, Hashimoto K & Panchenko AR (2011) Phosphorylation in protein-protein binding: effect on stability and function. *Structure* **19**: 1807–1815
- Normile D (2010) Spoiling for a fight with mold. *Science* **327**: 807
- O'Connell MJ, Osmani AH, Morris NR & Osmani SA (1992) An extra copy of nimE cyclinB elevates pre-MPF levels and partially suppresses mutation of nimTcdc25 in *Aspergillus nidulans*. *EMBO J.* **11**: 2139–2149
- Ohki Y, Funatsu N, Konishi N & Chiba T (2009) The mechanism of poly-NEDD8 chain formation *in vitro*. *Biochem Biophys Res Commun.* **381**: 443–447
- Oliver PT (1972) Conidiophore and spore development in *Aspergillus nidulans*. *J Gen Microbiol.* **73**: 45–54
- Olsen JV & Mann M (2004) Improved peptide identification in proteomics by two consecutive stages of mass spectrometric fragmentation. *Proc Natl Acad Sci USA.* **101**: 13417–13422
- Olsen JV, Blagoev B, Gnäd F, Macek B, Kumar C, Mortensen P & Mann M (2006) Global, *in vivo*, and site-specific phosphorylation dynamics in signaling networks. *Cell* **127**: 635–648
- Osmani AH, van Peij N, Mischke M, O'Connell MJ & Osmani SA (1994) A single p34cdc2 protein kinase (encoded by nimXcdc2) is required at G1 and G2 in *Aspergillus nidulans*. *J Cell Sci.* **107**: 1519–1528

- Osmani SA & Mirabito PM (2004) The early impact of genetics on our understanding of cell cycle regulation in *Aspergillus nidulans*. *Fungal Genet Biol.* **41**: 401–410
- Ozkaynak E, Finley D, Solomon MJ & Varshavsky A (1987) The yeast ubiquitin genes: a family of natural gene fusions. *EMBO J.* **6**: 1429–1439
- Pan ZQ, Kentsis A, Dias DC, Yamoah K & Wu K (2004) Nedd8 on cullin: building an expressway to protein destruction. *Oncogene* **23**: 1985–1997
- Park HS, Yu YM, Lee MK, Maeng PJ, Kim SC & Yu JH (2015) Velvet-mediated repression of β -glucan synthesis in *Aspergillus nidulans* spores. *Sci Rep* **5**: 10199
- Petroski MD & Deshaies RJ (2005) Function and regulation of cullin-RING ubiquitin ligases. *Nat Rev Mol Cell Biol.* **6**: 9–20
- Pfaffl MW, Horgan GW & Dempfle L (2002) Relative expression software tool (REST) for group-wise comparison and statistical analysis of relative expression results in real-time PCR. *Nucleic Acids Res.* **30**: e36
- Pfoh R, Lacdao IK & Saridakis V (2015) Deubiquitinases and the new therapeutic opportunities offered to cancer. *Endocr Relat Cancer* **22**: T35–54
- Pick E & Pintard L (2009) In the land of the rising sun with the COP9 signalosome and related Zomes. Symposium on the COP9 signalosome, Proteasome and eIF3. *EMBO Rep.* **10**: 343–348
- Pick E, Golan A, Zimbler JZ, Guo L, Sharaby Y, Tsuge T, Hofmann K & Wei N (2012) The minimal deneddylase core of the COP9 signalosome excludes the Csn6 MPN- domain. *PLoS One* **7**: e43980
- Pickart CM (2001) Mechanisms underlying ubiquitination. *Annu Rev Biochem.* **70**: 503–533
- Pickart CM & Fushman D (2004) Polyubiquitin chains: polymeric protein signals. *Curr Opin Chem Biol* **8**: 610–616
- Pierce NW, Lee JE, Liu X, Sweredoski MJ, Graham RL, Larimore EA, Rome M, Zheng N, Clurman BE, Hess S, Shan SO & Deshaies RJ (2013) Cand1 promotes assembly of new SCF complexes through dynamic exchange of F box proteins. *Cell* **153**: 206–215
- Pintard L, Kurz T, Glaser S, Willis JH, Peter M & Bowerman B (2003) Neddylolation and deneddylolation of CUL-3 is required to target MEI-1/Katanin for degradation at the meiosis-to-mitosis transition in *C. elegans*. *Curr Biol.* **13**: 911–921
- Pisa D, Alonso R, Rábano A, Rodal I & Carrasco L (2015) Different Brain Regions are Infected with Fungi in Alzheimer's Disease. *Sci Rep* **5**: 15015
- Piva R, Cancelli I, Cavalla P, Bortolotto S, Dominguez J, Draetta GF & Schiffer D (1999) Proteasome-dependent degradation of p27/kip1 in gliomas. *J Neuropathol Exp Neurol.* **58**: 691–696

- Pontecorvo G, Roper JA, Hemmons LM, MacDonald KD & Bufton AW (1953) The genetics of *Aspergillus nidulans*. *Adv Genet.* **5**: 141–238
- Pöggeler S, Nowrousian M & Kück U (2006) Fruiting-body development in ascomycetes. In: K. Fischer, (Ed.), *The Mycota I. Growth, Differentiation and Sexuality*. Springer-Verlag, Heidelberg: pp 325–355. doi: 10.1007/3-540-28135-5_16
- Prabakaran S, Lippens G, Steen H & Gunawardena J (2012) Post-translational modification: nature's escape from genetic imprisonment and the basis for dynamic information encoding. *Wiley Interdiscip Rev Syst Biol Med.* **4**: 565–583
- Pratt MR, Abeywardana T & Marotta NP (2015) Synthetic Proteins and Peptides for the Direct Interrogation of α -Synuclein Posttranslational Modifications. *Biomolecules* **5**: 1210–1227
- Punt PJ & van den Hondel CA (1992) Transformation of filamentous fungi based on hygromycin B and phleomycin resistance markers. *Methods Enzymol.* **216**: 447–457
- Purschwitz J, Müller S & Fischer R (2009) Mapping the interaction sites of *Aspergillus nidulans* phytochrome FphA with the global regulator VeA and the White Collar protein LreB. *Mol Genet Genomics* **281**: 35–42
- Purschwitz J, Müller S, Kastner C, Schöser M, Haas H, Espeso EA, Atoui A, Calvo AM & Fischer R (2008) Functional and physical interaction of blue- and red-light sensors in *Aspergillus nidulans*. *Curr Biol.* **18**: 255–259
- Rabut G & Peter M (2008) Function and regulation of protein neddylation. ‘Protein modifications: beyond the usual suspects’ review series. *EMBO Rep.* **9**: 969–976
- Randle SJ & Laman H (2015) F-box protein interactions with the hallmark pathways in cancer. *Semin Cancer Biol.* doi: 10.1016/j.semcancer.2015.09.013. [Epub ahead of print].
- Ravid T & Hochstrasser M (2008) Diversity of degradation signals in the ubiquitin-proteasome system. *Nat Rev Mol Cell Biol.* **9**: 679–690
- Reinstein E & Ciechanover A (2006) Narrative review: protein degradation and human diseases: the ubiquitin connection. *Ann Intern Med.* **145**: 676–684
- Reyes-Turcu FE, Horton JR, Mullally JE, Heroux A, Cheng X & Wilkinson KD (2006) The ubiquitin binding domain ZnF UBP recognizes the C-terminal diglycine motif of unanchored ubiquitin. *Cell* **124**: 1197–1208
- Reyes-Turcu FE, Shanks JR, Komander D & Wilkinson KD (2008) Recognition of polyubiquitin isoforms by the multiple ubiquitin binding modules of isopeptidase T. *J Biol Chem.* **283**: 19581–19592

- Rock KL, Gramm C, Rothstein L, Clark K, Stein R, Dick L, Hwang D & Goldberg AL (1994) Inhibitors of the proteasome block the degradation of most cell proteins and the generation of peptides presented on MHC class I molecules. *Cell* **78**: 761–771
- Rodríguez-Romero J, Hedtke M, Kastner C, Müller S & Fischer R (2010) Fungi, hidden in soil or up in the air: light makes a difference. *Annu Rev Microbiol.* **64**: 585–610
- Rodway H, Llanos S, Rowe J & Peters G (2004) Stability of nucleolar versus non-nucleolar forms of human p14(ARF). *Oncogene* **23**: 6186–6192
- Rogers S, McCloy R, Watkins DN & Burgess A (2015) Mechanisms regulating phosphatase specificity and the removal of individual phosphorylation sites during mitotic exit. *Inside the Cell*: doi: 10.1002/icl3.1035. [Epub ahead of print].
- Romero-Calvo I, Ocón B, Martínez-Moya P, Suárez MD, Zarzuelo A, Martínez-Augustín O & de Medina FS (2010) Reversible Ponceau staining as a loading control alternative to actin in Western blots. *Anal Biochem.* **401**: 318–320
- Roux KJ, Kim DI & Burke B (2013) BioID: a screen for protein-protein interactions. *Curr Protoc Protein Sci* **74**: Unit 19.23.
- Ruger-Herreros C, Rodríguez-Romero J, Fernández-Barranco R, Olmedo M, Fischer R, Corrochano LM & Canovas D (2011) Regulation of conidiation by light in *Aspergillus nidulans*. *Genetics* **188**: 809–822
- Saha A & Deshaies RJ (2008) Multimodal activation of the ubiquitin ligase SCF by Nedd8 conjugation. *Mol Cell* **32**: 21–31
- Sarikas A, Hartmann T & Pan ZQ (2011) The cullin protein family. *Genome Biol.* **12**: 220
- Sarikaya-Bayram O, Bayram Ö, Feussner K, Kim JH, Kim HS, Kaeffer A, Feussner I, Chae KS, Han DM, Han KH & Braus GH (2014) Membrane-bound methyltransferase complex VapA-VipC-VapB guides epigenetic control of fungal development. *Dev Cell* **29**: 406–420
- Sarikaya-Bayram O, Bayram Ö, Valerius O, Park HS, Irniger S, Gerke J, Ni M, Han KH, Yu JH & Braus GH (2010) LaeA control of velvet family regulatory proteins for light-dependent development and fungal cell-type specificity. *PLoS Genet.* **6**: e1001226
- Sarikaya-Bayram Ö, Palmer JM, Keller N, Braus GH & Bayram Ö (2015) One Juliet and four Romeos: VeA and its methyltransferases. *Front Microbiol.* **6**: 1
- Saunders DG, Aves SJ & Talbot NJ (2010) Cell cycle-mediated regulation of plant infection by the rice blast fungus. *Plant Cell* **22**: 497–507
- Scharf DH, Heinekamp T & Brakhage AA (2014) Human and plant fungal pathogens: the role of secondary metabolites. *PLoS Pathog.* **10**: e1003859

- Scheel H & Hofmann K (2005) Prediction of a common structural scaffold for proteasome lid, COP9-signalosome and eIF3 complexes. *BMC Bioinformatics* **6**: 71
- Scherer M & Fischer R (1998) Purification and characterization of laccase II of *Aspergillus nidulans*. *Arch Microbiol* **170**: 78–84
- Schmidt MW, McQuary PR, Wee S, Hofmann K & Wolf DA (2009) F-Box-directed CRL complex assembly and regulation by the CSN and CAND1. *Mol Cell* **35**: 586–597
- Schnell JD & Hicke L (2003) Non-traditional functions of ubiquitin and ubiquitin-binding proteins. *J Biol Chem.* **278**: 35857–35860
- Schrader EK, Harstad KG & Matouschek A (2009) Targeting proteins for degradation. *Nat Chem Biol* **5**: 815–822
- Schulman BA & Harper JW (2009) Ubiquitin-like protein activation by E1 enzymes: the apex for downstream signalling pathways. *Nat Rev Mol Cell Biol.* **10**: 319–331
- Schulman BA, Carrano AC, Jeffrey PD, Bowen Z, Kinnucan ER, Finnin MS, Elledge SJ, Harper JW, Pagano M & Pavletich NP (2000) Insights into SCF ubiquitin ligases from the structure of the Skp1-Skp2 complex. *Nature* **408**: 381–386
- Schwarz SE, Rosa JL & Scheffner M (1998) Characterization of human hect domain family members and their interaction with UbcH5 and UbcH7. *J Biol Chem.* **273**: 12148–12154
- Seiler S & Justa-Schuch D (2010) Conserved components, but distinct mechanisms for the placement and assembly of the cell division machinery in unicellular and filamentous ascomycetes. *Mol Microbiol.* **78**: 1058–1076
- Seo J & Lee KJ (2004) Post-translational modifications and their biological functions: proteomic analysis and systematic approaches. *J Biochem Mol Biol.* **37**: 35–44
- Serino G & Deng XW (2003) The COP9 signalosome: regulating plant development through the control of proteolysis. *Annu Rev Plant Biol* **54**: 165–182
- Sewall TC, Mims CW & Timberlake WE (1990a) Conidium differentiation in *Aspergillus nidulans* wild-type and wet-white (*wetA*) mutant strains. *Dev Biol* **138**: 499–508
- Sewall TC, Mims CW & Timberlake WE (1990b) *abaA* controls phialide differentiation in *Aspergillus nidulans*. *Plant Cell* **2**: 731–739
- Sharon M, Mao H, Boeri Erba E, Stephens E, Zheng N & Robinson CV (2009) Symmetrical modularity of the COP9 signalosome complex suggests its multifunctionality. *Structure* **17**: 31–40

- Sheaff RJ, Groudine M, Gordon M, Roberts JM & Clurman BE (1997) Cyclin E-CDK2 is a regulator of p27Kip1. *Genes Dev.* **11**: 1464–1478
- Shen LN, Liu H, Dong C, Xirodimas D, Naismith JH & Hay RT (2005) Structural basis of NEDD8 ubiquitin discrimination by the deNEDDylating enzyme NEDP1. *EMBO J.* **24**: 1341–1351
- Shevchenko A, Tomas H, Havlis J, Olsen JV & Mann M (2006) In-gel digestion for mass spectrometric characterization of proteins and proteomes. *Nat Protoc* **1**: 2856–2860
- Shi Y (2009) Serine/threonine phosphatases: mechanism through structure. *Cell* **139**: 468–484
- Shin YC, Tang SJ, Chen JH, Liao PH & Chang SC (2011) The molecular determinants of NEDD8 specific recognition by human SENP8. *PLoS One* **6**: e27742
- Sigoillot FD, Berkowski JA, Sigoillot SM, Kotsis DH & Guy HI (2003) Cell cycle-dependent regulation of pyrimidine biosynthesis. *J Biol Chem.* **278**: 3403–3409
- Sigoillot FD, Evans DR & Guy HI (2002) Growth-dependent regulation of mammalian pyrimidine biosynthesis by the protein kinase A and MAPK signaling cascades. *J Biol Chem.* **277**: 15745–15751
- Singer JD, Gurian-West M, Clurman B & Roberts JM (1999) Cullin-3 targets cyclin E for ubiquitination and controls S phase in mammalian cells. *Genes Dev.* **13**: 2375–2387
- Singer R, Atar S, Atias O, Oron E, Segal D, Hirsch JA, Tuller T, Orian A & Chamovitz DA (2014) Drosophila COP9 signalosome subunit 7 interacts with multiple genomic loci to regulate development. *Nucleic Acids Res.* **42**: 9761–9770
- Skowyra D, Craig KL, Tyers M, Elledge SJ & Harper JW (1997) F-box proteins are receptors that recruit phosphorylated substrates to the SCF ubiquitin-ligase complex. *Cell* **91**: 209–219
- Sohn KT & Yoon KS (2002) Ultrastructural study on the cleistothecium development in *Aspergillus nidulans*. *Mycobiology* **30**: 117–127
- Soldati T & Schliwa M (2006) Powering membrane traffic in endocytosis and recycling. *Nat Rev Mol Cell Biol.* **7**: 897–908
- Son S & Osmani SA (2009) Analysis of all protein phosphatase genes in *Aspergillus nidulans* identifies a new mitotic regulator, fcp1. *Eukaryot Cell* **8**: 573–585
- Spasser L & Brik A (2012) Chemistry and biology of the ubiquitin signal. *Angew Chem Int Ed Engl.* **51**: 6840–6862
- Steinberg G (2007) Hyphal growth: a tale of motors, lipids, and the Spitzenkörper. *Eukaryot Cell* **6**: 351–360

- Stinnett SM, Espeso EA, Cobeno L, Araujo-Bazan L & Calvo AM (2007) *Aspergillus nidulans* VeA subcellular localization is dependent on the importin alpha carrier and on light. *Mol Microbiol.* **63**: 242–255
- Stoker AW (2005) Protein tyrosine phosphatases and signalling. *J Endocrinol.* **185**: 19–33
- Stratmann JW & Gusmaroli G (2012) Many jobs for one good cop - the COP9 signalosome guards development and defense. *Plant Sci.* **185-186**: 50–64
- Streich FC & Lima CD (2014) Structural and functional insights to ubiquitin-like protein conjugation. *Annu Rev Biophys* **43**: 357–379
- Su H, Li J, Osinska H, Li F, Robbins J, Liu J, Wei N & Wang X (2013) The COP9 signalosome is required for autophagy, proteasome-mediated proteolysis, and cardiomyocyte survival in adult mice. *Circ Heart Fail.* **6**: 1049–1057
- Suelmann R & Fischer R (2000) Mitochondrial movement and morphology depend on an intact actin cytoskeleton in *Aspergillus nidulans*. *Cell Motil Cytoskeleton* **45**: 42–50
- Suzuki S, Sarikaya-Bayram O, Bayram Ö & Braus GH (2013) *conF* and *conJ* contribute to conidia germination and stress response in the filamentous fungus *Aspergillus nidulans*. *Fungal Genet Biol.* **56**: 42–53
- Szewczyk E, Chiang YM, Oakley CE, Davidson AD, Wang CC & Oakley BR (2008) Identification and characterization of the asperthecin gene cluster of *Aspergillus nidulans*. *Appl Environ Microbiol.* **74**: 7607–7612
- Szewczyk E, Nayak T, Oakley CE, Edgerton H, Xiong Y, Taheri-Talesh N, Osmani SA & Oakley BR (2006) Fusion PCR and gene targeting in *Aspergillus nidulans*. *Nat Protoc* **1**: 3111–3120
- Taheri-Talesh N, Xiong Y & Oakley BR (2012) The functions of myosin II and myosin V homologs in tip growth and septation in *Aspergillus nidulans*. *PLoS One* **7**: e31218
- Takeshita N, Manck R, Grün N, de Vega SH & Fischer R (2014) Interdependence of the actin and the microtubule cytoskeleton during fungal growth. *Curr Opin Microbiol.* **20**: 34–41
- Takeshita N, Wernet V, Tsuizaki M, Grün N, Hoshi HO, Ohta A, Fischer R & Horiuchi H (2015) Transportation of *Aspergillus nidulans* Class III and V Chitin Synthases to the Hyphal Tips Depends on Conventional Kinesin. *PLoS One* **10**: e0125937
- Tesfaigzi J, Smith-Harrison W & Carlson DM (1994) A simple method for reusing western blots on PVDF Membranes. *Biotechniques* **17**: 268–269
- Thrower JS, Hoffman L, Rechsteiner M & Pickart CM (2000) Recognition of the polyubiquitin proteolytic signal. *EMBO J.* **19**: 94–102

- Timberlake WE (1990) Molecular genetics of *Aspergillus* development. *Annu Rev Genet.* **24**: 5–36
- Tomoda K, Kubota Y, Arata Y, Mori S, Maeda M, Tanaka T, Yoshida M, Yoneda-Kato N & Kato JY (2002) The cytoplasmic shuttling and subsequent degradation of p27Kip1 mediated by Jab1/CSN5 and the COP9 signalosome complex. *J Biol Chem.* **277**: 2302–2310
- Tomoda K, Yoneda-Kato N, Fukumoto A, Yamanaka S & Kato JY (2004) Multiple functions of Jab1 are required for early embryonic development and growth potential in mice. *J Biol Chem.* **279**: 43013–43018
- Ubersax JA & Ferrell JE Jr (2007) Mechanisms of specificity in protein phosphorylation. *Nat Rev Mol Cell Biol.* **8**: 530–541
- Uhle S, Medalia O, Waldron R, Dumdey R, Henklein P, Bech-Otschir D, Huang X, Berse M, Sperling J, Schade R & Dubiel W (2003) Protein kinase CK2 and protein kinase D are associated with the COP9 signalosome. *EMBO J.* **22**: 1302–1312
- van der Veen AG & Ploegh HL (2012) Ubiquitin-like proteins. *Annu Rev Biochem.* **81**: 323–357
- Varadan R, Assfalg M, Haririnia A, Raasi S, Pickart C & Fushman D (2004) Solution conformation of Lys63-linked di-ubiquitin chain provides clues to functional diversity of polyubiquitin signaling. *J Biol Chem.* **279**: 7055–7063
- Varadan R, Assfalg M, Raasi S, Pickart C & Fushman D (2005) Structural determinants for selective recognition of a Lys48-linked polyubiquitin chain by a UBA domain. *Mol Cell* **18**: 687–698
- Verma R, Aravind L, Oania R, McDonald WH, Yates JR 3rd, Koonin EV & Deshaies RJ (2002) Role of Rpn11 metalloprotease in deubiquitination and degradation by the 26S proteasome. *Science* **298**: 611–615
- Vittal V, Stewart MD, Brzovic PS & Klevit RE (2015) Regulating the Regulators: Recent Revelations in the Control of E3 Ubiquitin Ligases. *J Biol Chem.* **290**: 21244–21251
- Vlach J, Hennecke S & Amati B (1997) Phosphorylation-dependent degradation of the cyclin-dependent kinase inhibitor p27. *EMBO J.* **16**: 5334–5344
- Vlachostergios PJ, Voutsadakis IA & Papandreou CN (2012) The ubiquitin-proteasome system in glioma cell cycle control. *Cell Div.* **7**: 18
- von Zeska Kress MR, Harting R, Bayram Ö, Christmann M, Irmer H, Valerius O, Schinke J, Goldman GH & Braus GH (2012) The COP9 signalosome counteracts the accumulation of cullin SCF ubiquitin E3 RING ligases during fungal development. *Mol Microbiol.* **83**: 1162–1177
- Wada H, Kito K, Caskey LS, Yeh ET & Kamitani T (1998) Cleavage of the C-terminus of NEDD8 by UCH-L3. *Biochem Biophys Res Commun.* **251**: 688–692

- Walden H, Podgorski MS, Huang DT, Miller DW, Howard RJ, Minor DL Jr, Holton JM & Schulman BA (2003) The structure of the APPBP1-UBA3-NEDD8-ATP complex reveals the basis for selective ubiquitin-like protein activation by an E1. *Mol Cell* **12**: 1427–1437
- Walsh G & Jefferis R (2006) Post-translational modifications in the context of therapeutic proteins. *Nat Biotechnol.* **24**: 1241–1252
- Walther A & Wendland J (2003) Septation and cytokinesis in fungi. *Fungal Genet Biol.* **40**: 187–196
- Wang J, Hu Q, Chen H, Zhou Z, Li W, Wang Y, Li S & He Q (2010) Role of individual subunits of the *Neurospora crassa* CSN complex in regulation of deneddylation and stability of cullin proteins. *PLoS Genet.* **6**: e1001232
- Wang X & Martin DS (2015) The COP9 signalosome and cullin-RING ligases in the heart. *Am J Cardiovasc Dis* **5**: 1–18
- Wang Z, Xu A, Hou X, Chen F, Cao W, Yu J, Liao M & Tang J (2014) COP9 signalosome subunit 6 binds and inhibits avian leukosis virus integrase. *Biochem Biophys Res Commun.* **453**: 527–532
- Watson IR, Li BK, Roche O, Blanch A, Ohh M & Irwin MS (2010) Chemotherapy induces NEDP1-mediated destabilization of MDM2. *Oncogene* **29**: 297–304
- Wee S, Geyer RK, Toda T & Wolf DA (2005) CSN facilitates Cullin-RING ubiquitin ligase function by counteracting autocatalytic adapter instability. *Nat Cell Biol.* **7**: 387–391
- Wei N & Deng XW (1999) Making sense of the COP9 signalosome: A regulatory protein complex conserved from Arabidopsis to human. *Trends Genet.* **15**: 98–103
- Wei N, Chamovitz DA & Deng XW (1994) Arabidopsis COP9 is a component of a novel signaling complex mediating light control of development. *Cell* **78**: 117–124
- Wei N, Serino G & Deng XW (2008) The COP9 signalosome: more than a protease. *Trends Biochem Sci.* **33**: 592–600
- Welchman RL, Gordon C & Mayer RJ (2005) Ubiquitin and ubiquitin-like proteins as multifunctional signals. *Nat Rev Mol Cell Biol.* **6**: 599–609
- Whittaker RH (1969) New concepts of kingdoms or organisms. Evolutionary relations are better represented by new classifications than by the traditional two kingdoms. *Science* **163**: 150–160
- Wilkinson KD, Urban MK & Haas AL (1980) Ubiquitin is the ATP-dependent proteolysis factor I of rabbit reticulocytes. *J Biol Chem.* **255**: 7529–7532
- Wolf DA, Zhou C & Wee S (2003) The COP9 signalosome: an assembly and maintenance platform for cullin ubiquitin ligases? *Nat Cell Biol.* **5**: 1029–1033

- Wolkow TD, Harris SD & Hamer JE (1996) Cytokinesis in *Aspergillus nidulans* is controlled by cell size, nuclear positioning and mitosis. *J Cell Sci.* **109**: 2179–2188
- Wu JT, Chan YR & Chien CT (2006) Protection of cullin-RING E3 ligases by CSN-UBP12. *Trends Cell Biol.* **16**: 362–369
- Wu K, Yamoah K, Dolios G, Gan-Erdene T, Tan P, Chen A, Lee CG, Wei N, Wilkinson KD, Wang R & Pan ZQ (2003) DEN1 is a dual function protease capable of processing the C terminus of Nedd8 and deconjugating hyper-neddylated CUL1. *J Biol Chem.* **278**: 28882–28891
- Wu S, Zhu W, Nhan T, Toth JI, Petroski MD & Wolf DA (2013) CAND1 controls *in vivo* dynamics of the cullin 1-RING ubiquitin ligase repertoire. *Nat Commun* **4**: 1642
- Xiang X & Plamann M (2003) Cytoskeleton and motor proteins in filamentous fungi. *Curr Opin Microbiol.* **6**: 628–633
- Xirodimas DP, Sundqvist A, Nakamura A, Shen L, Botting C & Hay RT (2008) Ribosomal proteins are targets for the NEDD8 pathway. *EMBO Rep.* **9**: 280–286
- Yang X, Menon S, Lykke-Andersen K, Tsuge T, Di Xiao, Wang X, Rodriguez-Suarez RJ, Zhang H & Wei N (2002) The COP9 signalosome inhibits p27(kip1) degradation and impedes G1-S phase progression via deneddylation of SCF Cul1. *Curr Biol.* **12**: 667–672
- Yoshida A, Yoneda-Kato N & Kato JY (2013) CSN5 specifically interacts with CDK2 and controls senescence in a cytoplasmic cyclin E-mediated manner. *Sci Rep* **3**: 1054
- Yu JH (2010) Regulation of Development in *Aspergillus nidulans* and *Aspergillus fumigatus*. *Mycobiology* **38**: 229–237
- Zhou C, Wee S, Rhee E, Naumann M, Dubiel W & Wolf DA (2003) Fission yeast COP9/signalosome suppresses cullin activity through recruitment of the deubiquitylating enzyme Ubp12p. *Mol Cell* **11**: 927–938
- Zhou L & Watts FZ (2005) Nep1, a *Schizosaccharomyces pombe* deneddylating enzyme. *Biochem J.* **389**: 307–314

Abbreviations

A (Ala)	alanine
aa	amino acid
Asex	asexual growth conditions
AspGD	<i>Aspergillus</i> Genome Database
ATP	adenosine triphosphate
BiFC	bi-molecular fluorescence complementation
BLAST	basic local alignment search tool
bp	base pair
BSA	bovine serum albumin
CADRE	Central <i>Aspergillus</i> Data REpository
CBB	calmodulin binding buffer
CBP	calmodulin-binding protein
CDK	cyclin-dependent kinase
CEB	calmodulin elution buffer
cDNA	complementary DNA
cl	cleistothecium
cm	centimeter
co	conidiophore
COP	constitutive photomorphogenic
CRL	cullin-RING ligase
CSN	COP9 signalosome
C-terminus	carboxy terminus
CulA/CUL1	cullinA/1
CulC/CUL3	cullinC/3
D	Germany
D (Asp)	aspartate
DenA/DEN1	deneddylase A/1
DIC	differential interference contrast
DipA	DenA interacting phosphatase
DNA	deoxyribonucleic acid
DTT	dithiothreitol

DUB	deubiquitinating enzyme
DUF	domain of unknown function
EDTA	ethylenediaminetetraacetic acid
EGTA	ethyleneglycol-bis(2-aminoethylether)-N,N,N',N'- tetraacetic acid
Fe	iron
FM4-64	N-(3-Triethylammoniumpropyl)-4-(6-(4-(Diethylamino) Phenyl) Hexatrienyl) Pyridinium Dibromide
FphA	fungal phytochrome A
G	glycine
GFP	green-fluorescent protein
h	hour
H (His)	histidine
H2A	histone
K (Lys)	lysine
kb	kilobase
kDa	kilo Dalton
L (Leu)	leucine
LaeA	lack of aflR expression
LB	lysogeny broth
LC-MS/MS	liquid chromatography-mass spectrometry/mass spectrometry
Mb	mega basepairs
µg	microgram
mg	milligram
min	minute
µl	microliter
ml	milliliter
MM	minimal medium
mM	millimolar
Mn	manganese
MPN	Mpr1p and Pad1p N-terminal
mRNA	messenger RNA
N (Asn)	asparagine
NaF	sodium fluoride
nat	nourseothricin

NCBI	National Center for Biotechnology
Nedd8 (N8)	neural precursor cell expressed developmentally downregulated
NimX	never in mitosis
N-terminus	amino terminus
OE	overexpressed
ORF	open reading frame
PAGE	polyacrylamide gel electrophoresis
PCI	proteasome-LID, CSN, eIF3
PCR	polymerase chain reaction
pers. comm.	personal communication
pfam	protein family
phleo	phleomycin
PPM	phosphatase metallo-dependent
PPP	phosphor-protein phosphatase
PTM	posttranslational modification
ptrA	pyrithiamine
R (Arg)	arginine
Q (Gln)	glutamine
qRT	quantitative real-time
Rbx1	RING box protein
rcf	relative centrifugal force
RFP	red-fluorescent protein
RING	really interesting new gene
RNA	ribonucleic acid
rpm	revolutions per minute
RT	room temperature
S (Ser)	serine
SCF	Skp1-cullin-F-Box protein complex
SDS	sodium dodecyl sulfate
sec	second
t	time
TAP	tandem affinity purification
TBS/T	Tris buffered saline with tween
TCA	trichloroacetic acid

ABBREVIATIONS

TEV	tobacco etch virus
Tris	2-Amino-2-hydroxymethyl-propane-1,3-diol
Ub	ubiquitin
UBL	ubiquitin-like
ULP	ubiquitin-like protease
UPS	ubiquitin-proteasome system
UTR	untranslated region
UV	ultra-violet
VapA	VipC associated protein A
VapB	VipC associated protein B
VeA	<i>velvet</i> protein A
Veg	vegetative growth conditions
VipC	VeA interacting protein C
WT	wild type
YFP	yellow-fluorescent protein
Zn	zinc
Δ	deletion

List of Figures

Figure 1: Posttranslational modifications of proteins.	4
Figure 2: Mechanism of phosphorylation and dephosphorylation of proteins.	5
Figure 3: Structures of ubiquitin and the ubiquitin-like protein Nedd8.	8
Figure 4: Nedd8 maturation and its ligation cascade.	9
Figure 5: Protein degradation by the ubiquitin-proteasome system.	11
Figure 6: Attachment of Nedd8 promotes CRL activity.	13
Figure 7: Subunit composition of the COP9 signalosome deneddylase.	14
Figure 8: Regulation of CRL activity by dynamic alterations of its architecture.	18
Figure 9: Life cycle of <i>Aspergillus nidulans</i>	22
Figure 10: Light-dependent regulation of <i>A. nidulans</i> development.	26
Figure 11: Influence of CSN and DenA on CulA or CulC deneddylation.	55
Figure 12: Changes in deneddylase activity and its consequences for the cellular pool of neddylated proteins.	57
Figure 13: Changes in deneddylase activity and its consequences for the cellular pool of neddylated CulA or CulC.	58
Figure 14: Impact of altered deneddylase activity on asexual development and stress response.	60
Figure 15: Protein amount of DenA-GFP in various <i>csn</i> deletion strains during development.	63
Figure 16: Enrichment of phosphorylated DenA from vegetative cultures.	64
Figure 17: Identification of DenA phosphorylation sites.	67
Figure 18: Influence of amino acid substituted DenA phosphorylation sites on its protein stability.	69
Figure 19: Influence of amino acid substituted DenA phosphorylation sites on asexual development.	70
Figure 20: <i>dipA</i> gene locus and multiple alignment of its deduced metallophosphatase domain.	72
Figure 21: Asexual colony formation of wild type, <i>dipA</i> mutant and <i>dipA</i> complementation strains.	74
Figure 22: Impaired development of strains lacking a functional DipA.	75

Figure 23: Hyphal morphology of <i>dipA</i> deletion strain.	76
Figure 24: Protein localization and occurrence of DipA.	78
Figure 25: Cytoplasmatic interaction between DenA and DipA.....	79
Figure 26: Dynamic co-transport of DenA-DipA interaction complex.	81
Figure 27: DenA protein level in <i>dipA</i> deletion strain.....	82
Figure 28: Effect of <i>dipA/csnG</i> double deletion on development.	83
Figure 29: Effect of <i>dipA/csnG</i> double deletion on DenA stability.....	84
Figure 30: Substrate specificity of the fungal deneddylases CSN and DenA.....	88
Figure 31: Model for auxiliary DenA function to compensate CSN associated defects.	92
Figure 32: DenA degradation mediated by the COP9 signalosome.	94
Figure 33: Phosphorylation of DenA regulates its stability and fungal development.	99
Figure 34: CSN and DipA target different subpopulations of DenA for degradation.	101
Figure 35: Putative impact of DipA on central regulators of fungal development.	106

List of Tables

Table 1: <i>Aspergillus nidulans</i> strains constructed and used in this study.....	31
Table 2: Plasmids constructed and used in this study.	41
Table 3: Oligonucleotides used in this study.	43

Acknowledgements

First of all, I thank Prof. Dr. Gerhard H. Braus for supporting my research. I started my scientific career with the diploma thesis in his department and continued with my doctorate. During all this time I could count on his expertise and I remember many inspiring work-related as well as private discussions. I am deeply grateful that he allowed me to visit both national as well as international conferences and introduced me to a many outstanding researchers.

My special thanks to Prof. Dr. Stefanie Pöggeler for being in my thesis committee. During a voluntary placement as a young student in her group she inspired me to use a fungus as a model organism in order to answer scientific questions. I appreciate her helpful suggestions and advices, especially during my doctoral studies.

I am also grateful to Prof. Dr. Rolf Daniel, PD Dr. Michael Hoppert, Prof. Dr. Kai Tittmann and Prof. Dr. Kai Heimel for being members of my examination board.

I wish to thank all the members of my department. Above all, I have to mention Rebekka Harting, as we shared many profitable and motivating discussions during my doctorate and diploma. Beside this I really enjoyed our rare moments when the SGE was winning. I really appreciated the time with my colleague Mirit Gulko. It was always a pleasure working with you and I deeply valued your honesty and I will miss our conversations. My gratitude goes to Gaby Heinrich for her excellent support with experiments, but also for providing us with enormous amounts of home-made chocolate cakes. I also thank Cindy Meister and Anna Köhler for all the pleasant moments in our lab as well as for the relaxing atmosphere. I wish you all the best. Many thanks go to my students Sina, Rita and Florian.

I would like to thank the “mensa-group”. Basti Joehnk, Jennifer Gerke, Dominik Schneider, Christoph Sasse, Fruzsina Bakti, Karl Thieme and many more. Thanks for the numerous moments, where one could recharge the positive energy.

Many thanks to Julian and Dome for sharing all the nice things that life has to offer.

My deepest thanks to my parents and brothers for their endless support during my doctoral work and life in general, and without this valuable book would not have been written.

Finally, I would like to thank my girlfriend for showing me the bright side of life.

Curriculum vitae

Personal details:

Josua Sebastian SchinkeBorn on October 16th, 1984

In Aalen, Germany

Academic Track Record

01/2012 - 11/2015

DoctorateProf. Gerhard Braus, Institute for Microbiology and Genetics,
Georg - August - University GöttingenThesis title: „Phosphorylation dependent stability control of the
deneddylase DenA and its impact on *Aspergillus nidulans*
development”

02/2011 - 01/2016

Research assistant

02/2010 – 11/2010

Diploma (Dipl. Biol.), Grade 1,5Prof. Gerhard Braus, Institute for Microbiology and Genetics,
Georg - August - University GöttingenTitle: “The *esdA* (essential for sterigmata development) - gene
and the asexual development of *Aspergillus nidulans*”

10/2005 – 11/2010

Academic Studies, Grade 1,5

Georg - August - University Göttingen

Biology - Focus on microbiology, biochemistry, zoology

Teaching

04/2014 – 09/2014

Supervision of the bachelor thesis “Analysis and Identification
of phosphorylation sites of the Deneddylase DenA in
Aspergillus nidulans”, of Margarita Stirz

03/2012 - 10/2012

Supervision of the master thesis “Consequences of DenA-CSN
interaction in *Aspergillus nidulans*”, of Sina Stumpf**Publications**

2016

J. Schinke, M.K. Gulko, M. Christmann, O. Valerius, S.K.
Stumpf, M. Stirz, G.H. Braus. The DenA/DEN1 Interacting
Phosphatase DipA Controls Septa Positioning and
Phosphorylation-dependent Stability of Cytoplasmatic
DenA/DEN1 during Fungal Development. PLoS Genetics.

2013

M. Christmann, T. Schmalzer, C. Gordon, X. Huang, Ö.
Bayram, **J. Schinke**, S. Stumpf, W. Dubiel, G.H. Braus.
Control of Multicellular Development by the Physically
Interacting Deneddylases DEN1/DenA and COP9
Signalosome. PLoS Genetics.

2012

M.R. von Zeska Kress, R. Harting, Ö. Bayram, M. Christmann,
H. Irmer, O. Valerius, **J. Schinke**, G.H. Goldman, G.H. Braus.
The COP9 signalosome counteracts the accumulation of cullin
SCF ubiquitin E3 RING ligases during fungal development.
Molecular Microbiology